Radiobiology of Combining Radiotherapy with Other Cancer Treatment Modalities

Vidhula Ahire, Niloefar Ahmadi Bidakhvidi, Tom Boterberg, Pankaj Chaudhary, François Chevalier, Noami Daems, Wendy Delbart, Sarah Baatout, Christophe M Deroose, Cristian Fernandez-Palomo, et al.

6 Radiobiology of Combining Radiotherapy with Other Cancer Treatment Modalities

Vidhula Ahire, Niloefar Ahmadi Bidakhvidi, Tom Boterberg, Pankaj Chaudhary, Francois Chevalier, Noami Daems, Wendy Delbart, Sarah Baatout, Christophe M. Deroose, Cristian Fernandez-Palomo, Nicolaas A. P. Franken, Udo S. Gaipl, Lorain Geenen, Nathalie Heynickx, Irena Koniarová, Vinodh Kumar Selvaraj, Hugo Levillain, Anna Jelínek Michaelidesová, Alegría Montoro, Arlene L. Oei, Sébastien Penninckx, Judith Reindl, Franz Rödel, Peter Sminia, Kevin Tabury, Koen Vermeulen, Kristina Viktorsson, and Anthony Waked

V. Ahire (✉)
Chengdu Anticancer Bioscience, Ltd., Chengdu, China

J. Michael Bishop Institute of Cancer Research, Chengdu, China

N. Ahmadi Bidakhvidi · C. M. Deroose
Department of Nuclear Medicine, University Hospitals Leuven, Leuven, Belgium

Nuclear Medicine and Molecular Imaging, Department of Imaging and Pathology, KULeuven, Leuven, Belgium
e-mail: niloefar.ahmadibidakhvidi@uzleuven.be; christophe.deroose@uzleuven.be

T. Boterberg
Department of Radiation Oncology, Ghent University Hospital, Ghent, Belgium

Particle Therapy Interuniversity Center Leuven, Department of Radiation Oncology, University Hospitals Leuven, Leuven, Belgium
e-mail: Tom.Boterberg@ugent.be

P. Chaudhary
Patrick G. Johnston Center for Cancer Research, Queen's University Belfast, Northern Ireland, United Kingdom
e-mail: p.chaudhary@qub.ac.uk

F. Chevalier
UMR6252 CIMAP, Team Applications in Radiobiology with Accelerated Ions, CEA-CNRS-ENSICAEN-Université de Caen Normandie, Caen, France
e-mail: chevalier@ganil.fr

N. Daems
Radiobiology Unit, Belgian Nuclear Research Centre, SCK CEN, Mol, Belgium

W. Delbart
Nuclear Medicine Department, Hôpital Universitaire de Bruxelles (H.U.B.), Brussels, Belgium
e-mail: wendy.delbart@bordet.be

S. Baatout
Radiobiology Unit, Belgian Nuclear Research Centre (SCK CEN), Mol, Belgium

Institute of Nuclear Medical Applications, Belgian Nuclear Research Center (SCK CEN), Mol, Belgium
e-mail: sarah.baatout@sckcen.be

C. Fernandez-Palomo
Institute of Anatomy, University of Bern, Bern, Switzerland
e-mail: cristian.fernandez@unibe.ch

N. A. P. Franken · A. L. Oei
Department of Radiation Oncology, Amsterdam University Medical Centers, Location University of Amsterdam, Amsterdam, The Netherlands

Center for Experimental and Molecular Medicine (CEMM), Laboratory for Experimental Oncology and Radiobiology (LEXOR), Amsterdam, The Netherlands

Cancer Biology and Immunology, Cancer Center Amsterdam, Amsterdam, The Netherlands
e-mail: N.A.P.Franken@amsterdamumc.nl

U. S. Gaipl
Translational Radiobiology, Department of Radiation Oncology, Universitätsklinikum Erlangen, Erlangen, Germany
e-mail: udo.gaipl@uk-erlangen.de; A.L.Oei@amsterdamumc.nl

L. Geenen
Radiobiology Unit, Belgian Nuclear Research Centre, SCK CEN, Mol, Belgium

Department of Radiology and Nuclear Medicine, Erasmus Medical Center, Rotterdam, The Netherlands

N. Heynickx
Radiobiology Unit, Belgian Nuclear Research Centre, SCK CEN, Mol, Belgium

Department of Molecular Biotechnology, Ghent University, Ghent, Belgium
e-mail: nathalie.heynickx@sckcen.be

S. Baatout (ed.), *Radiobiology Textbook*, https://doi.org/10.1007/978-3-031-18810-7_6

I. Koniarová
Department of Radiation Protection in Radiotherapy, National Radiation Protection Institute, Prague, Czech Republic
e-mail: irena.koniarova@suro.cz

V. K. Selvaraj
Department of Radiation Oncology, Thanjavur Medical College, Thanjavur, India

H. Levillain · S. Penninckx
Medical Physics Department, Hôpital Universitaire de Bruxelles (H.U.B.), Bruxelles, Belgium
e-mail: hugo.levillain@bordet.be; sebastien.penninckx@bordet.be

A. J. Michaelidesová
Nuclear Physics Institute of the Czech Academy of Sciences, Rez, Czech Republic

Faculty of Nuclear Sciences and Physical Engineering, Prague, Czech Republic
e-mail: michaelidesova@ujf.cas.cz

A. Montoro
Laboratorio de Dosimetría Biológica, Servicio de Protección Radiológica Hospital Universitario y Politécnico la Fe, Valencia, Spain
e-mail: montoro_ale@gva.es

J. Reindl
Section Biomedical Radiation Physics, Institute for Applied Physics and Measurement Technology, Universität der Bundeswehr München, Neubiberg, Germany
e-mail: judith.reindl@unibw.de

F. Rödel
Department of Radiotherapy and Oncology, Goethe University, Frankfurt am Main, Germany
e-mail: franz.roedel@kgu.de

P. Sminia
Department of Radiation Oncology, Amsterdam University Medical Centers, Location Vrije Universiteit/Cancer Center Amsterdam, Amsterdam, The Netherlands
e-mail: p.sminia@amsterdamumc.nl

K. Tabury
Radiobiology Unit, Belgian Nuclear Research Centre (SCK CEN), Mol, Belgium

Department of Biomedical Engineering, University of South Carolina, Columbia, SC, United States of America
e-mail: kevin.tabury@sckcen.be

K. Vermeulen
Institute of Nuclear Medical Applications, Belgian Nuclear Research Centre SCK CEN, Mol, Belgium
e-mail: koen.vermeulen@sckcen.be

K. Viktorsson
Department of Oncology/Pathology, Karolinska Institutet, Stockholm, Sweden
e-mail: Kristina.viktorsson@ki.se

A. Waked
Radiobiology Unit, Belgian Nuclear Research Centre, SCK CEN, Mol, Belgium

Laboratory of Nervous System Disorders and Therapy, GIGA Neurosciences, Université de Liège, Liège, Belgium
e-mail: anthony.waked@sckcen.be

Learning Objectives

- To understand the biological rationale and characteristics of conventional and alternative fractionation schemes used in clinical RT practice and get insight into the biological aspects (acceptability of high dose fractions, optimal dose-time) of hypofractionation regimen.
- To understand the definition and radiobiologic principles of Stereotactic Body Radiation Therapy (SBRT)/hypofractionation/boron neutron capture therapy (BNCT); and learn about their treatment planning and associated applications in clinical settings.
- To understand the basic concept of combining RT with various other treatment modalities that can enhance the effect of radiation by specifically targeting cancer cells or the immune system as well as for minimizing the adverse effects on normal cells.
- To understand the principles and clinical applications of both diagnostic and therapeutic radiopharmaceuticals.
- To grasp the different methods of spatial RT fractionation and how tissue is spared by using these methods.
- To learn basic principles of brachytherapy and understand the principles, treatment course and planning, application in clinical setting as well as the theory behind personalized radioembolization/selective internal radiotherapy (SIRT).
- To study the basic concepts and clinical applications of diagnostic/therapeutic radiopharmaceuticals and high linear energy transfer (LET) carbon ion irradiation.
- To get an overview of nanotechnology and how it can improve treatment of cancer as well as challenges of translating it into clinical settings.
- To acquire an understanding of the risk factors involved in acquiring secondary tumors after RT.

6.1 Physics

Radiotherapy (RT) relies on the effect of ionizing radiation (IR) to biological matter, i.e., cells. The radiation is transferring its energy to atoms and molecules present in the cells, which lie in the path of the radiation, and therefore ionizing them. These ionizations, i.e., the removal of electrons from the atom, lead to the breaking of chemical bonds in the molecules. If these ionizations occur in the cell nucleus, the DNA, carrier of the human genome, is damaged. In RT, the capability of radiation to damage the genome is exploited to kill tumor cells. The most important quantity to define the damage, which is caused, is the dose

$$D = \frac{\mathrm{d}E}{\mathrm{d}M} \tag{6.1}$$

i.e., the energy transferred from the ion to the matter (dE) by unit mass (dM). In general, one can say that the higher the dose, the larger the damage and the higher the probability of killing a cell. However, the same physical dose of different types of radiation can cause different damage in the cells. Various types of radiation are utilized for RT. These types of radiation can be distinguished by the so-called depth dose distribution, which is the dose which is transferred to matter along the path of radiation as shown in Fig. 6.1.

Electron radiation transfers most of its energy just after it interacts with matter, i.e., tissue, making it suitable for the treatment of tumors close to the skin. If one uses electrons with higher energy, such as the shown 250 MeV electrons, the dose peak can be shifted deeper into the tissue. However, this comes with the disadvantage that the maximum range is also longer, resulting in more dose to the normal tissue beyond the tumor. Furthermore, such electron beams are quite complicated to produce. For photon beams used in RT, the dose increases in the so-called build-up region until it reaches the maximal dose and then gradually decreases. The depth of the maximal dose can be a few μm (for kV beams, i.e., beams with particle energy in the kilovolt regime) or several mm or cm (for MV (megavolt) beams). In contrast to electrons and photons, particles such as protons or high linear energy transfer (LET) carbon ions show a totally different dose distribution depth. The ions deliver a low dose when entering tissue. With depth this transfer is slowly increasing, while the ion gets slower. With further energy loss and decreasing speed, the dose drastically increases and reaches a maximum just before the ion stops in the tissue. This unique dose distribution is called the Bragg curve in honor to the physicist William Henry Bragg, who discovered this behavior in 1904 [1]. To widen the treatment depth range, a spread-out Bragg peak (SOBP) is created by varying the energy of the incident proton beam. As a result, a uniform dose can be delivered to the tumor. The radiobiological impact of particles with high LET is higher compared to photons, and it increases dramatically in the distal edge and fall-off. The uncertainty in relative biological effectiveness (RBE) of ion beams is still a limitation in its clinical application and should be considered during the treatment planning as a part of the process leading to a robust treatment plan. A detailed description about the physical and biological interactions of radiation to biological matter and the consequences for the biological effect can be found in Chaps. 2 and 3.

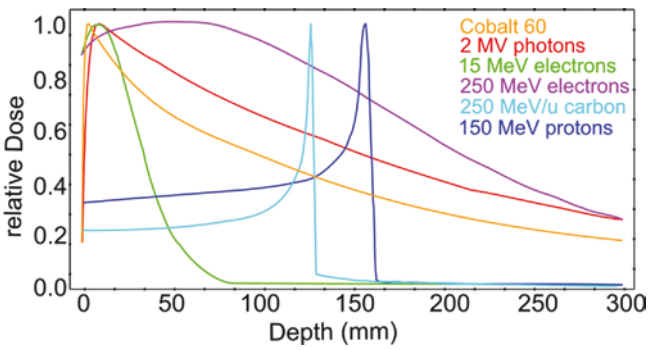

Fig. 6.1 Comparison of the relative depth dose distribution of 15 MeV electrons (green), 250 MeV electrons (purple), 2 MeV photons (red), 150 MeV protons (dark blue), and 250 MeV/u carbon (turquoise) and cobalt 60 (orange)

6.2 Conventional and Alternative Radiation Schemes

Box 6.1 Conventional and Alternative Radiation Schemes

- Typical conventionally fractionated irradiation schemes use 2 Gy fractions, 5 fractions per week for 3–7 weeks, depending on the tumor type.
- Alternative radiation schemes, i.e., either smaller or larger sized fractions, multiple fractions per day, or different overall treatment time should be based on the various biological processes and response characteristics of both the normal and malignant tissues in the exposed volume.

When using radiation for cancer treatment purposes, the total radiation dose is generally applied in a regimen with multiple small fractions, aiming to reach tumor kill while sparing adjacent normal, healthy tissues, and organs. Most tumors are treated with a conventional fractionation regimen, which is characterized by daily fractions of 1.8–2 Gy, 5 days per week, for a duration of 3–7 weeks,

Table 6.1 Characteristics of radiotherapy treatment regimen and involved radiobiological processes. (Reproduced with permission from [2])

Radiation treatment regimen	Conventional fractionation	Hyperfractionation	Accelerated fractionation	Hypofractionation	SBRT and SRS
Total dose (Gy)	70	≥70	<70	<70	<30
Fraction size (Gy)	1.8–2	<1.8	≥2	Mostly 2.5–10	Mostly ~12–25
Number of fractions per day	1	2–3	1	1	1
Treatment (days per week)	5	5	6	≤5	1 or a few
Overall treatment time (weeks)	7	7	Up to ~5	Up to ~5	–
Radiobiological reasoning—note the 6 **R**s of Radiobiology	Normal tissue sparing via **R**epair and **R**epopulation. Tumor control via **R**edistribution and **R**eoxygenation. **R**eactivation of the immune response.	Exploitation of differences in **R**adiosensitivity and **R**epair and—kinetics between normal and tumor cells. **R**eactivation of the immune response.	Overcoming tumor cell **R**epopulation. **R**eactivation of the immune response.	Overcoming tumor cell **R**epopulation.	Overcoming tumor cell **R**epopulation.

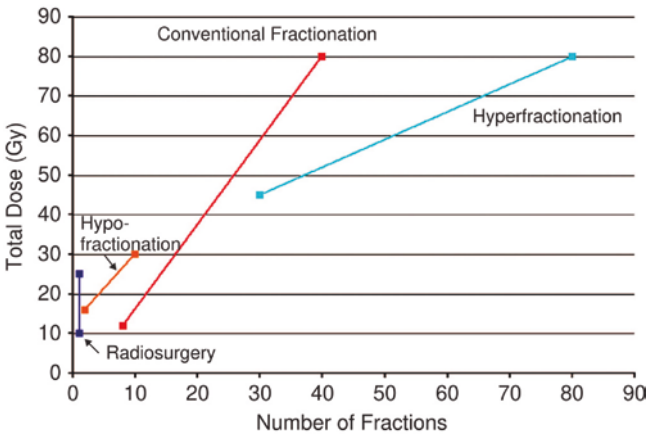

Fig. 6.2 Fractionation regimen used in clinical practice. (Reproduced with permission from [3])

reaching a total dose of 30–70 Gy. However, considering the radiation sensitivity and volume of the particular tumor type to be irradiated, as well as that of the normal tissue or organs at risk (OAR), an alternative irradiation regimen might be preferred. The use of an alternative radiation scheme should be motivated, either technically, e.g., by minimizing the volume of the normal tissue in the radiation field by using precision RT or on the basis of the biological characteristics of the malignant tissue, i.e., the 6R's (see Chap. 5). Apart from technical and radiobiological arguments, department logistics as well as patients' condition or patients' comfort might justify the choice of an alternative radiation treatment (Box 6.1). Typical characteristics of fractionation regimens and their radiobiological rationale are presented in Table 6.1 and discussed below.

The relationship between the number of fractions and the total dose for a clinical radiation regimen is presented in Fig. 6.2.

6.2.1 Hyperfractionation

The biological rationale of hyperfractionation is the advantage of application of multiple small-sized fractions compared with conventional 2 Gy fractions to further spare the normal tissues relative to the malignant tissues. Because of the higher total dose, hyperfractionation could increase the tumor control probability. To limit the duration of the overall treatment time, generally 2–3 fractions per day, typically ~1.4 Gy, separated 4–6 h between the fractions are given. Some hyperfractionation clinical trials, however, showed an increase in late normal tissue side effects, which has been ascribed to the short time interval between fractions for complete repair of sublethal DNA damages, since late-responding tissues do have long repair half times in the order of 2–4 h. Additionally, hyperfractionation puts a heavy logistical burden on the RT department and the patient, especially in children who may need anesthesia.

6.2.2 Hypofractionation and Accelerated Fractionation

The rationale of both hypo- and accelerated fractionation strategies can be found in shortening the overall treatment time to anticipate tumor cell proliferation/repopulation. Generally, fractions larger than 2 Gy fractions are applied with few fractions per week, allowing to shorten the overall treatment duration with a few weeks versus conventional regimens. The hypofractionation approach has become feasible because of currently available precision radiation techniques and technology, with optimized radiation dose distribution.

The drawback of using high fraction sizes, the rationale, pro- and contra biological arguments, is discussed in the next Sect. 6.3.

The term accelerated fractionation applies to the use of multiple fractions per day, or increasing the number of treatment days per week (e.g., continue radiation during the weekend) to deliver a higher average total radiation dose than conventionally used. Hence, the overall treatment time of accelerated regimen is reduced. Often, both hypo- and hyperfractionated irradiation fit in this definition of accelerated fractionation. A typical example is the Continuous Hyperfractionated Accelerated RadioTherapy (CHART) treatment scheme, with 36 fractions of 1.5 Gy, total dose of 54 Gy in 12 days. In that scheme three fractions of 1.5 Gy were applied per day, with an interfraction time interval of 6 h, for 12 days, including the weekend. Details regarding the CHART clinical trials and outcomes are available in the literature. In particular, head and neck cancer patients with high epidermal growth factor receptor (EGFR) expressing tumors benefited from CHART [4].

6.2.3 Stereotactic Radiotherapy: Radiosurgery

Historically, the term stereotactic radiotherapy was used for a type of external RT of the brain that uses dedicated equipment being a stereotactic frame fixed to the head with screws just penetrating the outer part of the skull. This frame was used to immobilize the head, position the patient, and create a stereotactic "space" with a coordinate system that allows target definition in an *X*-, *Y*-, and *Z*-axis. The term stereotactic radiosurgery (SRS) is used when a single fraction of stereotactically guided conformal irradiation is delivered to a coordinate-defined target. More modern fixation systems no longer require the placement of an invasive frame, but make use of advanced thermoplastic masks combined with position verification and adaptation systems of the treatment machine's table. Different delivery systems can be used for radiosurgery: the originally SRS-dedicated GammaKnife system (using 201 small 60-Co sources) or linac-based systems (linear accelerator, CyberKnife, Tomotherapy).

Typical indications are single (or up to 3–5) brain metastases, meningiomas, acoustic neuromas, or arteriovenous malformations, all smaller than 3 cm in diameter. Depending on the indication, doses range between 12 Gy (benign lesions) and 20–25 Gy (metastases). Some centers also use radiosurgery to treat benign conditions like epilepsy and trigeminal neuralgia, requiring doses of 20–25 Gy up to 60–80 Gy, respectively.

The appearance of the effect of radiosurgery usually takes several months and may be accompanied by an inflammatory reaction that mimics tumor growth in the first 1–3 years. In some cases, overt brain radionecrosis may develop, requiring treatment with steroids or rarely the need for surgical removal of the affected area (see also Chap. 5) (Box 6.2).

Box 6.2 Hypofractionation

- Hypofractionation is the use of radiation dose fractions considerably larger than the conventional fraction size of 2 Gy.
- Hypofractionation could be beneficial over conventional fractionation because of precision RT together with specific biological phenomena such as hypoxia and sensitivity to dose fractionation of both the tumor target volume and organs at risk.

6.3 Radiobiological Aspects of Hypofractionation

Fractionated RT, using multiple small-sized fractions of 1.8–2 Gy, is the standard treatment of cancer patients. Over many decades, large evidence has been obtained from experimental studies *in vitro* or *in vivo* and later in clinical studies regarding the biological rationale of fractionated irradiation. Abundant evidence exists on the differential effect of fractionation between late-responding normal tissues and early responding normal tissues or tumors. Most normal tissues and organs benefit from fractionated RT, meaning that they can tolerate a higher total dose, while tumors are only slightly spared by dose fractionation. The smaller the fraction size—taking the overall treatment time allowing tumor cell repopulation into account—the wider the therapeutic window. Having learned that fractionation is a great method to spare normal tissues while keeping tumor control equal, hypofractionation, i.e., the use of dose fractions substantially larger than conventional 2 Gy fractions (see also Chap. 5) sounds not as a good idea. However, for two main reasons, hypofractionation has gained importance in radiation oncology: α

(1) Clinical data have shown that some tumor types like prostate carcinoma, malignant melanoma, and liposarcoma, are almost as sensitive to fractionated irradiation as their surrounding normal tissues. Such tumors can tolerate a higher biological dose than formerly thought when treated with 2 Gy fractions, hence behaving like late-responding normal tissues and thus are relatively spared by fractionation. Indeed, these tumor types are characterized with a low $\langle \alpha/\beta$ value of ~1–2 Gy in the Linear Quadratic (LQ) model. Breast and esophageal cancers also have α/β values close to those for normal tissues, in the order of ~5 Gy. (2) With the implementation of high precision RT techniques, highly conformal 3D dose distributions to the target volume can be obtained, with minimal radiation exposure to adjacent critical normal tissues and OAR. The HyTEC initiative (Hy dose per fraction, hypofractionated Treatment Effects in the Clinic) is to systemically pool published peer-reviewed clinical data to further define dose, vol-

Table 6.2 Hypofractionation: pro and contra biological arguments

Pros
• If α/β ratio tumor < α/β ratio normal tissue
• Only if small normal tissue/OAR volumes are exposed: high conformity RT
• Direct vascular injury
• Shorter overall time: beneficial in case of rapid proliferating tumors
• If the onset of accelerated tumor cell repopulation is faster using high-dose fractions, dose reduction without loss of tumor control could be achieved while diminishing late toxicity
• "Biological dose" escalation, which might result in better tumor control
• Activation of the immune response to attack tumor cells inside the irradiated volume and at distance, the abscopal effect
• Lower probability of induction of secondary tumors
Cons
• Mostly, α/β ratio tumor > α/β ratio normal tissue
• High-dose fractions are detrimental for normal tissues: higher probability of normal tissue complications, unless dose gradients are steep and the irradiated volume small
• No benefit from sensitization of hypoxic tumor cells via reoxygenation between fractions
• Radiosensitizing agents are potentially less effective when combined with high-dose fractions

ume, and outcome estimates for both normal tissue complication probability and tumor control [5] for SRS and SBRT, where single high radiation doses are common practice. Under certain conditions, like high conformity of RT with steep dose gradients toward the surrounding normal tissues, hypofractionation could be beneficial over conventional fractionation. In this section, the radiobiological pro- and contra arguments of hypofractionation, listed in Table 6.2 are discussed.

6.3.1 Hypofractionation and the Linear Quadratic (LQ) Model

The validity of the LQ model at high fraction sizes above approximately 6 Gy is questionable, and alternative radiobiological models are proposed. However, a strong pro-argument was derived from clinical data from non-small cell lung cancer patients treated with SBRT, either with a single dose or hypofractionated with 3–8 fractions. From the study [6], it was evident that the clinically observed increase in tumor could be ascribed to radiation dose escalation, i.e., an increased Biologically Effective Dose (BED) according to the LQ equation. BED values were calculated for the various hypofractionation schemes including SBRT fraction sizes of 22 Gy. No adaptation or correction was made when using the conventional LQ model. The analysis showed a clear correlation between treatment outcome and the BED, even at extreme high BED values. Hence, there is still a discrepancy between theoretical and experimental validity of the LQ model. However, since the model describes the clinical data on tumor control over a wide range of dose, fraction sizes, and treatment durations [6], it might still be valid in predicting RT outcomes in certain conditions.

6.3.2 Hypofractionation, Hypoxia, and Reoxygenation

Hypoxia is a state of reduced oxygen availability or decreased oxygen partial pressure below a critical threshold (generally at pO_2 of 2.5 or 5 mmHg). The Oxygen Enhancement Ratio (OER) is around 3 for most cells: for sterilization of hypoxic cells, a three times higher irradiation dose is required than for normoxic cells. Hence, hypoxia can cause resistance to RT, which has been observed in many tumor types. Information about the role of oxygen in RT, the OER, and related radiation sensitivity is given in Chap. 5.

In fractionated RT, during the time interval between daily applied irradiation fractions and during the full course of RT, hypoxic cells can be re-oxygenated and become more sensitive to the next irradiation dose (see Chap. 5). If reoxygenation is efficient between dose fractions, the presence of hypoxic cells does not have a significant effect on the outcome of a multi-fractionation scheme. In a hypofractionation regimen, the time period to obtain full reoxygenation of hypoxic tumor cells might be too short. Animal data on the kinetics of reoxygenation of different tumor types demonstrated that full reoxygenation takes about 72 h [7]. Also, preclinical data and radiobiological modeling studies have demonstrated that tumor hypoxia is a greater detrimental factor for single dose treatments than for repeated conventional fraction sizes. To fully exploit reoxygenation between fractions, 6–8 fractions might be optimal, separated in a time frame of 72 h [7]. However, there are also advantages to large high-dose fractions of ~10 Gy. Relatively radioresistant hypoxic cells might be directly sterilized and vascular endothelial cells might be injured. Since one endothelial cell is subtending about 2000 tumor cells, direct vascular damage might largely contribute to tumor cell kill in hypofractionated RT [8].

6.3.3 Hypofractionation and Tumor Cell Repopulation

Tumor cell repopulation refers to an increase in the number of cells as a result of proliferation of surviving clonogenic tumor cells (see Chap. 5). Accelerated repopulation of tumor cells during the course of RT is starting after a lag period of ~4 weeks. One strategy discussed here is to cope with tumor cell repopulation by limiting the overall treatment time for fast repopulating tumors using a small number of higher sized fractions. As a consequence of high fraction sizes, the total irradiation dose should be reduced to overcome an increase in

late normal tissue toxicity. Hypofractionation allows shortening of the overall treatment time, which might be more effective than long duration conventional fractionation in the treatment of rapidly proliferating tumors. However, care should be taken when using too short schedules, because they could lead to an increase in acute toxicity.

To be noticed is the large LQ model based analysis of the tumor control probability (TCP) from randomized trials on in total 7283 head and neck cancer (HNC) patients, featuring wide ranges of doses, times, and fractionation schemes [9]. In the analysis, two different LQ based models were used, assuming a dose-independent (DI) and a dose-dependent (DD) acceleration of tumor cell repopulation. Accelerated Repopulation (AR) was assumed to be triggered by the level of tumor cell killing, with other words, to begin at a time when the surviving fraction of the tumor clonogenic cells falls below a critical value. This starting point of AR of tumor cells was assumed to be dose-dependent and therefore reached at an earlier time point after high fraction sizes than after low fraction sizes. The DD model of AR provided significantly improved descriptions of a wide range of randomized clinical data, relative to the standard DI model. This preferred DD model predicted that, for currently used HNC fractionation regimen, the last 5 fractions did not increase TCP, but simply compensated for increased accelerated repopulation (Fig. 6.3). A hypofractionation scheme of 25 fractions of 2.4 Gy (total dose of 60 Gy in 33 days) was found to be superior over 35 fractions of 2 Gy (total dose of 70 Gy in 47 days), both regarding the probability of tumor control and late normal tissue complications. In a next study, on basis of radiobiological model calculations with the DD model, an optimized hypofractionated treatment scheme for HNC patients was proposed with 18 daily fractions of 3 Gy, i.e., a total dose of 54 Gy in 24 days [10].

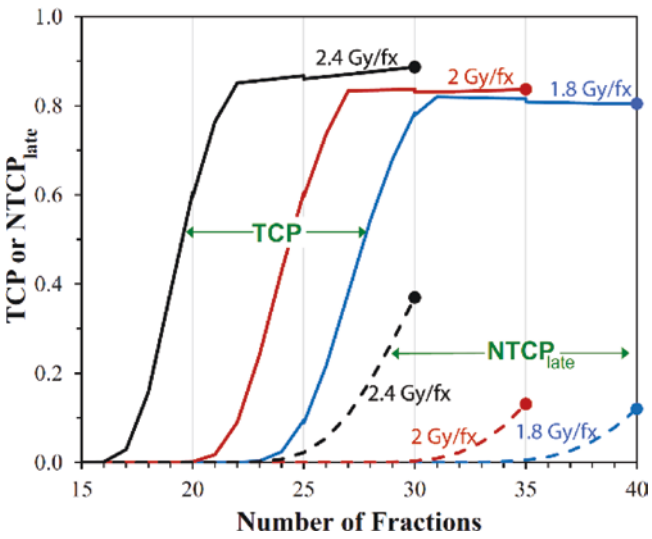

Fig. 6.3 Predicted TCP values by the DD model (solid curves) as a function of the number of fractions delivered, for stage $T_{1/2}$ head and neck cancer (HNC) patients. Dose per fraction (fx): 1.8 Gy (blue), 2.0 Gy (red) or 2.4 Gy (black), administered daily, 5 fx/week. NTCP late predictions for late toxicity (dashed curves) were made with the standard LQ model normalized to a 13.1% value (grade 3–5 late toxicity at 5 years) for 35 × 2 Gy fractions. The solid circles represent current standard treatment regimens. Thus, the final week of 5 fractions could be eliminated without compromising TCP, but resulting in significantly decreased late sequelae due to the lower total dose. (Reproduced with permission from [9])

6.3.4 Hypofractionation and the Immune Response

Radiation has long been thought to suppress the immune system, and total body irradiation is up to date applied for that reason. Studies in the past have demonstrated that local irradiation not only had a direct effect on tumor cells in the treatment volume, but also a systemic effect on the immune system (see Chap. 5). Therewith, local irradiation can induce abscopal effects, i.e., the immunological rejection of tumors or metastatic lesions distant from the irradiated site (see Chap. 5). Different radiation treatment schemes regarding the total dose and fraction size were shown to have diverse effects on the immune response, with a subsequent effect on combination therapy with immune-modulating agents [11]. The abscopal effect might best be exploited using 3–5 fractions of <10 Gy [12]. The immune-editing effects of radiation will probably also benefit from repeated intermediate high fraction sizes [13].

6.3.5 Hypofractionation and Radiosensitizing Agents

Hyperthermia and chemotherapeutic agents, e.g., cisplatin, gemcitabine, temozolomide and targeted drugs such as inhibitors of PARP-1 and EGFR may potentiate the effects of radiation. The LQ model is a very suitable tool to quantify the effects of the combination of irradiation and radiosensitizers, which can be either additive or synergistic. The most commonly used test to study interaction between irradiation and modulating agents is the clonogenic assay (see Chap. 3), being the golden standard test for determination of cell survival. LQ model analysis of the typical shaped cell survival curve allows to separately establish the effect of combination therapy on the ⟨ and ® α/β parameters of the model. The parameter ⟨ α determines the effectiveness at low doses, on the initial slope of the cell survival curve, while the parameter ® β represents the increasing contribution from cumulative damage thought to be due to interaction of two or more separate lesions. Preclinical studies have shown that most radiosensitizing agents cause an increase of the α-parameter, while the β-parameter is rarely affected [14]. With conven-

tional small-sized dose fractions, the value of the α-parameter therefore determines to a large extent the effectiveness of combination treatments. The interaction between chemotherapeutic agents and high-dose irradiation fractions will be minimal. For clinical hypofractionation regimen, it is to be expected that effects of radiosensitizing agents are smaller than when combined with conventional fractionation regimen.

6.3.6 Hypofractionation and Risk for Secondary Cancer

Long-term follow-up studies that address carcinogenic effects of fractionated high-dose RT describe the incidence of secondary malignancies, type of induced cancers, latency time, risk period as well as the shape of the dose–risk relationship curve. The dose–risk curve following curative RT is organ specific and is either linear, plateau, or bell-shaped. Radiobiological—LQ model based—calculations for estimation of the cancer risk following exposure to irradiation showed that both carcinoma and sarcoma risk decreased with increasing fraction size [9]. Via model calculations, it has been estimated that hypofractionated RT has the potential to reduce the second cancer risk [15].

6.4 External Beam Radiotherapy Strategies

6.4.1 Stereotactic Body Radiation Therapy (SBRT)

Box 6.3 Stereotactic Body Radiation Therapy (SBRT)

- The basic principle of SBRT is to deliver a tumoricidal dose to the target in a few fractions and minimize dose to normal tissue using highly conformal radiation.
- The high-dose per fraction used in SBRT can cause vascular damage through endothelial cell apoptosis and stem cell death.
- SBRT is commonly used in treatment of tumors in lung, liver, spine, prostate, and pancreas.

6.4.1.1 Definition

Stereotactic Body Radiation Therapy (SBRT) also known as Stereotactic Ablative Radiotherapy (SABR) refers to stereotactic image-guided delivery of highly conformal radiation to a small extracranial target using high-dose per fraction delivered in 1–5 fractions with a tumor-ablative intent [16]. The key requirements for SBRT are small well-circumscribed tumors (maximum cross-sectional diameter up to 5 cm), stringent patient immobilization, small or no margin for beam penumbra, high conformality and accurate radiation delivery as well as image guidance for geometric verification [17].

6.4.1.2 Radiobiologic Principles of SBRT

The aim of SBRT is to deliver tumoricidal dose to target in a few fractions and minimize dose to normal tissue by delivering highly conformal radiation under image guidance. A high-dose per fraction is more tumoricidal than conventional fractionation dose by its direct damaging action on tumor cells [6]. As discussed in Chap. 5 and earlier in this chapter, the effect on late-responding normal tissues is greater with high-dose per fraction. Few malignancies such as prostate cancer have low α/β values in the range of 1.5–3 Gy and show high sensitivity to fractionation (similar to late-responding normal tissues). In such malignancies, hypofractionation leads to better therapeutic benefit. On the other hand, delivering high-dose per fraction can increase toxicity in acute-responding tissues(see Chap. 5). To minimize this, a highly focused and conformal dose is delivered to the tumor with a steep dose gradient. It is achieved by reducing planned target volume (PTV) margins under image guidance, using multiple non-coplanar beams with careful treatment planning, and by delivering the total dose in two to five fractions (2–3 fractions per week) [7].

As discussed in Chap. 5, the bigger the tumor size the more is the hypoxic component and vice-versa. The advantage of reoxygenation seen during conventional fractionation is compensated in hypofractionated SBRT by selectively treating small tumors, which are relatively well oxygenated with a little hypoxic component. Furthermore, the hypoxic cells in tumors are depopulated by the direct damaging effect of large doses per fraction [6]. The same effect is responsible for overcoming the disadvantage of lack of reassortment of tumor cells to sensitive phases of cell cycle during fractionation. The high-dose per fraction counteracts the differences in radiosensitivity of cells in different phases of cell cycle by causing cell cycle arrest and interphase death in all phases (see Chap. 3).

Unlike conventional fractionation RT, owing to the short overall treatment time, tumor cell repopulation and interfraction repair of sublethal damage do not play a major role during SBRT (see Sect. 6.3). This is beneficial in terms of tumor control but detrimental to normal tissues.

However, when the treatment time of an individual fraction is prolonged for more than half an hour, intrafraction repair of some sublethal damage in rapidly proliferating tumor cells may occur [7]. However, such longer fraction treatment time and faster intrafraction repair result in greater loss of BED [18]. This can be overcome by increasing the dose rate with use of flattening filter free (FFF) beams.

It is postulated that the radiobiologic effect of SBRT also depends on two other mechanisms. One is the vascular damage due to endothelial cell apoptosis caused by high-dose per fraction. It has been reported that this occurs due to the structural abnormalities of tumor vessels that are dilated, tortuous, elongated and have a thin basement membrane [19]. The second mechanism is through radiation-induced immunologic responses. The strong T-cell response triggered after exposure to high-dose per fraction RT enhances cytotoxic effects [12]. In addition, SBRT when combined with immune checkpoint inhibitors, i.e., Programmed Cell Death Protein-1/Programmed Cell Death Ligand-1 (PD-1/PD-L1) targeting antibodies, e.g., pembrolizumab or cytotoxic T-lymphocyte-associated protein-4 (CTLA4) antibodies, e.g., ipilimumab has shown to trigger an immunologic response that produces an abscopal effect [12] as described in Chap. 5.

Conventional fractionation RT is modelled by the LQ model cell survival curve but at higher dose per fraction, it is thought that LQ model overestimates the effects of radiation [20]. Therefore, alternative radiobiological models like universal survival curve (USC) were proposed. Instead of the BED in the LQ model, USC calculates the standard effective dose (SED) which is the total dose administered in 2 Gy per fraction to produce the same effect [21]. There are arguments that the LQ model still holds good till a certain level of dose per fraction.

6.4.1.3 Treatment Planning

The RT treatment planning for SBRT involves various steps allowing proper delivery of SBRT. After appropriate patient selection, VacLoc bags are used for stringent patient immobilization and setup. The next step is to acquire treatment planning images using computed tomography (CT)/magnetic resonance (MR)/^{18}F-fluorodeoxyglucose (^{18}FDG) positron emission tomography (PET) simulator with patient setup in treatment position with immobilization devices [22]. Usually, images are taken in 1–3 mm slice thickness and scan length extends at least 5–10 cm superior and inferior beyond RT treatment field borders for coplanar beams and 15 cm for non-coplanar beams [22]. For tumors in the thorax and upper abdomen, respiration-induced organ and tumor motion may be an issue. Therefore, motion management strategies are utilized while treating these tumors (Table 6.3).

For SBRT, the target volumes and OARs are contoured as per the The International Commission on Radiation Units and Measurements (ICRU) 50 and 62 reports. The RT treatment planning is based on the American Association of Physicists in Medicine Task Group (AAPM TG) 101 recommendations [22]. Unlike uniform dose prescription in conventional RT, in SBRT, dose is prescribed to the low isodoses (e.g., 80% isodose line) with small or no margin for beam penumbra to improve sharp dose falloff outside the target volume, thereby reducing dose to adjacent normal tissues. Hence, dose heterogeneities and hotspots occurring within the target volumes are accepted in SBRT, unlike traditional RT where homogeneous dose distribution is desired. For obtaining an optimal SBRT treatment plan with better target dose conformality as well as isotropic dose gradient, multiple planar or non-coplanar treatment beams are used, and treatment is delivered using multileaf collimator (MLC) of width 5 mm or less [24]. The calculation grid size used in the

Table 6.3 Motion management methods in radiotherapy. Adapted from [23]

Motion management method	Rationale
Free breathing technique • Based on 4D CT	Generating of internal target volume (ITV) which covers the full range of tumor motion
Motion dampening techniques • Abdominal compression using paddle, pneumatic belts, etc. • Breath holding technique such as deep inspiratory breath hold (DIBH), active breath coordinator (ABC)	Limiting the diaphragm expansion and tumor motion by devices or by controlling breathing
Respiratory gating technique • Internal gating using internal surrogates for tumor motion • External gating using external devices to monitor respiration, a surrogate for tumor motion [such as real-time position management (RPM) system]	Treating the tumor only in discrete phases of respiratory cycle
Real-time tumor tracking • ExacTrac (Kilo-Voltage image-based system) • Cyberknife (Kilo-Voltage image-based robotic system) • Calypso (radiofrequency localization system)	Intrafraction tumor localization and repositioning of treatment beam toward the target

treatment planning system (TPS) affects the accuracy of calculated dose distribution. Hence, an isotropic grid size of 2 mm or finer is recommended.

The normal tissue tolerances derived from conventional fractionation studies do not apply to the high fractional doses delivered in SBRT. Therefore, bioeffect measures such as BED, normalized total dose (NTD), and equivalent uniform dose (EUD) are calculated to evaluate the effectiveness and safety of SBRT dose distributions [18, 25, 26]. BED and NTD are used to determine the biologic effectiveness of different dose fractionation schedules, whereas EUD is applied to rank different treatment plans based on their expected tumor effect [22]. The normal tissue tolerances for different SBRT fractionation schemes are still evolving. Apart from the traditional metrics reported in a RT treatment plan, SBRT plans must specify conformity index (CI = prescription isodose volume/PTV), heterogeneity index (HI = highest dose received by 5% of PTV/lowest dose received by 95% of PTV), and intermediate dose spillage (D50% = volume of 50% of prescription isodose curve/PTV or D2 cm = maximum dose at 2 cm from PTV) [22].

Recent advances in RT techniques and machines facilitate delivery of SBRT. Volumetric modulated arc therapy (VMAT) is an advanced RT technique that delivers radiation dose continuously in arcs where gantry rotation speed, treatment aperture, and dose rate vary simultaneously [27]. The newer linear accelerators (LINAC) capable of delivering flattening filter free (FFF) beams increases dose rate from 300 to 600 monitor units (MU)/min to 1200 to 2400 MU/min. Thereby, the time required to deliver the large number of MUs needed for high-dose per fraction in SBRT is decreased [28]. The FFF beams also have other advantages such as less off-axis beam hardening, less photon head scatter, less field size dependence, and less leakage outside beam collimators [29].

6.4.1.4 Clinical Applications

The clinical application of SBRT gained much interest over the past two decades. SBRT is commonly used in treatment of malignant tumors in lung, liver, pancreas, prostate, kidney, and spine (Table 6.4). It is also widely recommended for treating oligometastatic disease that has spread to liver, lung, bone, adrenals, or lymph nodes. Its clinical utility in breast cancer as well as head and neck cancers is being investigated. The common cancer subsites and clinical scenarios where SBRT has a role are summarized in Table 6.4.

Numerous phase 1/2 clinical trials have shown encouraging results regarding safety and efficacy of SBRT in different types and stages of cancer [31]. However, the major drawbacks of these trials are the adoption of variable radiation dose, fractionation schemes, and limited number of treated patients. Therefore, randomized phase 3 trial results on clinical outcomes and long-term toxicities are needed to recommend SBRT as the standard of care.

Table 6.4 Clinical application of SBRT at various cancer subsites. (Adapted from [30])

Cancer subsite	Indications
Lung	• Early-stage inoperable non-small cell lung cancer (NSCLC)—T1, T2, usually <5 cm, N0
	• Boost following definitive chemoradiation for locally advanced NSCLC
	• Recurrence/re-irradiation
	• Oligometastatic disease
Liver	• Hepatocellular carcinoma (HCC)—unresectable/medically inoperable patients, unsuitable/refractory to radiofrequency ablation, or transarterial chemoembolization
	• Oligometastatic disease
	• Portal vein tumor thrombosis (PVTT)
Pancreas	• Locally advanced unresectable disease—radical SBRT/SBRT boost following conventional fractionated RT
	• Borderline resectable disease—poor performance status
	• Re-irradiation
Prostate	• Low risk—SBRT monotherapy
	• Low volume intermediate risk—SBRT monotherapy/boost
	• High/very high/node positive disease—SBRT boost
	• Residual disease after RT—salvage/re-irradiation
Spine metastases	• Primary spinal cord neoplasms: medically inoperable/adjuvant/salvage SBRT
	• Spine metastases: limited disease, life expectancy more than 3 months, medically inoperable
	• Re-irradiation
Kidney	• Unilateral, medically inoperable disease
	• Bilateral/recurrent contralateral disease
Head and neck	• Re-irradiation: single, small volume recurrence, node negative
	• SBRT boost following definitive chemoradiation in locally advanced nasopharyngeal cancer
	• Palliation

6.4.2 FLASH Radiotherapy at Ultra-High Dose Rate

6.4.2.1 Principles

FLASH RT is emerging as a new tool for sparing normal tissue from ablative doses, as it is able to protect normal tissue while maintaining antitumor ablation [32]. FLASH RT targets tumors with ultra-high dose rates (>100 Gy/s) to reduce the administration time from minutes to less than 200 ms, as this is key to sparing normal tissue [32]. The biological mechanism behind the sparing of normal tissue, known as the "FLASH effect," is based on the following hypothesis:

The oxygen depletion hypothesis describes the rapid consumption of local oxygen by ultra-high dose rates resulting in transient radioprotection and transient local tissue hypoxia. It is known that hypoxic tissue is more radioresistant because the low concentration of molecular oxygen during radiation-induced DNA damage allows DNA repair, while in the presence of molecular oxygen, the DNA lesion binds to molecular oxygen and produces peroxyl radicals leading to the degradation of nucleic acids and lipids [32]. Therefore the oxygen depletion hypothesis suggests that FLASH RT may be able to prevent or reduce Reactive Oxygen Species (ROS)-mediated cellular damage [33]. However, this hypothesis has recently been challenged as studies showed that FLASH RT does not significantly decrease tissue oxygen concentration compared with conventional RT when measured with a solid optical sensor [34]. The differential ROS-damage recovery hypothesis describes that normal and tumor cells have different capabilities to "detoxify" themselves from ROS [32]. According to this hypothesis, normal cells have a greater capacity to eliminate peroxidized compounds compared to tumors. This would explain why tumors exposed to FLASH RT respond equally under either physiologic or hypoxic conditions.

6.4.2.2 Main Indications

Preclinical studies of FLASH RT confirmed its efficacy in various animal models (mice, pigs, cats, zebrafish) as well as in different tissues (lung, brain, intestine, skin) and led to the first use of FLASH RT in the clinic. One example is a man that had a cutaneous lymphoma that had spread over the entire surface of his skin. He had already received several sessions of conventional RT and the skin's tolerance was exhausted. FLASH RT was indicated as a way to spare the skin while achieving equivalent tumor control to conventional RT. The lesion received 15 Gy as a single dose in 90 ms. The treatment was successful, with no skin toxicity and complete ablation of the tumor as reported 6 months after treatment [33] (Fig. 6.4).

Apart from this successful case, the current use of FLASH RT in the clinic is limited to enrolling participants in clinical trials. However, in the near future patients with tumors in organs described as late-responding tissues would be good candidates for FLASH RT, as preclinical studies have shown that ultra-high dose rates dramatically reduce the incidence of pulmonary fibrosis and neurocognitive impairment. Patients with painful bone metastases in the extremities would also be good candidates to investigate the feasibility and safety of FLASH RT.

Fig. 6.4 Temporal evolution of the treated lesion: (**a**) before treatment with the limits of the PTV delineated in black; (**b**) at 3 weeks, at the peak of the skin reaction (grade 1 epithelitis NCI-CTCAE v 5.0); (**c**) at 5 months. (Reproduced with permission from [33])

6.4.2.3 Treatment Course

Before starting treatment with FLASH RT, one needs to be aware of the importance of the radiation source, the quality of the radiation, and the physical parameters of the beam.

- Radiation sources are currently standardized to deliver dose rates of about 0.1–0.4 Gy/s in 2 Gy daily fractions. FLASH RT, on the other hand, relies on facilities capable of delivering ultra-high dose rates in large doses in one or more pulses over microseconds. This capability has only been achieved in a few places by modifying clinical devices to deliver photons, protons, or electrons. There are large irradiation facilities such as the European Synchrotron that can deliver X-rays at dose rates of up to 16,000 Gy/s [35]. However, clinical trials using synchrotrons are not yet an option.
- The quality of the radiation must also be considered, as most research on FLASH RT has been done with electrons. FLASH RT with electrons has been shown to be effective in at least one human patient, while FLASH RT with photons and protons is still in the preclinical phase. Regardless of preclinical or clinical status, the quality of radiation needs to be considered to account for (1) the impact of the linear energy transfer on the mechanisms behind the FLASH effect and (2) the use of a continuous beam in the case of protons versus a pulsed beam in the case of electrons and synchrotron X-rays [32].
- The physical parameters of FLASH RT need to be defined much more precisely than in conventional RT. A team of experts from Switzerland has suggested that the number of pulses, the instantaneous intra-pulse dose rate (≥104 Gy/s), and the total exposure time (<100 ms) should be included in all studies of FLASH RT [33, 35]. These parameters mostly derive from FLASH RT with electrons and therefore should be carefully applied to FLASH RT with photons or protons.

In summary, FLASH RT is not yet actively used in the clinic. However, it is now clear that FLASH RT requires very precise management of the radiation quality and beam.

6.4.2.4 Therapeutic Intent

The patient population that would benefit from clinical trials with FLASH RT are those who still have radioresistant tumors for which even the most sophisticated intensity-modulated RT has not been successful. In this context, FLASH RT could be combined with immunotherapy to achieve a synergistic effect. This strategy is supported by the immune hypothesis, which builds on the oxygen depletion hypothesis by proposing that FLASH RT protects circulating and resident immune cells that are normally radiosensitive. This radiosensitivity is particularly important when radiation fields affect bone marrow and/or circulating blood cells [36], as doses as low as 0.5 Gy can reduce lymphocyte survival by 90% [37]. Therefore, FLASH RT has the potential to spare immune cells from the radiation dose and allow recognition of tumor antigens to potentially trigger an antitumor immune response [33].

6.4.3 Boron Neutron Capture Therapy (BNCT)

Box 6.4 Boron Neutron Capture Therapy (BNCT)

- The basic principle of BNCT is selective targeting of tumor cells while sparing normal tissues using boron-carrier agents and low-energy neutrons.
- Three boron-delivery agents approved for human clinical trials are sodium borocaptate (BSH), boronophenylalanine (BPA), and sodium decaborane (GB-10).
- The clinical trials on BNCT were conducted predominantly in brain malignancies, malignant melanoma, and recurrent head and neck cancers.

6.4.3.1 Principles

The basic principle of BNCT is to deliver a boron-containing drug that selectively attaches to cancer cells and has a large cross-section capable of capturing a low-energy neutron. After administration of the boron-containing compound, the patient is exposed to a beam of thermal or epithermal neutrons. The compound goes into an excited state after neutron capture and undergoes a nuclear fission reaction to produce densely ionizing alpha particles. The range of these high LET particles in tissues is limited around 7.6 μm on an average (range 5–9 μm) [38, 39]. Therefore, these particles lead to localized release of a substantial amount of energy within the tumor, sparing the normal tissues. The boron neutron chemical reaction is as follows:

$$^{10}B_5 + {}^{1}n_0 \rightarrow {}^{11}B_6 \rightarrow {}^{7}Li_3 + {}^{4}He_2 + \text{gamma ray} + 2.4\,\text{MeV} \quad (6.2)$$

A photon of 0.48 MeV is released in most of the fission events which is useful for monitoring the reaction and has little significance in terms of cell killing [40]. Similarly, the radiobiologic effect of the low-energy thermal neutrons themselves is little.

6.4.3.2 Boron Compounds

The success of BNCT largely depends on the properties of the boron compound used. An ideal boron compound should be non-toxic, have a high absolute boron concentration in tumors, have high specificity for malignant cells, and accumulate in low concentrations in adjacent normal tissues and blood [40]. To summarize, an ideal boron-carrier compound should have a high tumor-to-normal tissue ratio (around 3–4:1) [41].

Based on the molecular weight, there are two classes of boron compounds such as low-molecular weight (LMW) agents and high-molecular weight (HMW) agents. The LMW agents can cross the cell membrane and retain inside the cell. Examples are sodium borocaptate and boronophenylalanine. HMW agents are boron-containing monoclonal antibodies, bispecific antibodies, liposomes, nanoparticles, or conjugates of epidermal growth factor. They are highly specific to tumors but cannot cross the blood–brain barrier in adequate concentration to be of some utility clinically. However, they can be used only when blood–brain barrier is disrupted, or when delivered directly intracerebrally [41].

The boron-carrier agents that are approved for human clinical trials are sodium mercaptoundecahydro-closo-dodecaborate ($Na_2B_{12}H_{11}SH$) also known as sodium borocaptate (BSH), (L)-4-dihdroxy-borylphenyalanine also known as boronophenylalanine (BPA) and sodium decaborane (GB-10) [42]. Among the three, only BPA has a relatively higher tumor-specific uptake. It gets concentrated in cells synthesizing melanin. BPA is capable of taking up ^{18}F, therefore ^{18}F incorporated BPA positron emission tomography (PET) imaging is done to assess the boron concentration in tumor cells [43].

6.4.3.3 Source of Neutrons

The low-energy neutrons used in BNCT are produced from nuclear reactors through nuclear fission reactions and are either thermal neutrons or epithermal neutrons (Table 6.5).

Thermal neutrons have the same average kinetic energy as gas molecules in the environment, which is little. Whereas epithermal neutrons are intermediate energy range neutrons formed during the transition of energetic neutrons to slow/thermal neutrons [44]. If a tumor at a depth of more than few centimeters is to be treated effectively with BNCT using thermal neutrons, then the normal tissues at the surface will be irradiated with a very high dose. Whereas with epithermal neutrons, the very high surface dose can be avoided

Table 6.5 Neutrons used in BNCT and their characteristics. (Adapted from [41])

Type of neutrons	Energy (eV)	Characteristics
Thermal/slow neutrons	0.025	1. Attenuates rapidly in tissues 2. Half value layer is about 1.5 cm 3. Reacts with boron to produce high-LET particles
Epithermal	1–10,000	1. Peak dose at about 2–3 cm 2. Rapid falloff beyond peak dose 3. Do not react with boron but degrades to thermal neutrons by collisions with hydrogen atoms in tissues

[41]. But the depth dose distribution with both the types of neutrons is poor. In addition, the low-energy neutrons produced in nuclear reactors are contaminated with gamma rays and fast neutrons, both of which have different radiobiologic properties. Apart from this, there are capture reactions taking place with the naturally occurring isotopes in tissues such as ^{1}H, ^{12}C, ^{14}Ni, ^{16}O, ^{35}Cl, etc. These contaminants cause biologic damage even in normal tissues without ^{10}B concentration.

6.4.3.4 Treatment Planning

The dose in the radiation field is expressed as RBE-weighted dose, Gy_w. A weighted dose is used to take into consideration the radiobiological effects of alpha particles, gamma rays, fast neutrons and capture reactions occurring with the use of nuclear reactor-generated neutron beams. The weighting factor depends on the boron-delivery agent used, which determines the concentration of ^{10}B in cells and which in turn dictate the effectiveness of BNCT [42, 45]. Boron levels in a patient's blood can be measured but the concentration in tumor cells and adjacent normal tissues are based on earlier experimental studies [42]. Therefore, different weighting factors are used for tumor cells and normal tissues in the region of interest.

The Monte Carlo method is utilized for RT dose calculation. Unlike conventional dose planning algorithms, the Monte Carlo method takes into consideration the influence of inhomogeneities on dose delivered by primary radiation as well as scattered radiation [46]. This makes it appropriate from the BNCT standpoint where the dose contribution is from different by-products of nuclear fission reactions and contaminants in low-energy neutron beams from nuclear reactors. RT is delivered in single fraction or multiple fractions using oppositional or multiple fields.

6.4.3.5 Clinical Applications

The early human clinical trials carried out in Brookhaven National Laboratory and Japan did not show encouraging results with BNCT. It was widely tried out for treating

central nervous system (CNS) malignancies. In these trials, ^{10}B-enriched boric acid derivatives were used as boron-delivery agents, which showed high blood-to-tumor ^{10}B concentration leading to endothelial damage in blood vessels but with no therapeutic benefit [47]. In the Japanese trials, BSH was used as a boron-carrier agent [48]. Though BSH achieved better tumor-to-blood concentration compared to previous boron-carrier agents used, it was however excluded by normal blood–brain barrier, and the ^{10}B concentration in brain tumors was suboptimal [49, 50]. In addition, the thermal neutrons used in these trials were poorly penetrating. Therefore, open craniotomy and general anesthesia during the entire treatment time (about 4–8 h) were needed to deliver BNCT [50]. The shortcomings of earlier studies were rectified in the modern clinical trials. In majority of the subsequent trials, high energy epithermal neutron beam was used instead of thermal neutron beam. Thereby, avoiding the need for open craniotomy. Instead of previous boron-carrier agents, newer agents such as BPA were used, either alone or in combination with BSH.

The recent trials have aimed to find the optimal radiation fractionation, radiation fields, radiation dose, normal tissue tolerance, and pharmacokinetics of boron-carrier agents used in BNCT for treatment of different cancer subsites. In the twenty-first century, there were clinical studies experimenting and expanding the role of BNCT in other cancer subsites such as recurrent head and neck cancers as summarized in Appendix. However, there are no randomized controlled clinical trials on BNCT reported so far.

6.4.3.6 Limitations and Future Directions

There are few limitations that hamper the widespread use of BNCT in cancer treatment. The main shortcoming is the lack of ^{10}B carrier agents capable of achieving high tumor specificity and boron concentration. Secondly, the poor penetration of thermal neutrons into tissues. Thirdly, usage of nuclear reactors as the source of thermal neutrons for BNCT. The problems with nuclear reactors are that the low energy-neutron beams produced from them are contaminated with gamma rays and fast neutrons, which can cause damage to normal tissues even without boron concentration. Additionally, there is a shortage of nuclear reactors capable of delivering BNCT with a treatment delivery and monitoring room and they are also often located far away from population center. Fourthly, the interaction of low-energy neutrons with normal tissues results in capture reactions that cause biological damage.

Currently, active translational and clinical research focused on overcoming the above hurdles are being conducted. Newer boron-carrier agents based on purines, pyrimidines, thymidines, nucleotides, nucleosides, peptides, and porphyrin derivatives are being designed [39, 51, 52]. To avoid the hindrances associated with nuclear reactor-based treatment, alternative sources of neutrons such as radioactive decay of californium-252 (^{252}Cf) and particle accelerators are being investigated. ^{252}Cf is not available in the required amount to be utilized for BNCT [40]. On the other hand, particle accelerator-based treatment appears to be a promising alternative and would make hospital-based delivery BNCT feasible. However, the applicability of results from previous clinical trials conducted in reactor-based treatment centers to a larger population to be treated in particle accelerator-based treatment centers in future is questionable and warrants further studies [50].

6.5 Radiotherapy Combined with Other Cancer Treatment Modalities

Combining RT with other oncological treatments is central for clinical management of tumors. A key approach is to combine RT with other pharmaceutical treatments. Given that RT has an effect on diverse cellular signaling networks, there are a number ways to combine it with agents and/or regiments that affect such processes, e.g., chemotherapy, targeted therapy, immunotherapy, hyperthermia, hormonal therapy, short-term starvation, etc. (Fig. 6.5).

6.5.1 RT Combined with Chemotherapy

RT is often combined with chemotherapy in a diverse set of tumor types to increase locoregional control as well as to combat metastatic growth [53]. These combined regiments have emerged as a result of exploring chemotherapeutic agents that presented some single drug activity in a certain cancer malignancies for additive or synergistic effect when combined with RT at doses and time frames that had acceptable toxicity [54].

Combined chemotherapy and RT might refer to sequential association or to concomitant association. Chemotherapy may sensitize for RT by influencing one or several cellular effects including chromosome or DNA damage and subsequent repair, effect on cell cycle progression allowing cells to be accumulating in a RT sensitive phase, impact on different cell death routes including apoptosis, mitotic catastrophe as well as on autophagy. Moreover, in the tissue such combination may also impact on the hypoxic tumor environment/reoxygenation status. In a clinical setting it is most likely that a key benefit is the inhibition of tumor cell proliferation by drugs during the radiation interfraction interval [54].

The combined use of chemotherapy with RT has typically translated into a significant benefit in overall survival in sites where RT plays a substantial role.

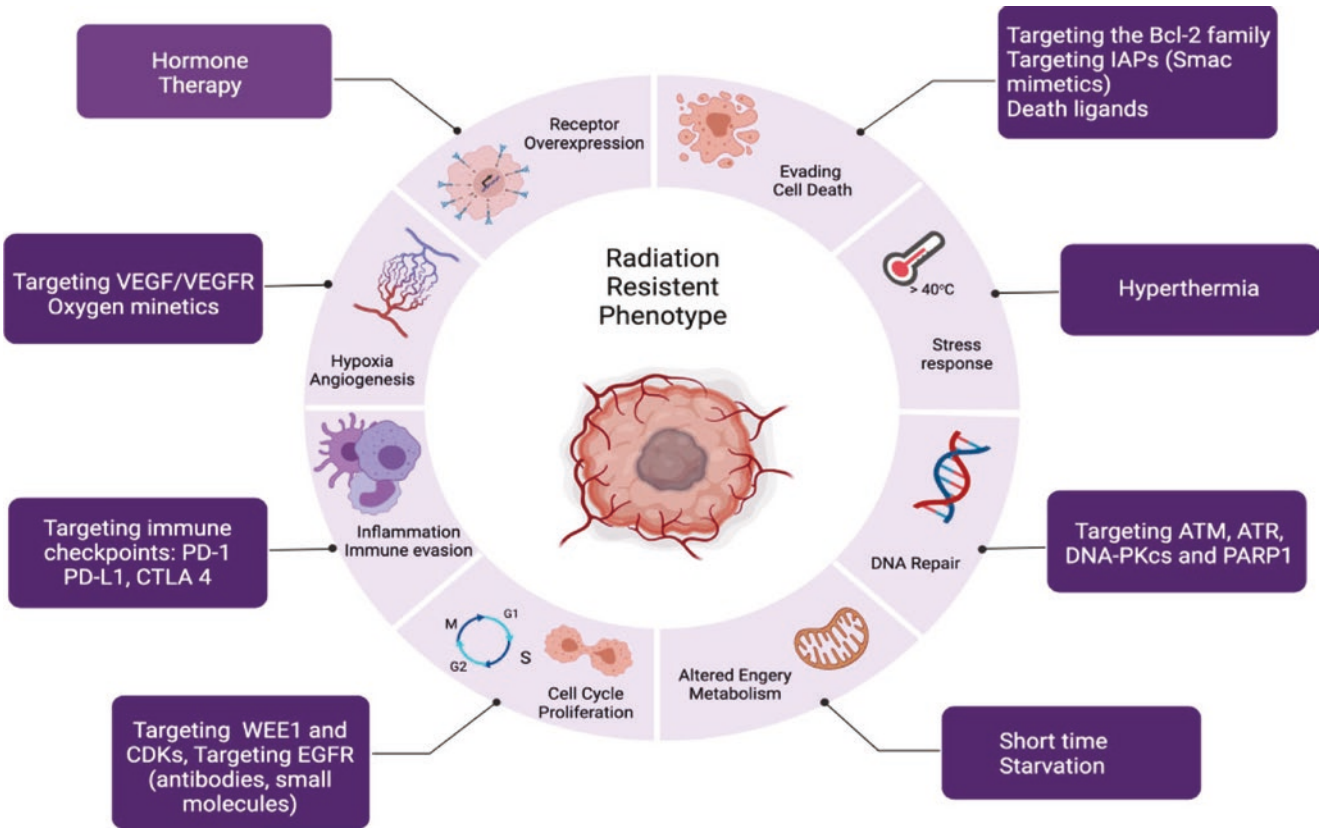

Fig. 6.5 Overview of radiotherapy combinations influencing different hallmarks of cancer

Concurrent RT and chemotherapy yielded an almost 10% higher survival rate relative to RT alone. Unfortunately, the complication rates of combined regimens are also higher than those of RT only [54].

Concomitant administration of chemotherapy and radiation gives increased early normal tissue toxicity due to inhibition of stem cell or precursor-cell proliferation. Late normal tissue damage is likely to be enhanced through inhibition of DNA repair, and by specific mechanisms of drug toxicity in sensitive tissues [55].

Several randomized trials with concomitant chemoradiotherapy have been conducted in most cancer types showing a significant increase in locoregional control in many disease sites with a consequent improvement in patient survival. Meta-analyses of available data of randomized trials in head and neck cancer (HNC) undertaken a few years ago showed that despite a high initial response rate, multi-agent chemotherapy given before radiation treatment (i.e. in a neoadjuvant setting) has a small impact on the locoregional control and survival rates [54]. Numerous single institutions and cooperative groups have investigated the use of concurrent RT and chemotherapy in the management of patients with localized esophageal and gastric cancer, either as definitive or adjuvant therapy. A significant body of information suggests that chemotherapeutic agents such as 5-fluorouracil, capecitabine, cisplatin, oxaliplatin, carboplatin, mitomycin C, gemcitabine, irinotecan, docetaxel, and paclitaxel have a greater additive effect when used in combination with RT [54].

In all the reported studies, the therapeutic ratio (defined as the advantage in efficacy over the disadvantage in toxicity) was, however, less clearly assessed and/or reported. In general, an increase in early toxicity was observed in all the trials. For late toxicity, systematic reporting of data is lacking, but the few available reports also indicate an increase in late radiation effects.

A drug may sensitize the radiation or may kill cells by independent means. Alternatively, a drug may inhibit cellular repopulation or act as a cytoprotector. Limited studies have presented drug mechanisms mathematically in order to estimate the equivalent radiation effect of a drug. In fact if cytotoxic drug effects could be expressed in terms of equivalent biologically effective dose of radiation, then relative contributions of radiation and chemotherapy in combined treatments could be assessed and consequently optimum schedules could be designed [54].

An ideal global model of tumor control in an attempt to simulate clinical reality would incorporate the effects of radiation dose, fractionation, hypoxia, blood flow, and concomitant drug therapy [55].

Chemotherapy combined with RT improves the therapeutic ratio by the following mechanisms:

1. Spatial cooperation—consists of administering the chemotherapeutic agent and RT separately in different anatomical sites.
2. Toxicity independence—both treatments have different side effects, the treatment with the combination modality is less toxic.
3. Normal tissue protection—chemotherapy drugs with a protective effect against normal tissue allow a higher dose of radiation to be administered.
4. Radiosensitivity—is a mechanism that leads chemotherapeutic agents to enhance the cytotoxic effects of RT treatment. Increased damage from radiation, inhibition of repair processes, interferance with the cell cycle progression through different phases, exerting greater activity against hypoxic cells, and helping to improve RT are some mechanisms of radiosensitivity that can influence these treatments.

Combination of chemotherapy with RT can be in three ways, with a sequential treatment where RT is followed by chemotherapy or chemotherapy is followed by RT. These treatments can reduce large tumor mass with a first modality and with the second one can increase the effectiveness, and thus control the disease. In concurrent treatment, chemotherapy and RT are given together. RT can be given daily, while chemotherapy could be given once a week or every 3–4 weeks. Finally, alternative treatment would be based on giving chemotherapy and RT on alternately weeks, such as every 1–3 weeks, with no concurrent treatments. This last option would reduce side effects and also allow full administration of the dose for each modality.

Molecular mechanisms of interaction between combination therapies [53]:

1. Enhance DNA/chromosome damage and repair

   Little is known about the capacity of chemotherapeutic agents to increase the efficiency with which IR induces DNA damage. Several commonly used chemotherapy agents have been shown to inhibit the repair of radiation damage (i.e., DNA and/or chromosome damage). Some of these drugs inhibit the repair processes by interfering with the enzymatic machinery involved in the restoration of the DNA/chromosome integrity.
2. Cell cycle synchronization

   Many of the chemotherapeutic agents inhibit cell division, that is, they exert their action on proliferating cells.

   Due to this cell cycle selective cytotoxicity by the cell cycle phase after the action of chemotherapeutic drugs, the remaining surviving cells will synchronize.

   If RT is given when cells are synchronized in the most radiosensitive phase of the cell cycle, then the effect of radiation is enhanced.
3. Enhanced apoptosis

   Apoptosis is a mechanism of cell death induced by chemotherapeutic agents. These can trigger one or more pathways of apoptosis. To ensure a robust apoptotic response, chemotherapeutics must be incorporated into DNA. The combination of these therapies, where RT is very effective in inducing DNA single strand breaks (SSBs) or double strand breaks (DSBs), could facilitate the incorporation of these agents into DNA and thus induce an enhanced apoptotic reaction.
4. Reoxygenation

   Hypoxia is associated with a worse response to RT treatment, and the reason is the inadequate diffusion of oxygen in the tumor mass due to insufficient tumor vascularization.

   If we combine the treatments, chemoRT, chemotherapy induces a certain degree of shrinkage in the tumor that facilitates the diffusion of oxygen in a more uniform way, increasing tumor oxygenation and therefore tumor radiosensitivity.
5. Inhibition of cell proliferation

   A mechanism of interaction between both treatments combined is the possible inhibition of cell proliferation, a mechanism that occurs during dose fractionation in RT. The exact timing and schedule between the chemotherapy and RT must be taken into account, since it would be best to administer the drug toward the end of radiation treatment because that is when tumor cell repopulation has been activated.

6.5.1.1 Side Effects of Combined Chemotherapy and Radiation Therapy

The combination of these treatments can increase both acute and late toxicity. ChemoRT as two cytotoxic treatments produces an increase in damage in the volume of damaged normal cells, being more evident during the concurrent chemoRT. By combining these therapies, if these side effects appear, you may require to reduce the dose of chemotherapy.

Side effects from combining chemotherapy with RT can be increased fatigue, lowering of blood counts, cardiac dysfunction, cognitive dysfunction, and second malignancies.

Some aspects to consider to reduce toxicity when combining both treatments are:

- If we optimize the schedule and sequence of the combined treatments, we can reduce toxicity.
- With an adequate selection of patients, we can avoid these side effects in patients with a poor performance status or patients with comorbidities.

Table 6.6 Chemotherapeutic agents used in combination with radiotherapy in different tumor types and associated side effects

Tumor type	Treatment	Side effects
Brain tumors	Carmustine	Myelosuppression
	Temozolomide	Neutropenia, anemia, thrombocytopenia, constipation
Head and neck cancer	Cisplatin	Nephrotoxicity, ototoxicity, nausea, vomiting, neurotoxicity/neuropathy
	Docetaxel	Myelosuppression
	Fluorouracil	Myelosuppression, gastrointestinal (GI) effects, mucositis, oral ulcers, diarrhea
Breast cancer	Cyclophosphamide	Hemorrhagic cystitis, myelosuppression, nausea, vomiting
	Docetaxel	Myelosuppression
	Doxorubicin	Cardiotoxicity (including recall effect)
	Methotrexate	Stomatitis, leucopenia and nausea
Lung cancer	Carboplatin	Nephrotoxicity, ototoxicity, nausea, vomiting, neurotoxicity
	Docetaxel	Myelosuppression
	Etoposide	Myelosuppression
Gastrointestinal cancer	Fluorouracil	Myelosuppression and mucositis
	Gemcitabine	Anemia, thrombocytopenia, nausea/vomiting
	Oxaliplatin	Nephrotoxicity, ototoxicity, nausea, vomiting and neurotoxicity
	Irinotecan	Diarrhea, immunosuppression
	Mitomycin C	Bone marrow damage, lung fibrosis, renal damage
Lymphoma	Bleomycin	Lung fibrosis
	DTIC (dacarbazine)	Loss of appetite, vomiting, low white blood cell or platelets count
	Doxorubicin	Cardiotoxicity
	Vinblastine	Peripheral neuropathy, bone marrow suppression
	Vincristine	Hair loss, constipation, difficulty walking, headaches, neuropathic pain, lung damage, or low white blood cell counts

- Using a genetic and molecular analysis of the tumor, we can avoid chemotherapy for patients with lower scores, avoiding chemotherapy toxicity.
- In patients with p16 oropharyngeal cancer, it has been possible to reduce the dose of RT and thus reduce toxicities.
- Advances in imaging techniques, such as IMRT and IGRT, have led to a decrease in the dose around normal tissues, resulting in minimizing the risk of complications from chemoRT.
- Finally, supportive care that involves adequate nutrition, adequate hydration, managing nausea, pain, and depression are essential to mitigate side effects when both therapies are combined (Table 6.6).

The incorporation of targeted therapies into treatment regimens helps to improve radiosensitization. Multimodal therapy uses these agents on a concurrent schedule [53].

Multimodal management for optimum cancer treatment with surgery, chemotherapy, and RT is one of the most significant advances in cancer treatment in the last 25 years. This combined therapy increases locoregional control and patient survival, as well as reduces the side effects of treatment, toxicities [53].

It is difficult to know the real underlying mechanisms of the interaction of this combination therapy of chemotherapy and RT, normally the clinical trials that are carried out do not allow to obtain this information [56] (Box 6.5).

Box 6.5 RT Combined with Chemotherapy

- RT and chemotherapy can, when combined, improve locoregional disease control.
- Concomitant administration of RT with chemotherapy gives increased early normal tissue toxicity but late toxicity of normal tissues may also be increased.

6.5.2 Combining RT with Targeted Therapy

Radiation-induced signaling is multifaceted, and these cellular events are affected by different growth factor signaling cascades controlled by oncogenic drivers and activated kinases in the tumors [57]. These radiation-induced signaling events as well as the tumor microenvironment interplay have been explored for RT sensitization purposes (Fig. 6.5).

Some of the RT sensitizing approaches based on targeting oncogenic drivers, DNA damage and repair, chromatin remodeling, cell cycle progression, cell death regulation and angiogenesis/hypoxia are shown in Table 6.7.

Table 6.7 RT sensitizing strategies and examples of drugs that are in clinical evaluation in combination with RT or in combined RT and chemotherapy regimen

Type of mechanism	Target or target mechanism	Example inhibitors	RT sensitized tumor	Reference or clinical trial No.[a]
DNA damage and repair	ATM	AZD1390	Glioblastoma, other brain tumors	NCT03423628
	ATR	BAY-1895344; M6620	Advanced solid tumor, esophageal cancers	[58] NCT03641547
	DNA-PKcs	Nedisertib, peposertib, AZD7648	Head and neck cancer, advanced solid tumors	[59] NCT03907969
	PARP	Olaparib, veliparib, rucaparib, niraparib	Breast cancer, prostate cancer, non-small cell lung cancer, small-cell lung cancer, glioblastoma/glioma, rectal cancer, cervical cancer, head and neck cancer	[60] NCT03542175; NCT04837209; NCT01477489; NCT02227082; NCT03945721; NCT03598257; NCT03109080; NCT03212742; NCT03581292; NCT01514201; NCT04790955; NCT04728230; NCT02412371; NCT01589419; NCT03644342; NCT02229656
Chromatin remodeling	Histone deacetylase (HDAC)	Vorinostat	Head and neck cancer	[61]
Cell cycle progression	WEE1	Adavosertib	Pancreatic cancer	[62]
	CDK 4/6	Palbociclib, ribociclib, abemaciclib	Glioma, breast cancer, head and neck cancer, meningiomas	[63] NCT03691493; NCT03870919; NCT04563507; NCT03024489; NCT03389477; NCT03355794; NCT02607124; NCT04585724; NCT04298983; NCT04923542; NCT04220892; NCT02523014
Cell death regulation	Bcl-2	AT-101 (Gossypol)	Head and neck cancer Brain tumors	[64] NCT00390403
	CD95/FAS ligand	Asunercept (APG101)	Glioblastoma	[65]
	SMAC mimetics	Xevinapant (Debio 1143)	Advanced head and neck cancer	[66]
Oncogenic drivers	EGFR	Erlotinib/ gefitinib/ osimertinib cetuximab	Non-small cell lung cancer, head and neck cancer	[67, 68]
	STAT3	Dovitinib	Hepatocellular carcinoma	[69]
Angiogenesis	VEGF, VEGFR2	Bevacizumab, vandetanib (Caprelsa)	Glioblastoma, esophagogastric cancer	[70, 71]
Hypoxia	Oxygen mimetic	Nimorazole	Head and neck cancer	[72]

[a]The trial number refers to its citation on https://clinicaltrials.gov/

6.5.2.1 Attacking DNA Damage Signaling and Repair for Radiation Therapy Sensitization

Three principal DNA damage response (DDR) kinases, the phosphatidylinositol-3-kinase-related kinases (PIKKs), ataxia-telangiectasia mutated (ATM), ATM- and Rad3-related (ATR), and the non-homologous end joining (NHEJ) component, DNA-dependent protein kinase, catalytic subunit (DNA-PKcs) are central in RT responses (see Chap. 3). These kinases execute their cellular action by phosphorylating targets that regulate DNA repair, e.g., histone H2AX, or cell cycle progression, e.g., WEE-1 and cell cycle checkpoint kinases (CHKs).

Multiple trials of ATR inhibitors are ongoing as single agents or combined with chemotherapy, yet fewer attempts have been made with ATR inhibitors and RT [60]. The ATR inhibitors BAY-1895344 and M6620 (see clinicaltrial.gov; NCT03641547) were tested in phase I trials in various solid tumors in an advanced stage setting including esophageal cancer [58]. As the kinase pocket of ATM is similar to other PIKKs, early attempts to develop specific inhibitors were unsuccessful [60]. However, the ATM inhibitor AZD1390 is currently undergoing trials in conjunction with RT in glioblastoma patients (NCT03423628). Attempts have also been made to target DNA-PKcs, a key component of the NHEJ repair cascade (see Chap. 3) [60]. Thus, AZD7648 has been demonstrated to enhance RT effect when combined with the

poly (ADP-ribose) polymerase (PARP) inhibitor olaparib in both tumor cell lines *in vitro* as well as in tumor-bearing mice. This DNA-PKcs inhibitor is at present tested further in a phase I clinical trial (NCT03907969). Moreover, other DNA-PKcs inhibitors are similarly evaluated when combined with RT in phase I trials involving patients with, e.g., head and neck (HNC) cancer where a clear improved local control was found.

Another class of DNA repair inhibitors is those targeting the PARP-1 repair enzyme [58, 60]. It has been demonstrated that in tumor cells which had mutations in certain DDR genes, e.g., BRCA1/2, causing impairment of their DNA damage sensing function, blockade of a back-up repair pathway, e.g., by PARP-1 inhibitors (PARPi) resulted in tumor-specific cell killing, a concept called synthetic lethality. Multiple PARPi, e.g., olaparib, rucaparib, and veliparib were developed and tested in different tumor types, e.g., breast cancer (BC), ovarian carcinoma (OC), and prostate cancer (PCa) (reviewed in [60]). In the context of RT, PARPis are currently tested or planned to be evaluated in several different tumor types (Table 6.7). Apart from the "BRCAness" tumor concept, the PARPi is also explored in tumors driven by other DDR-alterations, e.g., ATM and ATR.

6.5.2.2 Interfering with Cell Cycle Regulation to Improve RT Response

Multiple cyclin-dependent kinase 4 and 6 inhibitors (CDKIs), e.g., palbociclib, ribociclib, and abemaciclib which alter the cell cycle progression, have become an important new treatment of metastatic- or locally advanced BC including combinations with RT [63]. Albeit multiple studies are ongoing, no consensus has been reached underpinning the clinical benefit of combining RT with CDKIs [63]. For palbociclib, there are studies ongoing in BC and HNC, ribociclib is evaluated with RT in multiple trials as is abemaciclib (Table 6.7). In addition, there is an attempt to study abemaciclib in patients with solid tumors that have brain metastasis where CDK genomic testing is done (NCT03994796).

The CDK1/2 is in part controlled by the WEE1 G2 checkpoint kinase which via Ser/Th protein phosphorylation blocks their activity resulting in a G2/M cell cycle checkpoint activation. Indeed, the WEE1 inhibitor adavosertib was assessed alongside a dual RT and gemcitabine treatment regimen in advanced PCa patients where a clear response was evident by an increased overall survival [62].

6.5.2.3 Attacking Oncogenic Drivers and Downstream Signaling for RT Sensitization in a Precision Cancer Medicine Manner

Constitutively increased activity of epidermal growth factor receptors (EGFRs) by mutation or gene amplification (which is found in multiple tumor types) is responsible for resistance to CT/RT [68]. Moreover, downstream PI3K/AKT or Ras-Raf mitogen-activated protein kinases (MAPK) signaling cascades may also influence RT response via regulation of cell cycle, cell death signaling, or by interfering with the DDR network [73]. Treatment with the antibody cetuximab, a EGF ligand blocker has been shown to improve RT sensitivity in HNC. However, results presented from a meta-analysis covering 13 studies with 5678 patients on CT/RT-based treatment and receptor tyrosine kinase inhibition for solid cancers (ROCKIT) emphasized that targeting EGFR could not ameliorate overall survival yet causing increased toxicity [67]. In the context of metastatic Non-small cell lung cancer (NSCLC) driven by *EGFR* mutation, there is also an interest in combining small EGFR tyrosine kinase inhibitors (TKIs) together with RT for patients with oligometastatic disease as well as to consolidate tumor lesions resistant to a given EGFR targeting TKI [68].

The transcription factor signal transducer and activator of transcription 3 (STAT3) regulate inflammation, malignant cells initiation, progression, and therapy resistance. STAT3 is overexpressed in cancers of the gastrointestinal tract, NSCLC, OC, and brain tumors and thus it may cover a valuable target for precision therapy. One example is the drug dovitinib which was shown to sensitize hepatocellular carcinoma to RT by targeting Src homology region 2 (SH2) domain-containing phosphatase 1 (SHP-1)/STAT3 signaling [69].

6.5.2.4 Altering Cell Death Signaling for RT Sensitization

RT resistance is in part a result of impaired cell death initiation and/or execution (see Chap. 3) and targeted strategies aim to restore such signaling. Multiple signaling components of different apoptotic routes including the B-cell lymphoma 2 (Bcl-2) family members, inhibitor-of-apoptosis-proteins (IAPs), e.g., x-linked IAP (XIAP) or survivin and the Cluster of Differentiation 95 (CD95)/FAS signaling network have all been explored [74, 75]. Inhibition of the IAP survivin, for instance, is reported to increase apoptosis as well as autophagy, to impact on the cell cycle and to hamper DNA damage repair, resulting in a radiosensitization [75].

Another example is the pan-Bcl-2 inhibitor AT-101 (Gossypol), which sensitized HNC cells to RT-induced apoptosis indicating its therapeutic potential for tumors with high Bcl-2 expression levels [64]. An additional example is navitoclax (ABT-263) which impairs the anti-apoptotic function of Bcl-2/Bcl-xL and which was reported to potentiate RT cell death [76]. Finally, the anti-IAP smac mimetic, xevinapant (Debio 1143) has been tested in HNC in combination with cisplatin and RT where locoregional control was achieved in some patients [66]. Concerning RT sensitization via the extrinsic apoptotic route, focus has been on interfering with the FAS/CD95 signaling cascade

[65]. Thus, it was demonstrated in relapsed glioblastoma patients that addition of the Fc-fusion protein asunercept (APG101) which blocks ligand engagement prolonged patient survival.

6.5.2.5 Altering Hypoxia and the Tumor Microenvironment to Impart RT Refractoriness

Targeting the tumor microenvironment is another RT sensitizing approach that involves attack on hypoxia directly or the underlying aberrant angiogenesis/vascularity of tumors, respectively. By this, hyperbaric oxygen therapy (HBOT) and agents which are specifically activated in hypoxic tumor cells/parts of the tumor or are prodrugs which are triggered to activity under hypoxic conditions or impact on angiogenesis/vasculature (by impairing the function of the vascular endothelial growth factor (VEGF) or its receptor signaling) are tested. One prime example is the electron-affinic nitroimidazoles, such as the clinically proven oxygen mimetic nimorazole, which covers the standard of care in HNC patients that are given RT in some countries [72]. Moreover, it has been demonstrated in glioblastoma patients that temozolomide-based CT/RT can be enhanced resulting in improved progression free survival if an anti-VEGF monoclonal antibody bevacizumab (avastin) is included in the treatment regimen [71]. In contrast, addition of bevacizumab to capecitabine and RT did not improve outcome in rectal cancer [77]. Further, vandetanib (ZD6474), a tyrosine kinase inhibitor targeting VEGFR, was shown to improve outcome of esophagogastric carcinoma patients when applied after RT or different CTs [70] (Box 6.6).

Box 6.6 RT Sensitization with Targeted Therapy

- Inhibitors of the DDR signaling network, e.g., ATM, ATR, DNA-PKcs, and PARP-1 or interfering with cell some cycle regulating kinases offer sensitization for RT.
- Blockade of signaling from oncogenic drivers, e.g., growth factor regulated kinases via antibodies or small molecule inhibitors can sensitize tumors to RT.
- Restoring cell death pathways, e.g., apoptosis is another RT sensitizing strategy.
- Modulating the tumor microenvironment, e.g. hypoxia and aberrant angiogenesis allow for tumor RT sensitization.

6.5.3 RT Combined with Immunotherapy

6.5.3.1 Local and Systemic Modes of Action of Radiotherapy

For a very long time, it was assumed that the X-rays directly, or indirectly through the formation of ROS, only affect the radiation-sensitive DNA in the cell and that other structures are spared. However, today it is clear that in addition to the so-called targeted local effects of radiation on DNA, numerous so-called non-targeted effects occur, such as general stress responses of the irradiated cells, which then also can be transmitted to other cells and even the entire organism.

6.5.3.2 Radiotherapy as an Immune Modulator

Radiation-induced oxidative stress and DNA damage activate numerous signaling pathways in cells that influence the expression of genes and consequently trigger a broad spectrum of cellular responses ranging from promotion of cell survival to cell death (see Chap. 3). Thereby, the immunological phenotype of cells as well as the tumor microenvironment may change (see Chap. 5). It has been demonstrated that RT increases the expression of MHCI molecules, death receptors, and stress ligands on the tumor cell surface, and fosters the release of so-called damage-associated molecular patterns/danger-associated molecular patterns (DAMPs) such as adenosine triphosphate (ATP), HMGB1, and Heat Shock Protein 70 (HSP70) (see Chap. 5). Also, RT causes increased levels of immunostimulatory cytokines mainly through the induction of immunogenic tumor cell death (ICD) and in combination with additional immune stimulation [78].

Irradiation of tumors also affect immune cells that circulate through the tumor vasculature even though the functionality of the remaining immune cells is still appropriate. One has to keep in mind that different subtypes of immune cells differ in their radiosensitivity and antigen-presenting cells as key initiators of adaptive antitumor immune responses, are quite radioresistant [79]. RT has also immune suppressive properties directly on the tumor cells and their microenvironment. Local irradiation increases the expression of immune checkpoint molecules such as programmed death-ligand 1 (PD-L1) and induces the release of transforming growth factor (TGF)-beta. Which of these changes that predominates varies greatly from individual to individual and ultimately determines whether, in addition to the local effects of tumor cell killing, local and systemically acting antitumor immune responses are triggered by RT alone [80]. The immune responses triggered by local radiation and acting systemically are referred to as “abscopal effects” of RT (for definition see Chap. 5). However, since radiation has both immune-activating and immune-suppressing effects (Fig. 6.6), the abscopal effect is usually only

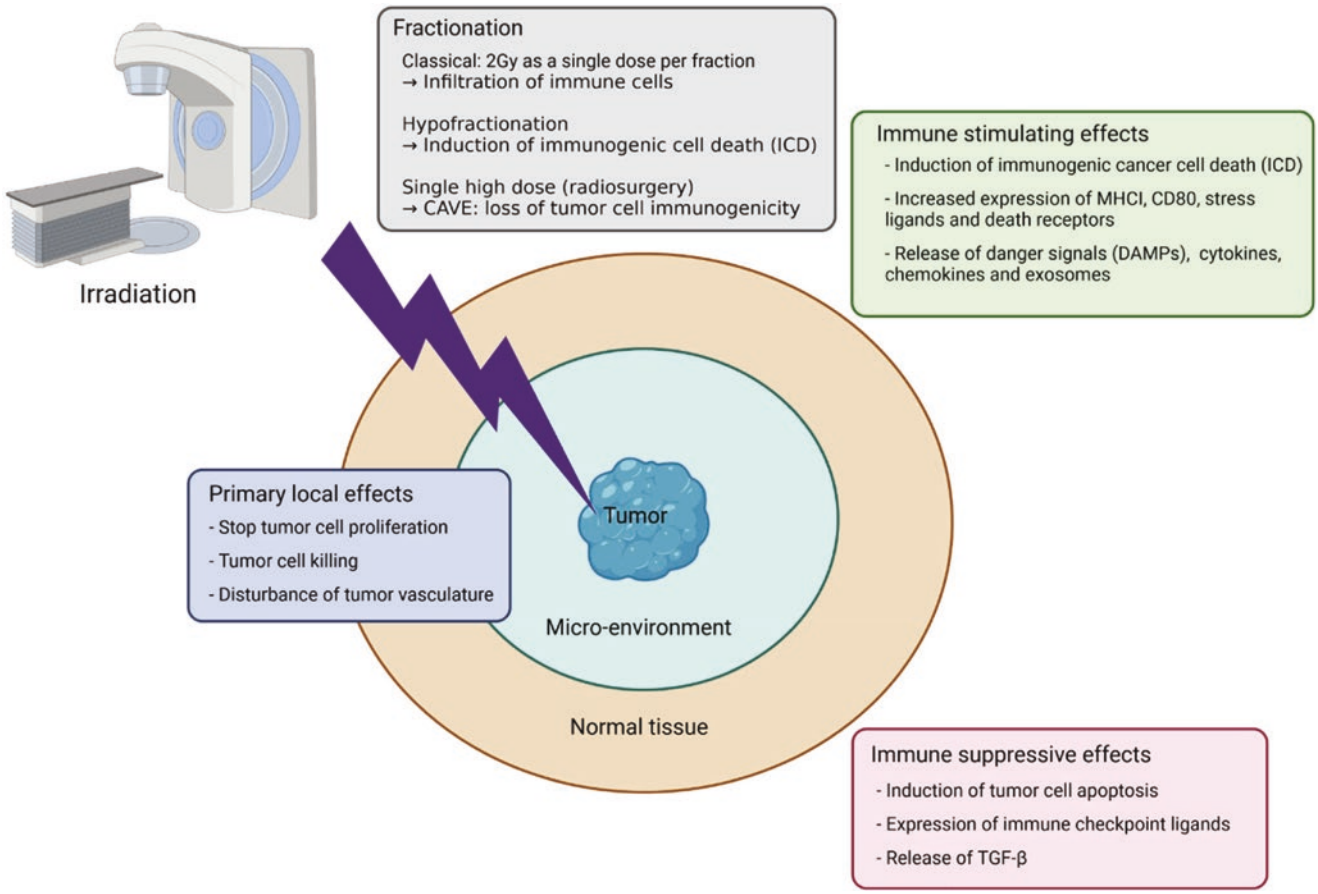

Fig. 6.6 Radiotherapy has multiple immune stimulating and immune suppressive effects which depend on dose

observed in the clinic when RT is used in combination with immunotherapies.

6.5.3.3 Rationale for Combination of Radiotherapy with Immune Therapies

If ICD is induced by local tumor irradiation and the tumor vasculature is changed in such a way that more immune cells can migrate into the tumor, this can already trigger effective antitumor immune responses [81]. In terms of radiation immunology, it is now believed that a single dose of 2 Gy is more likely to promote immune cell infiltration and a dose of >2 Gy is more likely to induce ICD [82]. Importantly, non-linear dose–effect relationships often prevail. For example, the immunogenicity of tumor cells is reduced again after irradiation with a single dose that is too high, because enzymes are activated that degrade the immunogenic DNA found in the cytoplasm after irradiation or because immune-suppressing immune checkpoint molecules (ICM) are increasingly expressed on the tumor cells [83].

Expression of immune suppressive ICM was the key starting point for a combination of radiation and immunotherapies. Inhibition of ICM in parallel with or shortly after RT has led to local and systemic antitumor immune responses in animal models and in the clinic, and the so-called radio-immunotherapies are increasingly being used in multimodal oncological treatment [84]. Further, immunologically-based patient selection based on induction chemo-immunotherapies is increasingly taking place [85]. Particularly exciting is the re-emergence of tumor vaccination in this context and the stratification of patients based on immunological factors of the peripheral blood (see Chap. 6) (Box 6.7).

Box 6.7 RT Combined with Immune Therapy

- Radiation affects DNA and via stress responses other cellular compartments.
- Radiation induces local and systemic effects.
- RT has both immune stimulatory and immune suppressive effects.
- Non-linear dose relationships also apply for radiation-induced immune effects.
- RT is well combinable with immune therapy.

6.5.4 RT Combined with Hormone Therapy (Radio-Hormone Therapy)

Box 6.8 RT Combined with Hormone Therapy

- Hormone sensitive tumors which are dependent on certain hormones for their growth can be slowed down or stopped by hormone therapies.
- In prostate cancer patients with a high risk of progression, hormone therapy in combination with RT is the treatment of choice as hormone therapy or RT alone remain inadequate

A combination of RT and hormone therapy is used in the management of breast and prostate cancers. Hormone therapy is considered to be quite effective and comparatively non-toxic in tumors that are driven by hormones such estrogen in breast cancer (BC) and testosterone in prostate cancer (PCa). The hypothalamic pituitary gonadal pathway controls the concentration of testosterone and estradiol in the serum. Estradiol is mainly produced in the ovaries of premenopausal women, however, in case of postmenopausal women; aromatase found in the peripheral fat tissue aids the peripheral conversion of adrenal androgens. Hormonal therapy is principally accomplished by chemical castration (usage of chemicals or drugs like the gonadotropin-releasing hormone agonists or luteinizing hormone-releasing agonists that stop the production of the sex hormone) in case of men with PCa and premenopausal women with BC (Box 6.8).

With respect to BC, approximately 50% of all premenopausal and 80% of all postmenopausal women suffer from a hormone receptor-positive malignancy. In the histochemical analysis of such tumor cases, the expression of estrogen (ER) and progesterone receptors (PR) are evaluated to understand the degree of positivity. The levels of ER/PR expression in BC are used as a guiding parameter for prognosis as well as for what systemic treatment to give. Recent studies have also shown that patients who overexpress the human epidermal growth factor receptor 2 (HER-2) have a low probability to benefit from hormone monotherapy. Hence it is necessary to target ER and PR as well as the HER-2 receptor. PCa can be hormone-dependent or non-dependent and have functional androgen receptors (AR). Hormone therapy is frequently part of curative therapy for both BC and PCa and where it is either used neoadjuvantly, i.e., for primary cancer size reduction before RT/radical surgery or adjuvantly, i.e., to decrease the risk of tumor recurrence.

6.5.4.1 Radiotherapy Combined with Tamoxifen for Breast Cancer

For ER/PR-positive BC patients, hormone therapy is usually given along with postoperatively RT. The combined treatment of tamoxifen with RT has shown a synergistic effect *in vivo* which can be attributed to the alterations in the tumor microenvironment. Further studies are required to shed light on the complex communications among the 17beta-estradiol and p53/p21(WAF1/CIP1)/Rb signaling pathways. IR is known to induce direct as well as indirect DNA damages via the ROS production. The DNA breaks generated; stimulate various signaling pathways associated with ATM (Ataxia telangiectasia-mutated gene), ATR (Ataxia telangiectasia-mutated gene Rad3-related), and DNA-PK (DNA-protein kinase). These kinases lead to the cell growth arrest after phosphorylation checkpoint kinase 2 (CHK2) or p53. The downstream effectors like p53/p21(WAF1/CIP1)/Rb, CDC25A, 14-3-3 sigma determine if the cell cycle arrest will be in the G1/S or G2/M transition. Interestingly, these pathways can be regulated at various stages by 17beta-estradiol (E2) in the irradiated cells. The ROS production can also be reduced by 17beta-estradiol, thereby reducing the subsequent effects of RT. This can be achieved either by reducing the p53 activation or by suppression of ROS induced DNA damage. Additionally, while 17beta-estradiol acts on S-phase kinase-associated protein 2 (SKP2) and P27 to allow G2/M transition, it also augments the expression of *CCND1* and *MYC* that control the cell cycle promoting the G1/S transition. In contrast, tamoxifen, with its anti-estrogen activity obstructs the effects of 17beta-estradiol. This anti-estrogenic effect can strengthen the IR induced growth inhibition as depicted in Fig. 6.7 [86].

The usage of TAM is however limited because of the pharmacological side effects like endometrial changes that can lead to endometrial cancers or the thromboembolic events. Keeping this in mind, other endocrine drugs that might endow a comparable efficiency with boosted acceptability in early disease conditions can be utilized. Hence, Letrozole (LTZ), an aromatase inhibitor, is considered as a potent drug in the adjuvant settings. It can be delivered after surgery or in combination with RT with a long-term follow-up to identify the treatment- associated cardiac side effects and evaluate cancer-specific results. LTZ, when combined with radiation, arrests cancer cells in the G1 phase with a significant decrease of cells in the S phase and G2 phase of the cell cycle [87]. Table 6.8 gives the list of hormone therapies for breast and prostate cancers.

6.5.4.2 Radiotherapy Combined with Androgen Deprivation Therapy (ADT) for Prostate Cancer

During the course of the disease, a majority of PCas express the androgen receptor (AR) which is known to specifically direct the cancer cell behavior and this has solidified the significance of androgen signaling in the pathogenesis of PCa [89]. Hence, androgen deprivation therapy (ADT) is a foundation of PCa therapy. ADT is typically utilized to cut down the levels of serum testosterone to a castrate level. This can be accomplished by surgical or chemical castration. Chemical castration can be accomplished by using estrogens or LHRHa; and it is likely to be reversible. The consequence of initial use of LHRHa results in follicle-stimulating hormone (FSH), luteinizing hormone (LH), and testosterone surge in

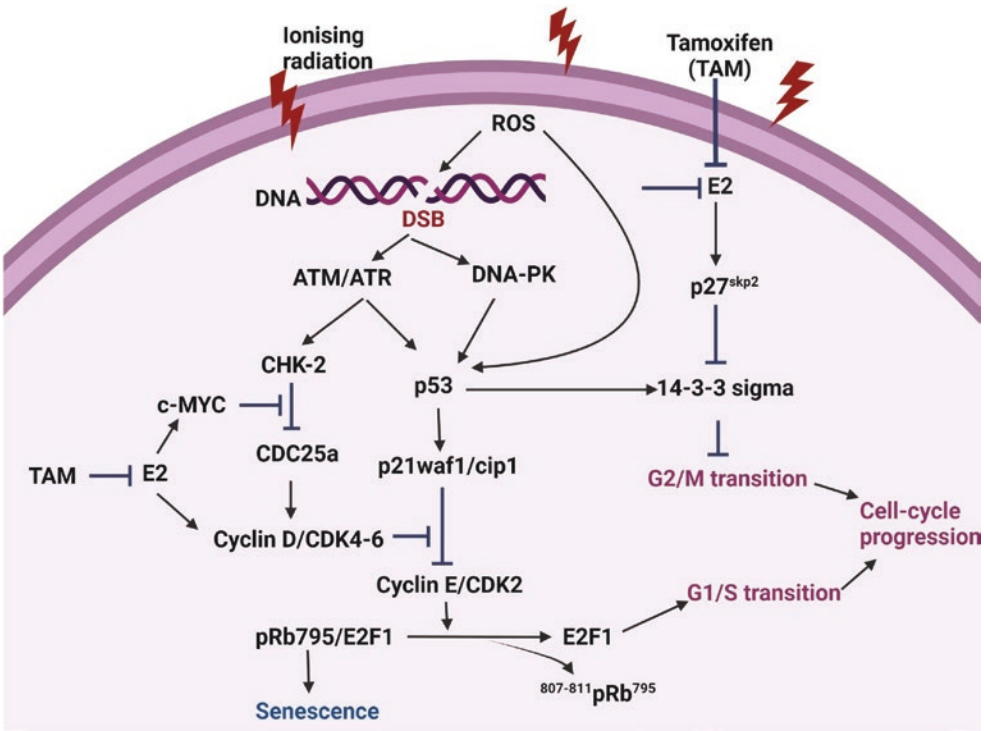

Fig. 6.7 Prospective direct genomic effect of estradiol, tamoxifen, and IR on inhibition of cell cycle progression. (Reproduced with permission from [86])

Table 6.8 Hormone therapies used for breast and prostate cancer. (Reproduced with permission from [88])

Drug	Type	Dose/route	Mode of action
Tamoxifen	Anti-estrogen	Orally, (20 mg) daily	For ER binding, competes with estradiol
Anastrazole	Non-steroidal aromatase inhibitor	Orally, (1 mg) daily	Inhibition of competitive aromatase
Exemestane	Steroidal aromatase inhibitor	Orally, (25 mg) daily	Irreversible aromatase inhibition
Goserelin	LHRH agonist	(3.6 mg) every 28 days or (10.8 mg) every 3 months SC	Reduced pituitary production of LH and FSH
Bicalutamide	Non-steroidal antiandrogen	Orally, (50 mg) combination dose or (150 mg) single agent daily	Competitive AR inhibition
Prednisolone	Corticosteroid	Orally, (5–10 mg) daily	Suppression of Adrenal

ER estrogen receptor, *LHRH* luteinizing hormone-releasing hormone, *LH* luteinizing hormone, *FSH* follicle-stimulating hormone, *AR* androgen receptor, *SC* subcutaneous, *IM* intramuscular

the serum, which makes the symptoms worse. Hence, patients are advised to take oral antiandrogens for 1–2 weeks prior to the LHRHa injection. ADT is mostly given with RT as a neoadjuvant therapy which can be continued throughout and even further than RT. Although evidence suggests that the combinatorial treatment of PCa with ADT and RT has improved therapeutic effects, there is still a lot of improvement that can be made on the biochemical front as demonstrated by the clinical trials. ADT might also boost the efficacy of RT by inhibiting successive PCa cell repopulation and by enhancing reoxygenation and radiosensitization. Many preclinical studies involving tumour cell lines *in vitro* and *in vivo* tumor xenografts have suggested that ADT works by suppressing the mechanisms associated with the DNA damage response, particularly the NHEJ repair. This increases the anticancer effect induced by RT. Preclinical studies have also shown that the synergistic effect of RT and ADT enhances apoptosis by suppressing the DNA repair machinery. The combinatorial treatment not only increases the tumor oxygenation but also radiosensitizes the PCa cells. The first phase III, EORTC 22863, study demonstrated a noteworthy overall survival when RT was combined with ADT in men with locally advanced PCa. The results showed that the combination arm had a significantly higher OS compared to that of the RT alone (58.1% vs. 39.8%, $p = 0.0004$). Short-term and long-term follow-up of the EORTC studies showed that only 74% patients exhibited a 5-year disease-free survival with combined RT and ADT [89, 90].

6.5.5 Radiotherapy Combined with Hyperthermia

Hyperthermia as an adjuvant treatment to RT or chemotherapy considers heating of the tumor (area) above a physiological temperature up to 40–43 °C for approximately an hour. Hyperthermia can be applied as whole body, local invasively (intraperitoneal, interstitial, or intracavitary) and locoregional.

Hyperthermia as a radiosensitizer or chemosensitizer has been proven its effectiveness in many different tumor types, such as locally advanced cervical cancer, recurrent breast cancer, malignant melanoma, and head and neck cancer. The size, location, and type of tumor(s) determine whether hyperthermia should be applied only locally in combination with RT or chemotherapy, or whether hyperthermia should be applied to a larger area in combination with only chemotherapy. Hyperthermia has also been demonstrated to regulate the innate and adaptive immune system [91, 92].

6.5.6 Hyperthermia in Clinical Settings

6.5.6.1 Hyperthermia Combined with Chemotherapy

For metastases from, e.g., colon or ovarian origin which are located in the peritoneal area, a heated chemotherapy solution can be circulated through the peritoneal area (called hyperthermic intraperitoneal chemotherapy; HIPEC) [93]. For urinary bladder cancer, a heat solution can be circulated through this organ (endocavity). Since all of these heated solutions are combined with chemotherapy, these hyperthermia setups will not be further discussed in this chapter. Generally, hyperthermia modifies the cytotoxicity of many chemotherapeutic agents. Furthermore, for some drugs, like the platinum compounds, hyperthermia was found to make resistant cells platinum-responsive again [94]. Whether hyperthermia has this effect on other drugs, needs to be investigated.

6.5.6.2 Hyperthermia Combined with Radiotherapy

Locoregional hyperthermia combined with RT is an approach for patients with locally advanced cervical carcinoma (deep hyperthermia) or recurrent breast cancer (superficial hyperthermia) in Europe and USA. Locoregional hyperthermia combined with RT has been used in the clinic already since the early 1980s [95]. It is also possible to implant a heat source in the tumor itself (interstitial), which mainly has been used for brain tumors or locally advanced head and neck tumors [96]. Hyperthermia weakens DNA damage repair enzymes and thereby retards the repair of radiation-induced DNA damage. An increased amount of unrepaired DNA damage causes more cells to die from the radiation injury. Importantly, the synergy between radiation and heat is highest when given simultaneously or closely together in time (within 4 h) [97].

6.5.6.3 Hyperthermia Combined with Immune Therapies

Based on the preclinical knowledge gained in the last few years [91, 92], ongoing clinical trials are conducted with complementary translational studies focusing on immune alterations of patients receiving hyperthermia in combination with RT and/or chemotherapy. These data will form the basis for the design of multimodal cancer therapies in which hyperthermia will be combined additionally to radio- and/or chemotherapy with immune therapies such as immune checkpoint inhibitors.

6.5.6.4 Techniques to Apply Hyperthermia

Hyperthermia can be applied using different techniques such as capacitive radiofrequency heating, radiative radiofrequency and microwave heating, infrared and laser, ultrasound, conductive heating, and by hyperthermic perfusion [63]. One of the most commonly used techniques which is validated within clinical trials is microwave heating and hyperthermia is induced with one or more antennas. An applicator containing one antenna is used for superficial hyperthermia, such as breast cancer or malignant melanomas. This applicator can be placed on the surface area. For deep hyperthermia, the patient lies on a mobile bed that can move through a circle with 4 or 6 antennas. This non-invasive method is used for deeper located tumors such as cervical cancers.

6.5.6.5 Mechanism of Action of Hyperthermia

Macroscopical effects of hyperthermia: Hypoxic and nutrient-deprived areas of a tumor are the least sensitive to RT or chemotherapy, while these areas are especially sensitive to hyperthermia. By local heating of the tumor, an increased blood flow occurs, which increases reoxygenation [95]. As a consequence, more radiation-induced DNA damages are formed and fixed (Fig. 6.8). Moreover, increased tumor perfusion by hyperthermia allows the chemotherapeutic agent to penetrate deeper into the tumor.

Microscopical effects of hyperthermia: Besides increasing the radiation-induced DNA breaks within cancer cells, hyperthermia temporality inhibits DNA DSB repair (Fig. 6.8). This occurs by degrading the essential BRCA2 protein, and thereby temporarily inhibiting the homologous recombination DNA repair pathway. In HPV-positive cervical cancers, hyperthermia was found to disrupt the interaction between the HPV protein (E6) which in normal circumstances suppresses p53. Activation of p53 in these cancer cells results in cell death [95].

Immune effects of hyperthermia: Dependent on the temperature, certain immunological processes are triggered by hyperthermia (Fig. 6.8). Starting with temperatures of 39 °C, an increased infiltration and activation of immune cells in the tumor can be observed in preclinical model systems. At higher temperatures, heat-induced cell death has certain characteristics of "immunogenic cell death" (ICD). This means that the dying and dead cells activate rather than suppress the immune system. In this scenario,

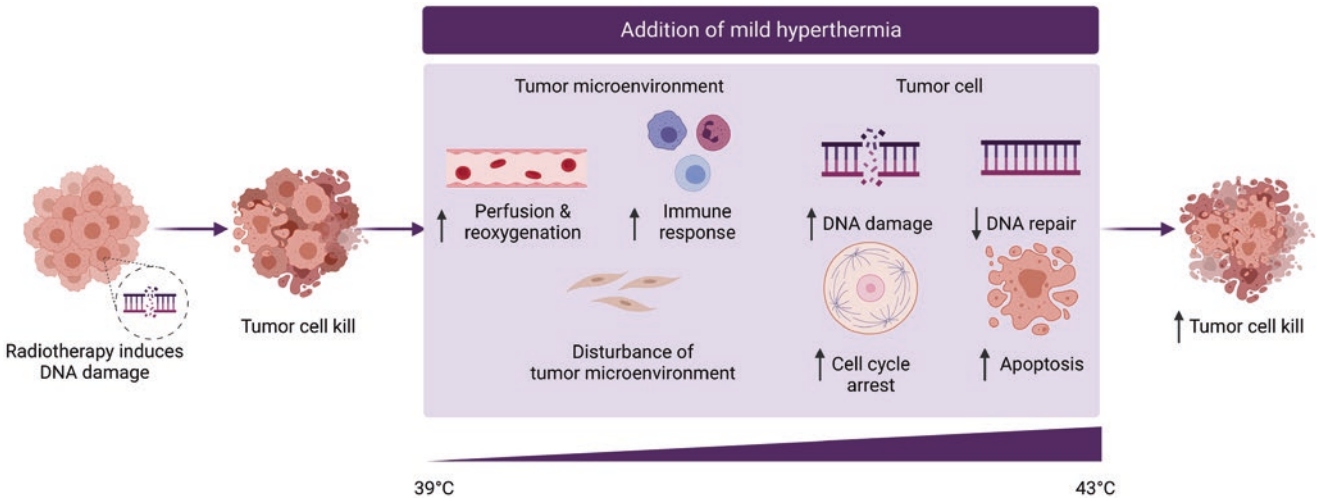

Fig. 6.8 Mild hyperthermia enhances radiotherapy by initiating multiple intracellular and intercellular processes. While radiotherapy induces DNA damages, hyperthermia can enhance the induction of radiation-induced DNA damage by increasing the perfusion and reoxygenation; hyperthermia can temporarily inhibit the DNA repair processes which causes cell cycle arrest and subsequently cell death of the tumor cells such as apoptosis; hyperthermia can also trigger an immune response and disturb the tumor microenvironment eventually all causes of increased tumor cell kill

the heat shock protein 70 (HSP70) is a major player. While inside the cell, it acts as chaperon and protects cells (known as thermotolerance), outside of the cell when being, e.g., released by heat-induced necrotic cells, it activates dendritic cells and delivers antigen to these key immune cells that bridge innate and adaptive immunity. Thus, dendritic cells take up tumor antigens, present them with co-stimulation to CD8+ T cells, and subsequently trigger cellular antitumor immunity by priming cytotoxic T cells [99]. Additionally, HSP70 can directly activate further cells of the innate immune system, such as natural killer cells [100]. Based on this preclinical knowledge gained in the last years, ongoing clinical trials are conducted with complementary translational studies focusing on immune alterations of patients receiving hyperthermia in multimodal settings.

6.5.6.6 Main Indications

Superficial tumors: Hyperthermia is, e.g., standard of care in the Netherlands, Germany, and Japan for patients with recurrent breast cancer (BC), who have received a full radiation treatment course for treatment of their primary tumor. Retreatment with a similar radiation dose as used for their primary tumors is not possible, therefore hyperthermia is applied to prevent severe radiation-induced toxicities. To accomplish the same effectiveness without severe normal tissue toxicity, RT is combined with hyperthermia. The latter gives a boost to the treatment effectiveness. Nevertheless, hyperthermia treatment is not refunded by insurances for treatment of most heatable tumor entities, since big randomized trials are still missing. Besides BC, malignant melanoma and head and neck cancers are prominent superficial tumor entities which are accessible for hyperthermia. The clinical outcomes using locoregional hyperthermia with RT and-/or chemotherapy have been summarized [101]. For soft tissue sarcomas, optimized strategies with multimodality approaches including chemotherapy, regional hyperthermia, and immunotherapeutic agents have been shown to improve survival in high-risk patients [102]. However, more randomized phase III studies, as carried out in an exemplary manner for soft tissue sarcoma [103], are urgently needed to bring hyperthermia as standard tumor therapy in multimodal settings into the clinics (Figs. 6.9 and 6.10).

Deeper located tumors: In most countries, RT combined with chemotherapy is standard treatment of care for cervical cancer patients. However, chemoradiation is less beneficial in tumors of higher stage, whereas hyperthermia as an adjuvant to RT has shown its additional value. Especially in this group, chemoradiation was found to be not very effective. Moreover, chemoradiation seems to result in more toxicities, whereas hyperthermia in addition to RT did not increase radiation-induced toxicities [104].

Treatment course: Both superficial and deep hyperthermia are applied in combination with either RT or chemotherapy. Depending on the tumor type, e.g., BC, cervical cancer, etc. and The International Federation of Gynecology and Obstetrics (FIGO) stage, a radiotherapy or chemotherapy scheme is chosen. While external beam RT is mainly given in daily fractions with low doses, hyperthermia is only applied once or twice per week, for 5 weeks in a row. For each treatment session, the target temperature

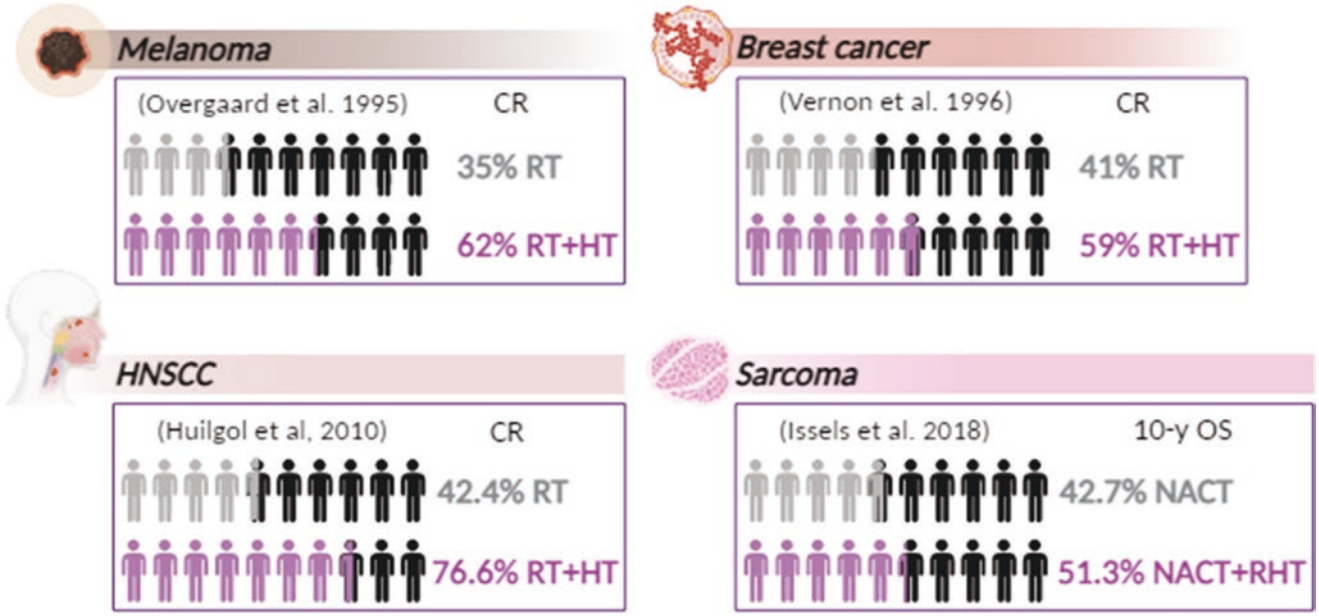

Fig. 6.9 Improved clinical responses after addition of hyperthermia in superficial tumor types. In malignant melanoma, superficial breast cancer and head and neck squamous cell carcinoma, complete responses were much better in patients treated with RT combined with hyperthermia, compared to RT alone. In soft tissue sarcoma, the addition of RT plus hyperthermia to neoadjuvant chemotherapy, leads to a8.6% higher 10-year overall survival

Fig. 6.10 The additional effect of hyperthermia in a deep located tumor (cervical cancer)

should be above 40 °C for approximately 1 h. Moreover, a short time interval on the day that both RT and hyperthermia are given can be more beneficial, but research is ongoing in providing more evidence [105, 106] (Box 6.9).

Box 6.9 RT Combined with Hyperthermia

- Hyperthermia enhances blood perfusion and reoxygenation, triggers an immune response, and disturbs the tumor microenvironment.
- Hyperthermia increases RT and chemotherapy-induced DNA damage, inhibits the DNA damage repair pathways, increases cell cycles arrest, and induces cell death such as apoptosis and necrosis.
- Hyperthermia was proven to be effective in many different tumor types, such as superficial breast cancer, soft tissue sarcoma, and cervical cancer.

6.5.7 RT Combined with Short-Term Starvation

Voluntary fasting is a part of religious services in many cultures like Buddhism, Christianity, Hinduism, etc. Fasting/short-term fasting (STS) is also known as calorie restriction (CR) which is associated with diets with a wide alteration in the growth factors and the metabolites levels. This produces a milieu that diminishes the cancer cell competency to get acclimatized and endure which results in improved outcomes for cancer therapy. In normal cells, STS and fasting selectively boost the chemotherapy resistance which is not the case with cancer cells. STS endorses rejuvenation of normal cells, thereby averting the toxic and harmful effects of the treatment. Clinical as well as *in vivo* studies suggest that the low calorie-fasting mimicking diet (FMD) cycles are promising and also safe, in patients that can barely endure STS/fasting. Hence, it can be predicted that

the combination of STS or FMDs with chemotherapy, immunotherapy as well as other therapies holds a promise in increasing the cancer treatment efficacy, preventing the acquired resistance and minimizing the aftereffects [107]. This can be correlated with one of the emerging hallmarks of cancer, i.e., the susceptibility of cancer cells to nutrient deficiency and their addiction for explicit metabolites. Three of the nutritional interventions of food withdrawal strategies like fasting, FMD, and calorie CR from the myriad of strategies have increasingly exhibited a valuable effect on metabolism and shown a promising anticancer activity. STS is typically done on an average of 3–5 successive days. In fasting, only water is consumed, for a timespan ranging from 12 h to 3 weeks. For CR, there is a 20–40% decrease in calorie ingestion with decrease in all constituents without intercepting the ingestion of minerals and vitamins, typically used by specialists as a synonym to dietary restriction.

Cancer cells are distinguished from normal cells by means of their irregular metabolic and signaling pathways that lead to circumventing the antiproliferative signals, distorted mitochondrial function, and increased glucose uptake. Fasting or STS exhibits a differential consequence on cancer cells and normal cells which can be attributed to drop in the glucose, insulin-like growth factor-1, and insulin levels, amplification in ketone bodies and insulin-like growth factor-binding protein 1 (IGFBP1). This phenomena force cancer cells to depend on the limited amounts of factors and metabolites that are present in the blood, thereby eventually resulting in cell death. The response mechanisms of differential stress sensitization (DSS) and differential stress resistance (DSR) caused by fasting/STS stimulate the normal cell protection but pushes the cancer cell toward cell death. One of the major classical responses of radiation is the dys-functioning of the cell cycle arrest [108].

There is a growing body of evidence from the preclinical studies on STS which enhances the efficacy of a wide variety of chemotherapy drugs that are used in treatments of several types of tumors. Some of clinical trials (NCT00757094, NCT00936364, NCT01304251, and NCT01954836) have proven to be safe and feasible with reduction in the chemotherapy associated side effects. Since STS has demonstrated favorable traits to fight cancer, it would be logical to combine STS with RT as it presents clinical gain. In preclinical studies, combining STS with RT has already exhibited enhanced RT effects. Clinical and preclinical trials of STS and RT are also picking pace to exhibit the efficacy of this combination. STS can be considered as a personalized dietary approach that can be conveniently combined with RT in clinics in the path forward (Box 6.10).

Box 6.10 RT Combined with Short Term Starvation

- Short-term starvation (STS) in combination with RT leads to an increased effect of RT on metastatic cancer cells, and at the same time also protects normal cells.
- Short-term starvation (STS) or fasting can particularly safeguard normal cells in mice and probably in patients receiving chemo without reducing the therapeutic effect on cancer cells.
- Fasting dependent decrease in IGF-1 and glucose are arbitrate components involved in the DSR and DSS effects.

6.6 Spatial Fractionation

Box 6.11 Spatial Fractionation I

- Spatial fractionation is a method that reduces damage to normal tissue.
- Small beams of radiation are applied in a grid-like pattern.
- High doses are applied in the beam path, while (almost) no or very low dose is delivered between the beams, resulting in high peak-to-valley dose ratio (PVDR).

Box 6.12 Spatial Fractionation II

- Spatial fractionation of photons is in clinical use.
- GRID therapy uses 2D pattern with beam width of ~1–1.25 cm and center to center (ctc) of 2.2–2.4 cm.
- LATTICE is the 3D extension of GRID therapy.

Box 6.13 Minibeam RT

- Minibeam RT (MBRT) is a modern therapy approach using protons and heavier ions, which is at the moment in preclinical stage or investigated in clinical trials.
- In proton MBRT, the beam widen and overlap in the tumor.
- Further sparing of healthy tissue can be achieved using interlacing methods.

The concept of spatial fractionation of radiation in tumor therapy aims to widen the therapeutic window by sparing healthy tissue by simply sparing parts of it from radiation. It was introduced as GRID therapy by Alban Köhler in 1909 by the use of a grid of centimeter-wide pencil beams in X-ray therapy [109]. In the 1990s, when more powerful X-rays became available from synchrotron facilities, GRID therapy was moved to the micro level with the development of microbeam radiotherapy (MRT) and to the submillimeter level in the later 2000s with minibeam radiotherapy (MBRT) [110]. It was then that GRID, MRT, and MBRT were classified under a broader term of spatially fractionated radiation therapy (SFRT).

In SFRT, the spatial arrangement of the radiation allows irradiating tumors with a heterogeneous dose, with high doses in the radiation channels and low doses in the so-called valleys in between.

In recent years, advances in the use of spatial fractionation in particle therapy have also been investigated. Proton minibeam radiotherapy (pMBRT) is making rapid progress [111]. Thanks to small-angle scattering, the radiation channels overlap and the tumor is irradiated with a homogeneous dose, while the normal tissue is spared due to the spatial fractionation of the dose (Box 6.11, 6.12, and 6.13).

Schematic representations of SFRT, proton and ion MBRT is shown in Fig. 6.11.

6.6.1 Parameters and Mechanisms

Spatial fractionation of radiation means that new parameters must be introduced and controlled in treatment planning and therapy. First and foremost, beam size and the distance between two beams become the most important variables. Beam size, or beam width, is the full width at half maximum (FWHM) of the lateral intensity profile of a beam. The distance between two beams, also called center-to-center distance (ctc), is defined as the length of the direct connection between the maximum intensity (also called center) of the two beams [112].

Another important quantity is the dose ratio between the dose in the center of the beam (peaks) D_P and the dose in the middle between two beams (valleys) D_V, the peak-to-valley dose ratio (PVDR):

$$\mathrm{PVDR} = \frac{D_P}{D_V} \tag{6.3}$$

The PVDR defines the strength of spatial fractionation. It is ~1 for homogeneous irradiation and approaches infinity for small valley doses [113].

The parameters of beam width, ctc, and PVDR determine the possibility of sparing normal tissue and also the dose applied to the tumor, thus influencing tumor control.

Finally, the geometric arrangement of the beams is also crucial. Spatial fractionation uses beams that have either a pencil (Fig. 6.12a, b) or a planar structure (Fig. 6.12c). Pencil

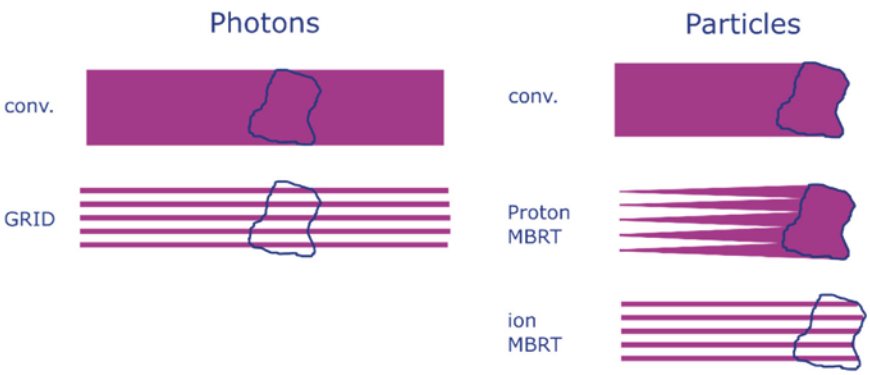

Fig. 6.11 Schematic view of spatial fractionation in RT. The blue object represents the tumor

Dose pattern	*Photon SFRT*	*Proton MBRT*	*Ion MBRT*
In the tumor	Heterogenous	Homogeneous	Heterogenous
In front of the tumor	Heterogenous	Heterogenous	Heterogenous
Behind the tumor	Heterogenous	No dose	Heterogenous

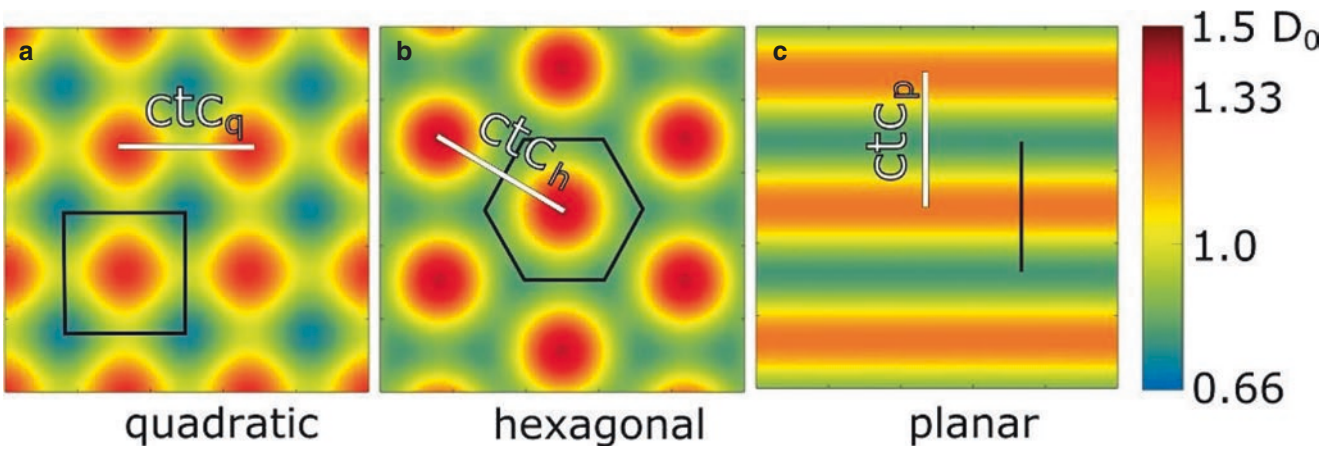

Fig. 6.12 Quadratic (**a**) and hexagonal (**b**) pencil minibeam and planar minibeam (**c**) arrangements on a 2D lattice with view direction in the direction of the beam. The dose is color coded and normalized to a mean dose D0. The black lines indicate the unit cell, and the white lines indicate the corresponding ctc. (Reproduced with permission from (CCBY) [112])

beams have a completely round or Gaussian shape and can be arranged in either a square or hexagonal lattice. For treatment planning, it is important to know the dimensions of a beam. For this purpose, the unit cell of a beam is used. The unit cell is the smallest unit in which a beam can be considered a beam and the entire dose distribution is covered. The unit cell is assembled to form the entire lattice and cover the tumor.

The basic mechanism of tissue sparing by spatial fractionation lies in the ability of undamaged cells in the vicinity of the radiation beam paths to migrate to this region and support wound healing. This is described as the dose-volume effect, i.e., the ability of skin and subcutaneous tissue in particular to tolerate more dose as the irradiated volume decreases. Furthermore, the microscopic prompt tissue repair is another beneficial effect resulting in better tolerance of tissue to submillimeter sized beams. When tissue is damaged in such small areas, capillary blood vessels can be rapidly restored within days or even hours by the regeneration of cells from the undamaged area. The intact blood vessels also support healing of the damaged tissue located between the beams. The extent to which the bystander effect plays a role is still unknown and is currently being investigated.

6.6.2 Spatial Fractionation of Photons

6.6.2.1 Photon SFRT in the Clinic

Spatial fractionation of photons is already being used clinically, but other treatment strategies are being tested simultaneously in preclinical and clinical studies. The application of photon SFRT in the clinic can be distinguished into GRID and LATTICE therapy. In GRID therapy, based on the original method of Koehler et al. in 1909, portions of the radiation field are blocked by the use of collimators placed in front of the patient to produce a non-conformal dose in both healthy tissue and tumor, as shown in a therapy plan in Fig. 6.13b [109].

Optimal geometries of collimators for tissue sparing and therapeutic outcome are hole sizes from 1 to 1.25 cm and ctc from 2.2 to 2.4 cm [114]. The pattern can be generated either with a block collimator with a defined hole pattern or with multileaf collimators (MLCs), which can be flexibly adapted to the needs of the treated tumor. The disadvantage of MLCs in the clinic is that treatment time is prolonged because each spot must be applied in a step-and-shoot procedure. Although faster irradiations are possible with MLCs by moving the target across the beam, this is currently only possible preclinically. A more advanced method is the hybrid use of an MLC and a block collimator, which combines the advantages of both methods but has the disadvantage of lower PVDR along the diagonal [115].

The efficiency of GRID therapy has been demonstrated in various clinical trials with different tumor types and by using different collimators [114, 115]. A modern approach to photon SFRT is LATTICE therapy, which can be used with arc-based therapy and is the 3D extension of GRID therapy. In LATTICE therapy, the beams are applied to form multiple small spheres of high dose, called vertices, in the tumor (Fig. 6.13a). The LATTICE application further reduces damage to normal tissue and has also been used in clinical trials [116].

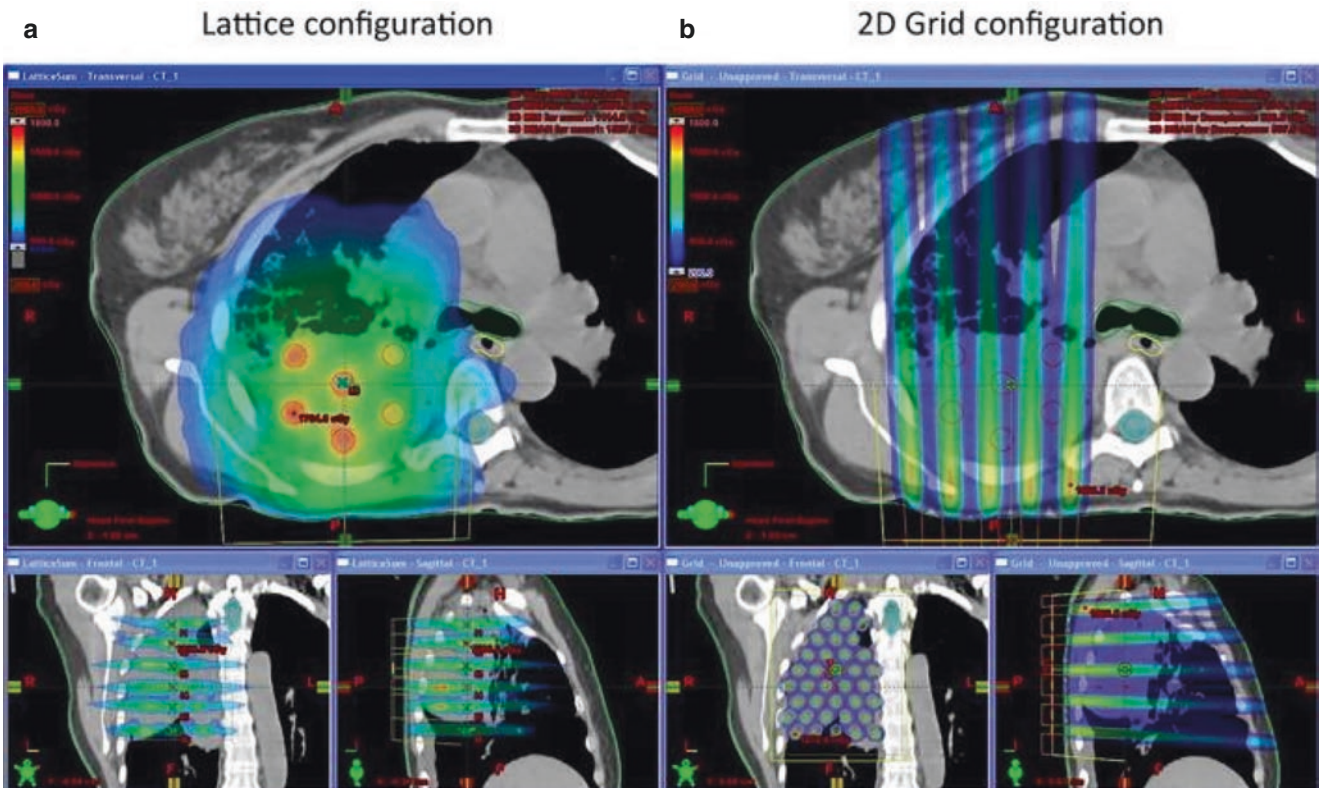

Fig. 6.13 Treatment planning of a lung tumor patient in LATTICE (**a**) and GRID (**b**) therapy. (Reproduced with permission from [114])

6.6.2.2 Photon SFRT in Preclinical Development

While the use of SFRT in the clinic started with GRID and LATTICE, there are two other spatially fractionated modalities that are being studied preclinically. These are MRT, which uses spatially fractionated photons in the form of rectangular beams 25–100 μm wide (Fig. 6.14), and MBRT, which also uses rectangular photon beams but 400–700 μm wide.

MRT has the distinction of using extremely thin microbeams, which exploits the dose-volume effect and allows very high doses of radiation (300–600 Gy) to be delivered with minimal toxicity to normal tissue. In addition, synchrotron facilities such as the European Synchrotron can deliver radiation at ultra-high dose rates (12,000–16,000 Gy/s), making synchrotron MRT a spatially fractionated FLASH RT [117].

The benefits of MRT over conventional RT are many:

- Normal tissue is spared from the effects of radiation by two unique mechanisms: (1) volumetric sparing due to spatial fractionation of microbeams and (2) sparing of normal tissue due to ultra-high dose rates, known as the FLASH effect [117]. More details of FLASH radiotherapy are discussed in Sect. 6.4.2.
- MRT produces unique vascular effects that preferentially damage tumor vessels rather than those of healthy tissue. Peak doses selectively affect rapidly growing "immature" tumor vasculature, triggering transient tumor ischemia and neutrophil infiltration [117].
- Strong immune responses have been observed after MRT. For example, MRT can activate natural killer and cytotoxic CD8+ T cells, induce higher levels of pro-inflammatory genes in tumors, trigger the release of chemokines that attract monocytes, and recruit leukocytes to malignant tissues [118].

MRT currently requires ultra-high dose rates to deliver the radiation fast enough to prevent the beam from smearing across tissue due to the cardiovascular motion. Therefore, preclinical and future clinical research on MRT is currently limited to synchrotron facilities. However, a compromise can be achieved by delivering photon MBRT, since beam smearing is not a problem with submillimeter beams. The same logic is now being applied to MBRT ion therapy research and will be discussed next.

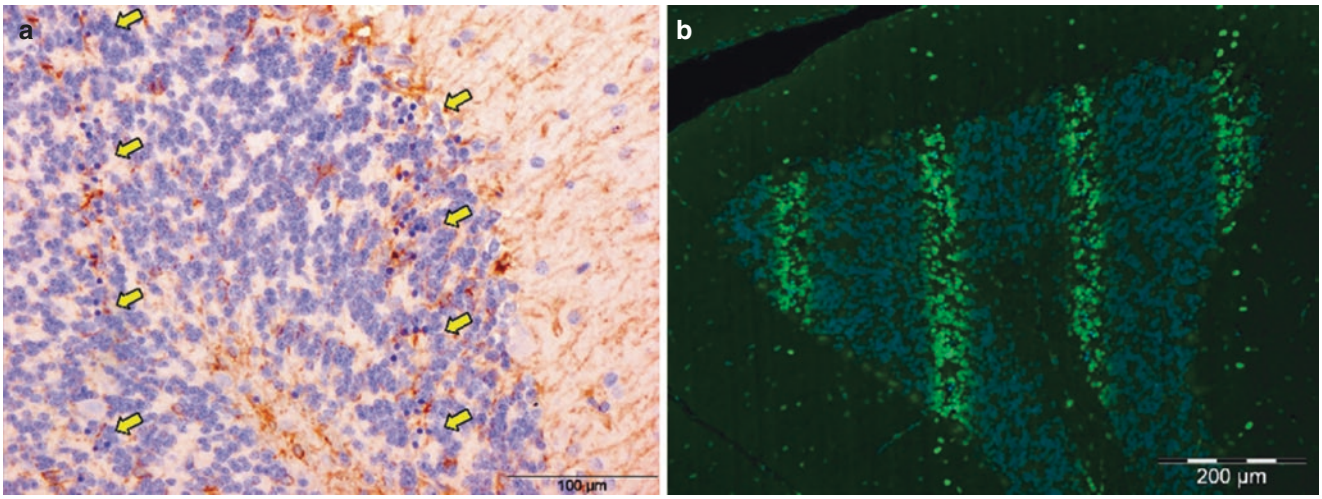

Fig. 6.14 Cerebellum of a rat 8 h after exposure to synchrotron MRT. The peak dose was 350 Gy, and each microbeam was 25 µm wide and spaced 200 µm from the center of the next microbeam. (**a**) H&E staining of the cerebellum. The track of the microbeams can be seen as two vertical bands of dark blue dots (yellow arrows) consisting of cells with nuclear pyknosis (irreversible condensation of chromatin in the nucleus of cells undergoing necrosis). (**b**) Immunostaining of a different section of the cerebellum with gamma-H2AX. The track of the microbeam can be seen as green staining, indicating large amounts of DNA damage. The blue color indicates nuclear staining with DAPI

6.6.3 Spatial Fractionation of Ions

The method of applying spatially fractionated RT using particles, also called minibeam RT, is still in its infancy. Preclinical research points to drastically lowered side effects, with at least same tumor control, thus clearly widening the therapeutic window. In MBRT, one distinguishes between proton MBRT and ion MBRT, most commonly carbon and helium. The major difference lies in the application of the dose to the tumor originating from different physical properties of the particles. When particles traverse matter, interactions with the atoms and molecules occur. At high energies, as used for therapy, the interactions are dominated by Coulomb interactions with the electrons of the target material. These mechanisms mainly cause the ions to lose energy and define the well-known Bragg curve of energy loss. But these interactions also cause scattering of the ions and thus deflection, called small-angle (Coulomb) scattering. In each interaction, the particle is only scattered by a small angle, causing a roughly gaussian broadening of an incident ion beam. The beam is thus widening with increasing penetration depth. The FWHM of the beam due to scattering, which is in the order of several millimeters for therapy relevant energies, is proportional to the ion charge z its kinetic energy E_{kin} and the distance covered in medium x:

$$\text{fwhm} \propto \frac{z}{E_{\text{kin}}}\left(\sqrt{x}\right)^3 \tag{6.4}$$

Therefore for helium and carbon ions, this results in a reduction of beam width compared to protons of a factor of ~2 and ~3, respectively, as shown in Fig. 6.15.

Therefore MBRT for protons works with the principle that the beams start to clearly widen, while traversing tissue as shown in Fig. 6.16. The planning is done in a way that at the beginning of the tumor, the beams overlap and the tumor is irradiated with a small PVDR or even a homogeneous dose distribution.

For helium and carbon, the beams don't overlap, thus giving potential for further sparing of healthy tissue also close to the tumor volume. Although there is evidence for tumor control using heterogeneous tumor dose, it seems appropriate to find a way of applying an (almost) homogeneous dose to the tumor [119]. This is achieved through so-called interlacing, where the beams of different irradiation fields are arranged in a way that in the tumor the dose peaks interlock and homogeneous dose distribution is formed. Figure 6.17 shows different possibilities of interlacing using either pencil or planar beams compared to single direction irradiation.

Up to now, the method of MBRT is still in the preclinical state and especially proton MBRT is investigated here, as the possible spreading is more promising as more proton therapy centers than other particle therapy centers exist worldwide. Up to now it could be shown that pMBRT has

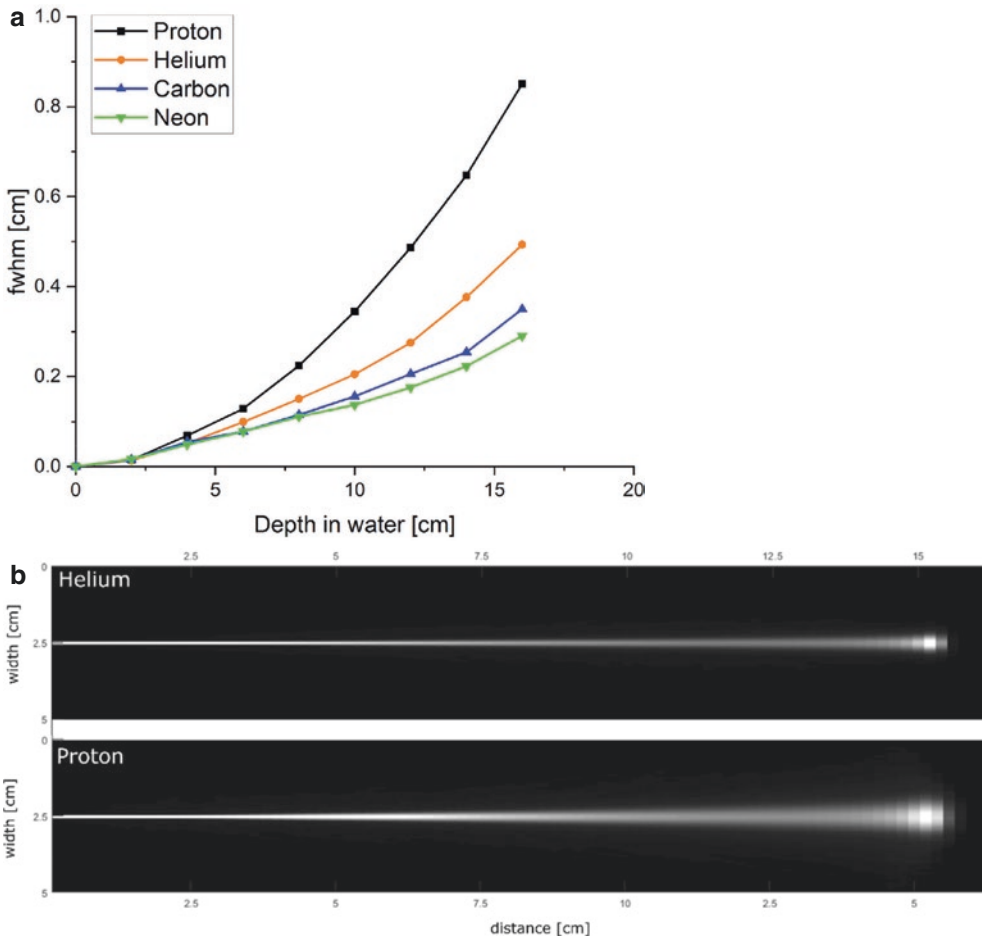

Fig. 6.15 (**a**) Beam width for proton, helium, and carbon ion beams with penetration depth. No incident beam size and divergence is used, both have to be added to the FWHM. (**b**) Widening of a helium ion and a proton beam with penetration depth

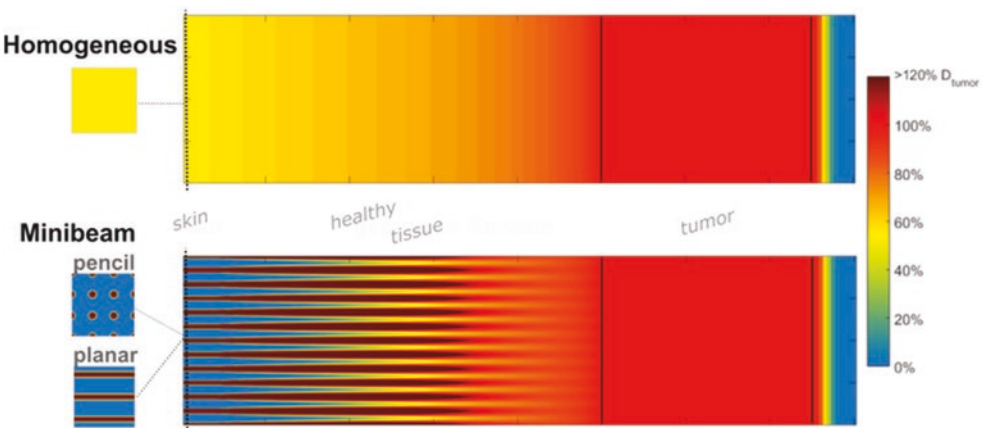

Fig. 6.16 Conceptual therapy plans comparing conventional proton therapy (homogeneous) with pMBRT (Minibeam) for a box-shaped tumor

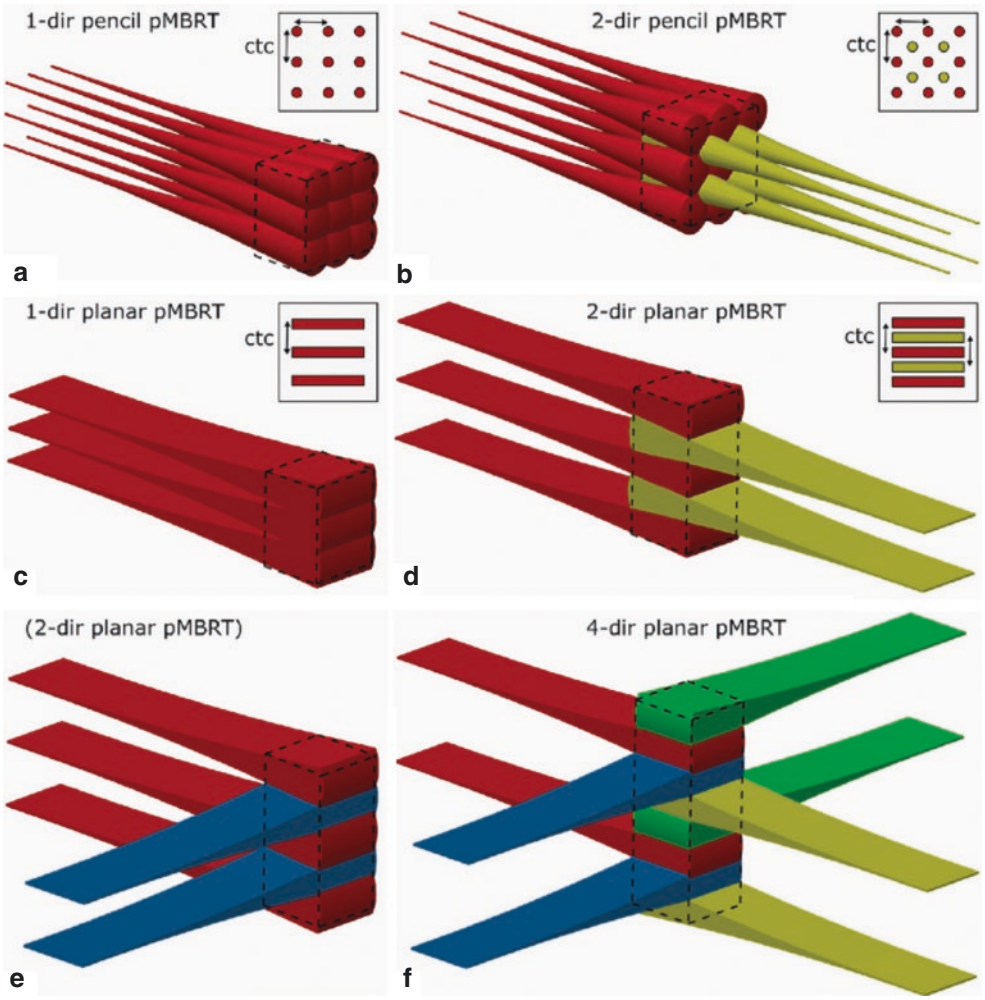

Fig. 6.17 Possible interlacing geometries in MBRT for pencil (**a**, **b**) or planar (**c**–**f**) beams for homogeneous irradiation of a box-shaped tumor (black dashed line). (Reproduced with permission (CCBY) from [119])

lower early and late side effects in the skin of mice and rats [113, 120]. Furthermore, in a rat brain model, it could be shown that less histological and behavioral changes occur after pMBRT [120]. Already tumor treatment was performed in glioma bearing rats, where animal survival could be clearly enhanced while tumor control was kept. First therapy planning in brain tumor patients shows reduced dose to organs at risk, while the same dose distribution in PTV could be achieved (Fig. 6.18) [121]. These promising preclinical results cleared the way for clinical trials. First results on treatment of ten patients treated with pMBRT, called proton GRID therapy, in a clinical study (NCT01255748) show the possible advantages of pMBRT, regarding sparing of healthy tissue and tumor control [122]. Furthermore, the integration of pMBRT to clinical facilities is under investigation and especially the combination with FLASH RT seems promising [113]. An important task which needs to be solved is the production of mini beams with a small enough size without producing secondary radiation, which can harm the patient. The two possible ways of minibeam production are via the focusing of a proton beam or via the use of a collimator. Both methods are complementary, and their use in clinical practice needs to be further investigated.

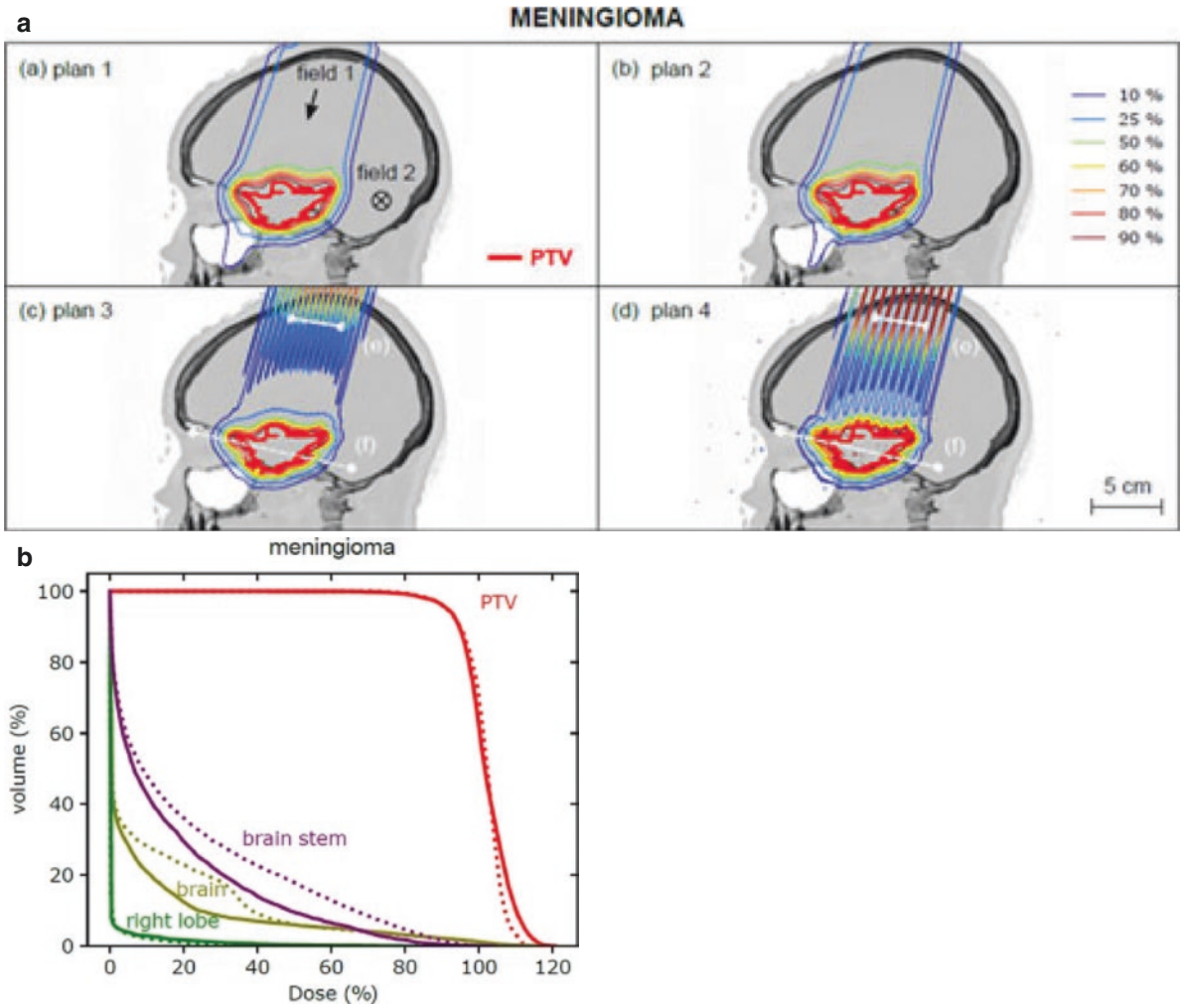

Fig. 6.18 (**a**) Treatment plan comparison of a meningioma patient. Plan 1 and 2 are homogeneous plans, with different planning methods. Plan 3 and 4 show single field pMBRT plans with ctc of 4 mm and 6 mm, respectively. (**b**) Comparison of dose-volume histograms for plan 2 (homogeneous, dashed line) and plan 3 (pMBRT, solid line)

6.7 Brachytherapy Strategies

6.7.1 Brachytherapy

Box 6.14 Brachytherapy

- According to the dose rate brachytherapy can be divided into three types: low dose rate (LDR) with dose rates 0.4–2 Gy/h, medium dose rate (MDR) with dose rates 2–12 Gy/h, and high-dose rate (HDR) with dose rates excessing 12 Gy/h.
- Brachytherapy can be delivered with sealed radionuclide sources and electronic brachytherapy using kV X-rays.
- Brachytherapy is mostly used for treatment of cervix, prostate, and skin cancers and some rare sarcomas.

6.7.1.1 Principles

Brachytherapy is a treatment technique in which radiation sources are placed into the tumor (or the tumor bed to be treated after surgery) or its proximity. For conventional brachytherapy, sealed radionuclide sources are used, but electronic brachytherapy with X-ray has recently become available. The advantage of brachytherapy is a very high dose gradient around the sources, which are, contrary to external RT, extremely close to the treated area. Sharp dose decrease allows for a high level of conformity when dose is delivered locally. However, the technique is available only for easily accessible treatment areas.

The fractionation scheme is different in comparison to the external RT with lower number of fractions and higher doses per fraction.

Usually, radionuclide implants are applied to deliver the treatment which can be either temporary or permanent. The radionuclides need to have convenient physical characteristics (half-life, type of disintegration, mean energy, nominal specific activity, etc.).

Table 6.9 Physical characteristics of radionuclides used for brachytherapy

Characteristic	^{192}Ir	^{60}Co	^{137}Cs	^{125}I	^{103}Pd
Type of disintegration	β^- (95.1%), Electron capture (4.9%)	β^-	β^-	Electron capture	Electron capture
Half-life	73.83 days	5.27 years	30.07 years	59.4 days	17.0 days
Mean gamma energy (keV)	372.2	1252.0	661.7	35.5	137.1
Nominal specific activity ($\times 10^5$ TBq/kg)	3.4	0.41	3.2×10^{-2}	6.5	27
Air kerma-rate constant ($\times 10^{-18}$ Gy m^2/(Bq s))	15	85	6.1×10^{-5}	9.9	9.0

According to the dose rate brachytherapy can be divided into three types: low dose rate (LDR) with dose rates 0.4–2 Gy/h, medium dose rate (MDR) with dose rates 2–12 Gy/h, and high dose rate (HDR) with dose rates exceeding 12 Gy/h (which is 0.2 Gy/min). Higher source energies are used for temporary brachytherapy with HDR sources compared to permanent LDR brachytherapy. Pulsed dose rate (PDR) uses series of short exposures of 10–30 min every hour to approximately the same total dose in the same overall treatment time as with the LDR. Characteristics of frequently used radionuclides are presented in Table 6.9.

Electronic brachytherapy is a non-invasive procedure and is a good option for skin cancers in the facial area, especially around the eye and nose. It is also an option after breast conserving surgery to treat the tumor bed when intraoperative RT is used according to an accelerated partial breast irradiation (APBI) procedure. Kilovoltage X-rays generators are used with voltage potential 30–50 kVp.

6.7.1.2 Main Indications and Modalities

There are several types of brachytherapy depending on the site and organ type to be treated [123].

Intracavitary brachytherapy uses sources that are placed in body or organ cavities. It is mostly used to treat early cervical and uterine (endometrial) cancer, but also in a heterogeneous group of gynecological cancers (ovary, fallopian tubes, body of the uterus, vagina, and vulva). Early rectal cancer can be treated with electron brachytherapy, but the standard of care in rectal cancer is still surgery, especially in case of bulky tumors and more advanced disease, preceded by radio(chemo)therapy.

Interstitial brachytherapy employs sources placed into the tumor, or to its proximity, using needles. It has primarily been used to treat prostate or breast cancer (PCa, BC), but recently it has also been combined with intracavitary brachytherapy to treat bulky cervix tumors. This combination improves coverage of the target volume which was not achievable intracavitary techniques only. PCa brachytherapy can be performed with permanent seeds (for LDR) or temporary sources (for HDR). For breast brachytherapy, interstitial multicatheter brachytherapy is used for boost or partial breast irradiation (PBI)/accelerated PBI (APBI). APBI treats only the lumpectomy bed with 1–2 cm margin, rather than the whole breast [124]. HDR sources are usually applied to deliver prescribed doses of 30.3–34 Gy in 7–10 fractions for APBI and 15–20 fractions with LDR/PDR (pulsed dose rate) or 8.5–10 Gy with HDR for breast boost treatment. Soft tissue sarcomas are sometimes also treated with brachytherapy alone or in combination with external RT after surgery.

When sources are placed into tubular organs such as trachea, lungs, esophagus, or bile duct, the term **intraluminal brachytherapy** is used. For lung cancer, the ability of patients to tolerate bronchoscopy is essential. The main indication is treatment of significant, endotracheal, or endobronchial symptoms. Endobronchial brachytherapy is mainly palliative, however it has been used with curative intent in a small number of cases of early-stage tumors with good results.

Skin cancer can usually be treated by placing the sources on the skin in the desired geometry, therefore it is sometimes referred to as **contact brachytherapy**. Skin cancer is a very common cancer, and brachytherapy is used mainly for areas such as face, scalp, ears, hands, legs, especially when surgery would result in poor cosmetic results or require (extensive) plastic reconstructions. Most cancers are either squamous or basal cell carcinomas. Contact applicators or surface molds can be used. The applied dose is tumor size dependent. For LDR and PDR brachytherapy, doses of 60–66 Gy are delivered to tumors less than 4 cm and 75–80 Gy for those more than 4 cm. For HDR brachytherapy, typical total dose is 30–40 Gy delivered in 8–10 fractions. Other options for skin treatment include superficial X-rays, orthovoltage X-rays, megavoltage photons, or electron beam irradiation.

Ocular brachytherapy can be used to treat uveal malignant melanoma. Currently, the most frequently used radionuclides are I-125, Ru-106/Rh-106, Pd-103, Cs-131.

Intravascular brachytherapy is a rarely used treatment option. It can be used to treat restenosis following percutaneous angioplasty of cardiac arteries. The sources are temporarily placed within cardiac stents in which restenosis has occurred to prevent restenosis. Typically, beta emission sources like P-32, Ir-192, or Rh-188 are used for the treatment. P-32 coated stents have also been used, but with the development of drug-eluting stents, intravascular brachytherapy has lost a lot of its attractivity.

The application of **brain brachytherapy** has decreased a lot since highly conformal RT radiotherapy and stereotactic radiosurgery are available. However, brachytherapy can still be used to treat gliomas with a maximum diameter of 5 cm if not too close to organs at risk.

6.7.1.3 Treatment Course

Three main radiobiology parameters in brachytherapy are dose rate, cell cycle redistribution, and reoxygenation.

Brachytherapy can be used as a single strategy or can be combined with other treatment modalities. When combining brachytherapy with external beam RT, total dose to the tumor and organs and risk must be considered. As an example, for the cancer of the cervix, both radiation treatment modalities are usually combined [125]. In such a case, the doses to the tumor and to the critical organs should be always considered as a summation of radiobiological doses to each structure. The LQ model l is recommended with the concept of equi-effective dose (EQD2) [126]. For simple estimations and HDR brachytherapy, the LQ model without any corrections can be applied to calculated EQD2. However, there are some radiobiological factors relevant to brachytherapy for continuous treatment or for multiple fractions per day. Repair rates (called μ values) are used to correct doses for repair of sublethally damaged cells. Average repair half-lives for mammalian tissues are usually 0.5–3 h. There exists evidence that tumor recovery half-lives are probably shorter than those for late-reacting normal tissues.

In fractionated treatment with HDR, there should be at least 6 or 8 h between individual fractions to enable the cells of normal tissues to repair. HDR brachytherapy delivers treatment with dose rates exceeding 12 Gy/h with 192-Ir or 60-Co sealed sources. Pulsed dose rate (PDR) brachytherapy is fractionated treatment but with a special time schedule. The treatment is delivered with continuous hourly pulses. This approach is supposed to give a similar effect as a hyperfractionation. It was shown that if the time interval between pulses does not exceed 1 h, overall treatment time is not modified, total dose is the same, and the dose rate is not above 0.5–0.6 Gy/h.

Radiobiological modeling demonstrated that the PDR technique rather than continuous LDR radiation allows to exploit differences between the half times for sublethal damage repair ($T_{1/2}$) of late-responding normal tissues and tumors. Repair half times for tumors are estimated to be in the range of 1–2 h, while for late-responding normal tissues, these could be as long as 3–4 h. By matching the pulse frequency with tissue repair kinetics, in a fixed overall treatment time, a therapeutic benefit, i.e., normal tissue sparing while keeping the same tumor control probability, can be obtained relative to continuous LDR radiation. On the basis of those modeling data, an office hours PDR boost regimen was designed for substitution of the continuous LDR boost in breast conserving therapy [127]. A next theoretical study on the optimal fraction size in hypofractionated HDR brachytherapy demonstrated large dependency on the treatment choices (the number of fractions, the overall time, and time between the fractions) and the treatment conditions (reference LDR dose rate tissue repair parameters). The data revealed that hypofractionated HDR might have its opportunities for widening of the therapeutic window for a specific combination of those choices and conditions.

In general, tumor reoxygenation occurs during fractionated treatment. In LDR brachytherapy, the contribution of reoxygenation is low. The lower the dose rate, the lower the oxygen enhancement ratio due to the reduction in sublethal damage repair capability in hypoxic cells.

It is well known that cells have different sensitivity to radiation due to their position in the cell cycle phases. With HDR brachytherapy, delivered in fractions, it can be more difficult to synchronize cells in these cell cycle phases. On the other hand, with LDR brachytherapy the cell distribution in certain cycle phases can be better and earlier synchronized. Cell cycle changes were also observed later for PDR, however, which were more long-lasting and more pronounced [128].

6.7.2 Radioembolization

Box 6.15 Radioembolization

- Radioembolization is based on a vascular selectivity process resulting in a differential effect that leads to a higher concentration of radioactivity within tumor tissue than in non-tumoral liver.
- Treatment course includes several steps, notably a treatment planification process aiming to personalize the activity of radioembolization to administer.
- Radioembolization is commonly used in treatment of primary and metastatic liver diseases.

6.7.2.1 Principle

Yttrium-90 radioembolization, also called Yttrium-90 selective internal radiotherapy (SIRT), is a type of brachytherapy based on intrahepatic arterial administration of yttrium-90 (^{90}Y)-loaded biocompatible microspheres (^{90}Y-microspheres) [129]. Two types of microsphere loaded with 90Y are commercially available: one made of resin (SIR-Spheres®, Sirtex, St. Leonards, Australia) and an alternative made of glass (TheraSphere®, Boston Scientific, Marlborough, MA, USA). The rationale for this approach is that both primary and metastatic tumors in the liver receive their blood supplies primarily from the hepatic artery, whereas the non-tumoral liver (NTL) is fed essentially entirely via the portal vein rather than the hepatic artery [130].

^{90}Y is a therapeutic radionuclide with a physical half-life of 2.67 days (64.05 h) and combined electron (β^-) and positron (β^+) emission. The maximum and average energies of β^- emissions from ^{90}Y are 2.28 MeV and 934 keV, with a mean tissue penetration of 4.1 mm and a maximum of 11 mm. As in other RTs, ^{90}Y β^- absorbed dose deposition induces direct or indirect damage to DNA in exposed tissue, leading to early or delayed cellular death [130]. To avoid

serious adverse events such as radiation pneumonitis secondary to lung contamination via hepato-pulmonary shunts or radioembolization-induced liver disease (REILD), the irradiation of liver malignancies is limited by unintended exposure to NTL and lung parenchyma.

Although the branching ratio is very low, the β^+ emission enables ^{90}Y-microsphere positron emission tomography (PET) imaging after radioembolization. It is also possible to image the ^{90}Y-microsphere distribution based on the β^- bremsstrahlung emission spectrum by bremsstrahlung emission computed tomography (BECT).

Therefore, the efficacy of radioembolization is based on a vascular selectivity process resulting in a differential effect that leads to a higher concentration of radioactivity within tumor tissue than in NTL. The stronger the differential effect, the more effective the treatment will be. Due to their size, the tumor's vascular properties, and the hemodynamics of the vascular system used for targeting, ^{90}Y-microspheres are permanently implanted into the micro-vessels of the tumor/NTL without any biological degradation (although physical decay of ^{90}Y still occurs).

6.7.2.2 Main Indications

Radioembolization has been broadly adopted as a locoregional therapy for advanced primary or metastatic liver disease [129, 130]. The most common indications for radioembolization are hepatocellular carcinoma (HCC), liver metastases from colorectal cancer (mCRC), intrahepatic cholangiocarcinoma (IH-CCA), and neuroendocrine tumors (NET) [129, 131]. Very little scientific evidence (level 1 or 2) derived from prospective randomized controlled trials supports the use of radioembolization as a first- or second-line treatment option in various treatment algorithms. Prospective data have been obtained for HCC and mCRC patients, and prospective studies in IH-CCA and NET are underway [132]. In the HCC management guidelines for the European Association of Medical Oncology (ESMO), radioembolization is considered as the last-line treatment. The ESMO guidelines for the management of mCRC patients include radioembolization as a second-line treatment for patients with liver-limited disease in whom the available chemotherapeutic options have failed.

6.7.2.3 Treatment Course

The treatment course, illustrated in Fig. 6.19, includes several steps [132]:

- First, patients are selected for radioembolization by the multidisciplinary tumor board, based upon individual characteristics. Radioembolization requires a holistic view of the patient and the disease. Disease stage, long-term and immediate treatment aims, morphological features [assessed using computed tomography (CT) or magnetic resonance imaging (MRI)], metabolic/functional properties [e.g., assessed using [^{18}F]-fluorodeoxyglucose (^{18}F-FDG) hybrid PET coupled with CT (PET/CT) imaging], and biological characteristics of the tumor, and the surrounding liver are all considered when establishing a radioembolization treatment plan.
- Then, a pre-treatment 3D hepatic CT angiogram is performed. The goal is to decide into which artery the ^{90}Y-resin microspheres will be injected and to determine the best catheter position to optimize the selectivity of treatment.
- To simulate the treatment, a 2D hepatic angiogram is performed, generally accompanied by a 3D cone-beam CT (CBCT). The catheter is placed at the position defined by the 3D CT angiogram, and ^{99m}Tc-labeled macroaggregated-albumin (^{99m}Tc-MAA) is injected into the hepatic artery. Given the similar median size of MAA particles (10–50 μm) and resin microspheres (20–60 μm), the MAA distribution pattern serves as a surrogate for how ^{90}Y-microspheres will localize.
- To visualize the distribution of ^{99m}Tc-MAA, planar scintigraphy, generally accompanied by hybrid single-photon emission CT and CT imaging (SPECT/CT), is acquired within 2 h after administration. This allows validation of the catheter position, identification of potential extrahepatic visceral contamination, and evaluation of the lung shunt and the targeting of the lesions; in addition, it can be used to determine the activity to administer in future therapy. This practice prevents post-therapy complications and selects patients with a good potential outcome.
- After this pre-treatment phase, treatment with ^{90}Y-microspheres is performed according to the pre-treatment catheter position and prescribed activity. With catheter-directed therapies such as radioembolization, it is important to verify that the position/location of the catheter during the ^{99m}Tc-MAA simulation is consistent with the position during the administration of ^{90}Y-microspheres to best reproduce the MAA distribution.
- Following administration of ^{90}Y-microspheres, a qualitative and quantitative assessment is performed (1) to verify that the treatment was performed as planned and identify any technical failures and (2) to detect any possible extrahepatic activity, which could cause serious complications such as gastrointestinal bleeding. Post-radioembolization imaging of ^{90}Y distribution may be performed using hybrid ^{90}Y-PET/CT or ^{90}Y-BECT/CT. However, many studies show qualitatively superior resolution and contrast with ^{90}Y-PET/CT relative to ^{90}Y-BECT/CT, and only ^{90}Y-PET/CT is available for quantification in clinical routine (^{90}Y-BECT/CT quantitative imaging is still under development).
- Finally, treatment response is evaluated. Clinical and biochemical assessment after radioembolization for any sig-

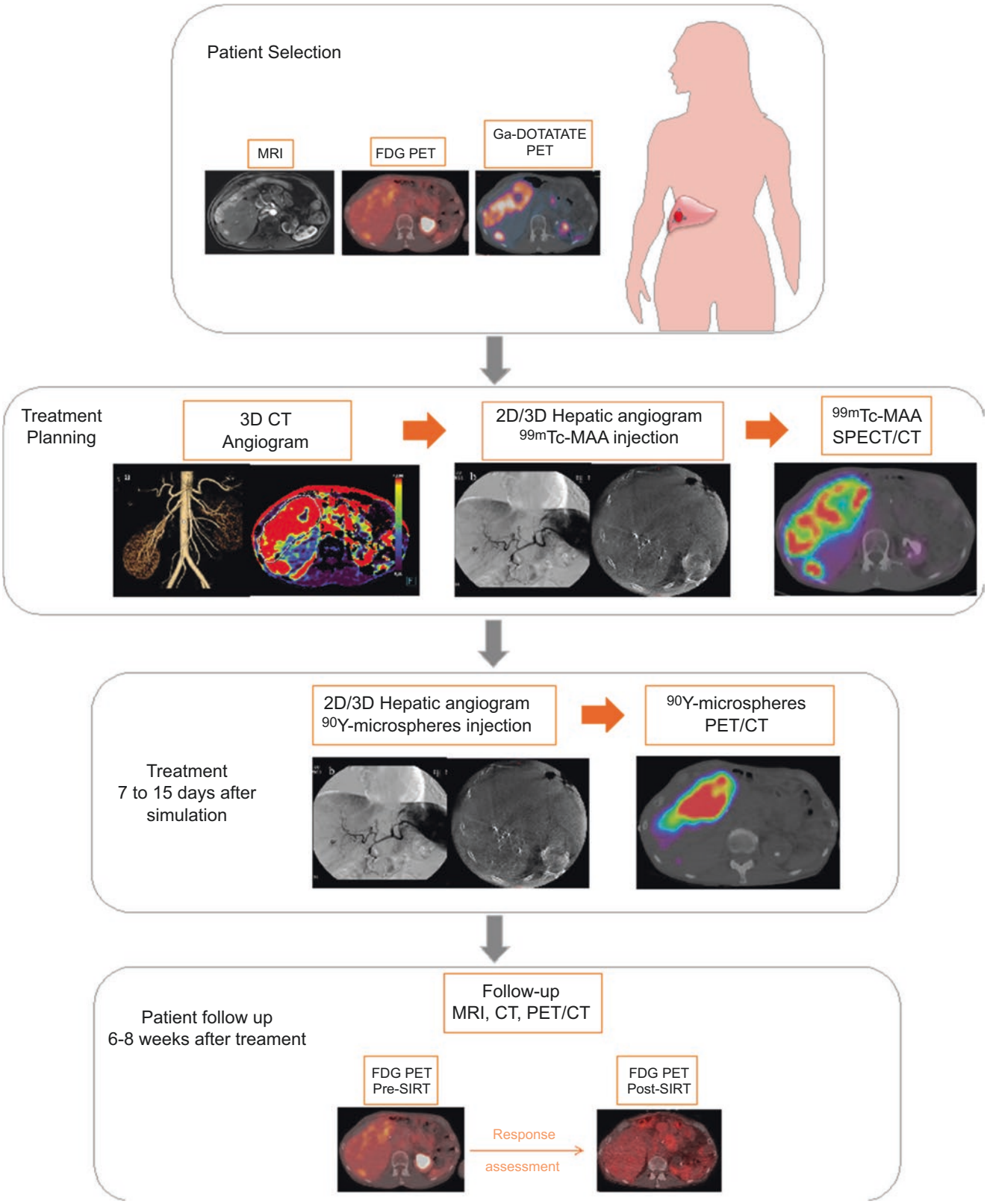

Fig. 6.19 ^{90}Y-resin microspheres radioembolization treatment course. Example of a patient treated for neuroendocrine neoplasia

nificant side effects is typically performed 1–2 months post-radioembolization. Imaging assessment of the tumor response should be performed 1–3 months post-radioembolization and every 2–3 months thereafter. The clinically relevant "treatment response," and thus the most suitable imaging technique, is defined differently depending on the type of tumor (e.g., variable ^{18}F-FDG avidity) and treatment intent (e.g., bridging-to-surgery, downstaging, etc.) [131].

6.7.2.4 Therapeutic Intent

Oncological Ambition

Curative setting: Radioembolization can be used in a preoperative setting (for solitary or limited-multifocal/oligometastatic tumor) when the ambition is to cure the patient. It can be used as bridging-to-surgery, to stabilize or slow down tumor growth and multiplicity thereby keeping a patient as a potential surgical candidate for liver resection or transplantation. Alternatively, radioembolization can be applied as a downstaging approach to induce a clinical shift from a non-resectable stage to a potentially resectable or transplantable stage by decreasing tumor size or number [129, 130].

Non-curative setting: In patients with advanced multifocal bilobar/lobar tumor distribution in whom curative approaches are not feasible, radioembolization can be used alone or in combination with other therapies as a life-prolonging treatment and palliative care [129, 130].

Radioembolization Field of Treatment

Whole-liver treatments: In the case of bilobar multifocal tumor distribution, the whole liver must be treated. Single injection within the common hepatic artery or a bilobar (left and right hepatic artery) approach is performed. The bilobar approach can be performed on the same day or staged (i.e., on separate days).

Lobar and segmental treatments: Unilobar or segmental treatments are considered when the disease is limited to a unique lobe or a segment. These approaches enable the preservation of the untreated liver, and if some loss of function in the treated lobe/segment is permissible, they allow more aggressive treatment.

Lobectomy and Segmentectomy: Radiation lobectomy, with the intent to induce contralateral lobe hypertrophy while achieving tumor control, may be considered in patients with unilobar disease and a small anticipated future liver remnant in an attempt to facilitate curative surgical resection.

Radiation: segmentectomy may be considered for localized disease (one or two segments) supplied by a segmental artery that is not amenable to other curative therapies because of tumor localization or patient comorbidities.

6.7.3 Personalized Radioembolization

Until recently, the prescription of 90Y-microspheres was based upon the body surface area method (resin microspheres) or on a dose limit to the whole treated liver volume without distinction between tumor and non-tumoral liver (glass microspheres). Both approaches lead to inherent risks of under- or overdosing, with considerable interpatient variations [130, 132]. To tackle those pitfalls, the concept of personalized radioembolization has recently emerged and provides an optimal framework to improve patient selection and maximize tumor response while sparing non-targeted tissues undesired toxicities. The patient-specific definition of a radioembolization therapeutic window is now assessed by integrating multidisciplinary teamwork, multimodal imaging techniques, advanced treatment planning algorithm, and by considering relationships between radiation dose and treatment outcomes. Precision radioembolization with dosimetry is now recommended as the standard approach in recent international recommendations [132, 133]. Recently, a prospective randomized phase II clinical study in HCC, the DOSISPHERE-01 trial, provided the first level one scientific evidence that personalized radioembolization significantly improves overall survival compared to the standard semi-empirical approach [134].

6.8 Radionuclide Therapy

The concept of using radiation to treat cancer and other diseases found its origin in the discovery of X-rays in 1895. After Pierre and Marie Sklodowska-Curie discovered radium as a source of IR further interest was sparked. However, it wasn't until the 1950s that external beam radiation became a key treatment modality for cancer. Since then, external beam RT has become one of the most efficient tools for treatment of locally confined cancers. However, its effect is limited for treatment of more advanced and disseminated disease. In the early twentieth century, first potential for using Iodine-131 as a targeted therapeutic was discovered by nuclear pioneers such as Saul Hertz [135]. This discovery was the start of the field of radionuclide therapy and today, several types of radionuclide therapy exist. Each of the different types will be discussed in this section.

6.8.1 Introduction to Radiopharmaceuticals

Cancer cells often express certain molecules on their membrane surface, called receptors, which are not or to a lesser extent present on healthy cells. These receptors on cancer cells can be targeted by several molecules, being a peptide, small molecule or (parts of) antibodies, which will be termed as the ligand. When talking about radiopharmaceuticals, the cancer-targeting moiety is linked to a chelator molecule, responsible for entrapping a radionuclide into the structure as shown in Fig. 6.20.

As already explained in Chap. 2, based on the purpose of the radiopharmaceutical, being diagnostic or therapeutic, different radionuclides can be used. For diagnostic purposes, gamma (γ)-emitting radionuclides are used. Radionuclides that are usually used for therapy are alpha (e.g., actinium-225), beta (e.g., lutetium-177), or Auger electron (e.g., iodine-125) emitters.

Upon binding of the ligand to its receptor, the radioligand complex gets internalized. Upon internalization, the radionuclide will emit its toxic IR from inside the cell and cause damage to cellular structures including DNA and cell membrane, resulting in cancer cell death, as shown in Fig. 6.21.

Radioligand therapy (RLT) can in theory be used to target any type of cells (over)expressing the target molecule and can thus be used to attack multiple (micro) metastases instead of only targeting the primary tumor, in contrast to external beam RT (EBRT) that focus on one or several, geographically limited target volumes. Furthermore, RLT enables specific targeting of cancer lesions (including metastatic cancer cells), while causing minimal damage to surrounding healthy tissues and thus minimizing the amount of side effects [136] (Box 6.16).

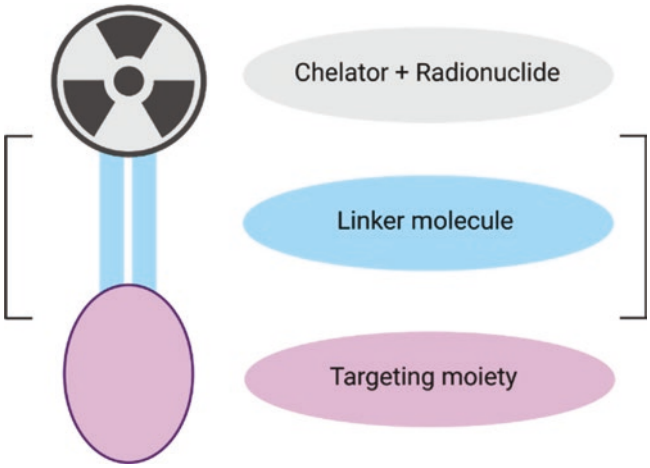

Fig. 6.20 Schematic representation of the structure of a radiopharmaceutical. The purple circle represents the cancer-targeting moiety, which can be a peptide, small molecule, or antibody. This targeting moiety is connected to a chelator (blue circle) entrapping a radionuclide (for diagnostics or therapy) directly to the targeting moiety or via a linker molecule (grey)

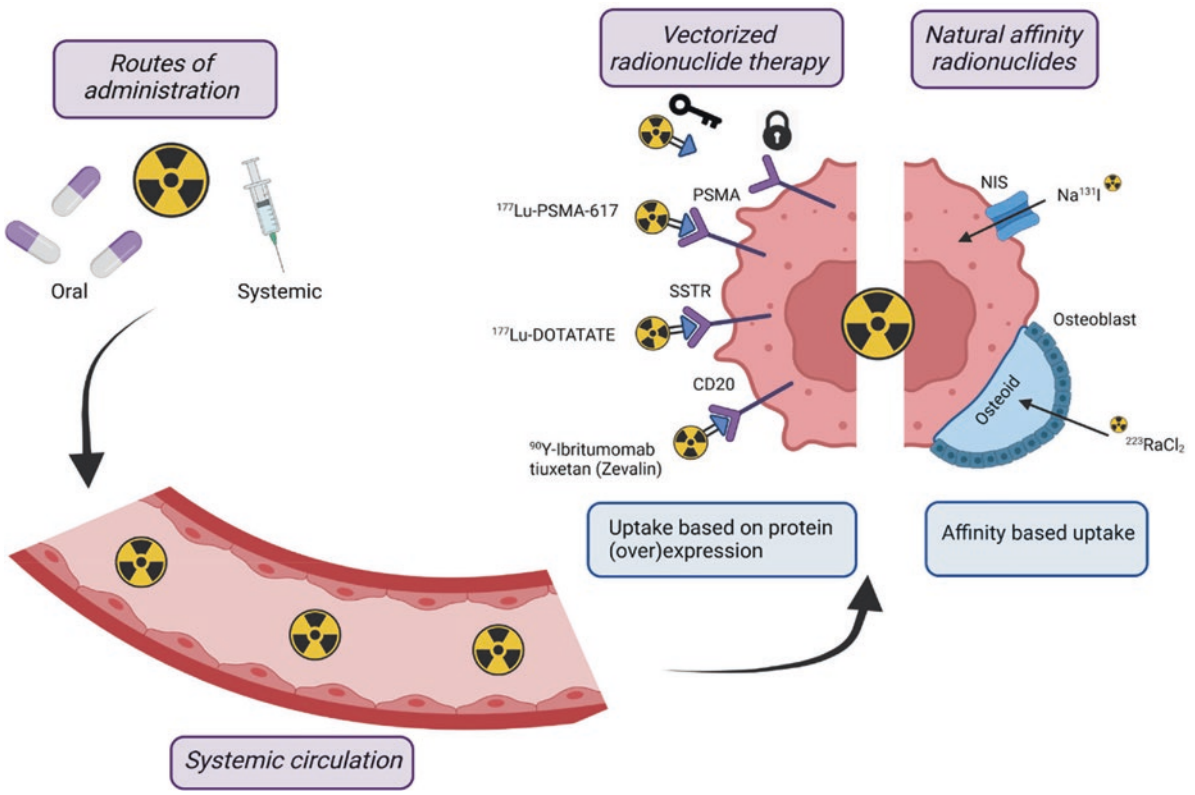

Fig. 6.21 Overview of the general principle or radioligand therapy. A radionuclide (either ingested orally or injected systemically) will enter the bloodstream. Via the bloodstream, the radionuclide will find its way to the target tissue either through its natural affinity for the target tissue (i.e., the natural affinity radionuclides) or via expression of certain molecules on the target tissue (i.e., vectorized radionuclide therapy)

Box 6.16 Radionuclide Therapy

- Human cancers express molecules on their membrane surface that can be targeted for therapy.
- A radioligand is comprised of a cancer-targeting moiety (small molecule, peptide, or (part of) antibody) linked to a chelator entrapping the radionuclide.
- Radioligand therapy enables specific targeting of cancer cells, with minimal harm to surrounding healthy tissues.

6.8.2 Radiotheranostics Approaches

Theranostics, the combination of therapy and diagnostics, is emerging in personalized medicine approaches. The main goal is to use diagnostic imaging to follow-up (radio)therapeutic interventions and improve or alter them along the way, thereby increasing efficacy and limiting toxicological effects. The ideal theranostic pair, i.e., for imaging or therapy, respectively, has the same pharmacokinetics, meaning that the pair should be distributed, metabolized, and cleared similarly [137]. If this is the case, the diagnostic counterpart can be used to accurately determine the accumulation and absorbed dose in different organs, including tumor, that would result upon injection of the therapeutic radiopharmaceutical. The imaging thus further allows selection of patients with high probability of response to the therapy (i.e., predictive biomarkers) and can provide guidance on the total activity of the therapeutic counterpart to be administered. It can also be used for treatment response evaluation in follow-up. Several therapeutic radionuclides (e.g., ^{177}Lu, ^{131}I) intrinsically decay via both particle- and γ-emission which can be used for both imaging and therapy that said after administration of vastly different injected activities [137]. Different radioisotopes of the same element have the greatest theoretical appeal to use in the theranostic approach. Examples are the radioisotopes of iodine ($^{123/124/131}$I), terbium ($^{149/152/155/161}$Tb), and yttrium ($^{86/90}$Y) [138]. Although the biological behavior of these radiopharmaceuticals will be similar, the use in clinical practice might be limited due to unfavorable decay properties, long $T_{1/2}$, availability, and cost of production. In this respect, radiopharmaceuticals which use the same vector molecule but different radiometals are often applied for this purpose as they have similar pharmacokinetics. A prime example is the somatostatin receptor targeting vector DOTATATE, which can be radiolabeled with the PET radionuclide ^{68}Ga and the therapeutic radionuclide ^{177}Lu, harnessing the diagnostic potential of PET (which have higher resolution and sensitivity for radioactivity) to enable efficient therapeutic approaches [139]. Of note, current efforts are being made to include [^{18}F]AlF into the armamentarium to eventually replace ^{68}Ga [140].

Radiotheranostics is being applied to the different branches of radiopharmaceutical development, including radioimmunotherapy (with, for example, nanobodies, antibodies, or similar affinity reagents), peptide receptor radionuclide therapy, radiolabeled microspheres/nanoparticles, and small molecules. This combination of therapy and diagnostics can help to reduce the toxic side effects by appropriate patient selection and determination of administered activity. The benefit and safety of using repeated treatment have also been proven in several studies.

A key aspect to note is the uptake and retention of the radionuclides at the target site. Logically, tumor-to-background ratios should be as high as possible for both diagnostic and therapeutic radionuclides. However, diagnostic imaging is typically performed in a time scale of several minutes to 1 h and thus optimally, radionuclides with a short $T_{1/2}$ should be applied. On the other hand, radionuclides with a longer $T_{1/2}$ are typically used for therapy, which can result in a more selective tumor irradiation, with higher dose to the tumor than to the healthy tissues (Fig. 6.22). The most important requirement for a therapeutic radiopharmaceutical is to

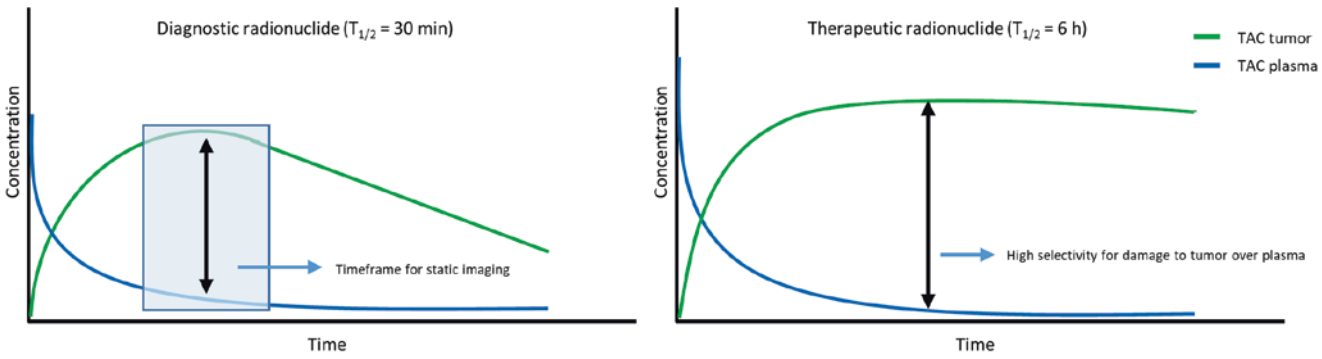

Fig. 6.22 Hypothetical representation of time-activity curves (TACs) of a vector radiolabeled with a diagnostic ($T_{1/2}$ = 30 min) and therapeutic radionuclide ($T_{1/2}$ = 6 h)

have a high ratio between the integral of the time-activity curve (previously known as the residence time) of the tumor vs. normal organs (Box 6.17).

Box 6.17 Radiotheranostics

- The theranostic approach makes use of diagnostic and therapeutic nuclear medicine.
- Theranostics utilizes different isotopes of the same element.
- Therapeutic radiopharmaceuticals can use radionuclides with a longer half-life compared to diagnostic radiopharmaceuticals.
- Radiopharmaceutical vector molecules can include peptides, antibodies, nanobodies, nanoparticles, and small molecules.

6.8.3 Natural Affinity Radionuclides

6.8.3.1 Principles

To obtain specific targeting, a radiopharmaceutical usually comprises a moiety capable of binding a cancer-specific overexpressed entity (e.g., a receptor, an enzyme, a transporter, etc.). However, this is not always required as certain elements show a natural affinity for certain tissues. Examples are iodine, which is concentrated in the thyroid gland, and radium, a calcium mimetic naturally taken up in remodeling bone. This enables specific targeting of these tissues without the need for elaborate organic chemistry nor radiochemistry.

Radiopharmaceutical development started with the research of Hamilton and Soley into diagnosis and treatment of thyroid disease. In the thyroid gland, iodine plays an important role in the production of thyroid hormones, which in turn have important functions in the human body. Naturally, because of the importance of iodine for the thyroid gland, all ingested iodine is taken up by the thyroid gland, where it is converted into iodide and remains trapped. Radioactive iodine (iodine-131) can be used to treat thyroid diseases because the thyroid gland is not able to distinguish between the stable iodine (iodine-127) and its radioactive isotope. Like stable iodine, iodine-131 is concentrated in the thyroid gland after ingestion. Treatment of thyroid disease using iodine-131 in the form of sodium-iodine ($Na^{131}I$) can be considered as a historic pillar of radiopharmaceutical design as the usage of $Na^{131}I$ has paved the way for further radiopharmaceutical development.

The primary site for metastasis in prostate cancer (PCa) is the bone, resulting in severe morbidity due to so-called skeletal related events (e.g., fractures) and bone marrow failure. To control the disease in castrate-resistant PCa patients, the Food and Drug Administration (FDA) approved radium-223 chloride ($^{223}RaCl_2$, Xofigo®) for treatment of bone metastasis in 2013. Radium-223 is an alpha-emitting radionuclide that accumulates in bone areas with increased bone turnover due to its similarity with calcium ions and its capability to form complexes with hydroxyapatite (which is the mineral component of bone). In the decay process of radium-223 to the stable lead-207, four alpha particles and two beta-particles are generated which induce local damage to bone sites with increased bone turnover, such as areas of bone metastasis.

6.8.3.2 Main Indications and Therapeutic Intent

$Na^{131}I$ is administered in patients suffering from benign thyroid disease such as an overactive thyroid (autonomic hyperthyroidism, Graves' Disease), goiter (enlarged thyroid), or well differentiated thyroid cancers (papillary or follicular thyroid cancer). The thyroid incorporates iodide in two forms of thyroid hormones, triiodothyronine (T3) and thyroxine (T4). These hormones control metabolism and protein synthesis. An overactive thyroid leads to increased metabolic rate, sweating, fatigue, tachycardia, intestinal problems, and other life debilitating issues. As iodide is taken up in the thyroid in large excess, it is a valuable approach in treating an overstimulated or enlarged thyroid. Due to the high uptake via the intestinal tract, $Na^{131}I$ is administered per os. Iodine-131 is taken up by the sodium-iodide symporter into the thyroid cells and will subsequently irradiate the thyroid cells. One potential side effect of this treatment is a complete loss of thyroid function (hypothyroidism), which can result in the necessity for daily lifelong thyroid hormone (levothyroxine) substitution. The occurrence of hypothyroidism depends on the type of indication, with a low fraction seen in autonomic disease but with a 100% occurrence in patients treated for thyroid cancer (with treatment occurring post-thyroidectomy to ablate the so-called remnant). Of note, these pills are generally inexpensive and are taken per os once daily [141].

To date, $^{223}RaCl_2$ is the only alpha-emitting radiopharmaceutical that has been FDA approved and is now in routine clinical use for treatment of bone metastasis in patients with metastatic castration-resistant prostate cancer. The ALSYMPCA phase III clinical trial investigated safety and efficacy of $^{223}RaCl_2$ compared to placebo (i.e., saline injection). The results of this trial led to the FDA approval of $^{223}RaCl_2$ for patients with metastatic castration-resistant prostate cancer with symptomatic bone metastasis as this clinical trial showed that treatment was well-tolerated, prolonged overall survival, and improved the quality of life of patients [142, 143].

6.8.3.3 Treatment Course

$Na^{131}I$ is typically administered as a pill or in rare cases as a liquid per os. The required activity to treat hyperthyroidism is typically small (148–370 MBq). Usually one treatment cycle will suffice to have a satisfying effect on the thyroid function after 2–3 months [144]. For patients suffering from differentiated thyroid cancer, the administered activity depends on the disease stage (after previous resection in so-called remnant ablation, used as adjuvant therapy, metastatic disease) and can range from 1.1 to 7.4 GBq [145]. Before treatment, patients need to have sufficient blood levels of thyroid-stimulating hormone (TSH) (TSH > 30 mU/L), by stopping uptake of thyroid hormone supplements or by injections of recombinant THS, to increase the uptake of the administered iodine radioisotope. Several days after treatment, a post-therapy scintigraphy is made to document the targeting of thyroid tissue and to detect potential metastatic disease. After ablation, levothyroxine treatment is started to compensate for the loss of thyroid function. Afterwards follow-up is necessary to assess therapy response and to rule out recurrence, with regular determination of thyroid function, thyroglobulin, and thyroglobulin antibodies.

Radium-223 dichloride is injected intravenously in adult patients with castration-resistant prostate cancer with bone metastases. The treatment schedule comprises six injections of 55 kBq per kg body weight at 4-week intervals. A single complete blood count is performed 10 days prior to administration of a treatment cycle. An additional complete blood count might be performed 2–3 weeks after administration if necessary. Clinical follow-up complemented with bone scintigraphy and CT is the cornerstone of follow-up, but with more recent evidence pointing to the utility of also modern imaging tools such as PET/CT or MRI. Several biomarkers, including prostate-specific antigen, lactate dehydrogenase, and alkaline phosphatase, might be checked during the treatment course to monitor treatment response, but they are not considered to be reliable indicators of treatment response.

6.8.4 Vectorized Radionuclide Therapy

6.8.4.1 Peptide Receptor Radionuclide Therapy

Principles

Peptide receptor radionuclide therapy (PRRT) consists of the injection of a tumor-targeting peptide into the systemic circulation of a patient. This radiopharmaceutical will subsequently bind to a specific peptide receptor leading to tumor-specific retention. Several receptors have been studied over the last few years, including the somatostatin receptor (SSTR), glucagon-like peptide-1 receptor, cholecystokinin type 2, and melanocortin receptors. At present, SSTR is the only target that is used in routine clinical practice. The SSTR is overexpressed on a range of tumors, including neuroendocrine tumors (NETs), which arise from neuroendocrine cells present in a range of organs (e.g., gastrointestinal tract, pancreas, and bronchi) and neural-crest derived tumors (e.g., pheochromocytoma, paraganglioma, neuroblastoma). Humans have five subtypes of SSTRs, with subtype 2 being the most important for theranostics. The randomized controlled trials PROMID and CLARINET have proven that treatment with non-radioactive somatostatin analogues (SSAs) leads to an antiproliferative effect in metastatic enteropancreatic NETs. In the late 1980s and early 1990s, the Rotterdam group uncovered the potential of using the SSTR for radionuclide-based imaging and demonstrated that radiolabeled SSAs have a high uptake and retention in tumoral tissue and a limited uptake in normal, mainly endocrine, organs. An interesting therapeutic avenue was explored: treatment of SSTR-positive tumors with radionuclide therapy (RNT). Several radiopharmaceuticals were developed in the last two decades including the first generation ^{111}In-pentetreotide (an Auger emitter), the second generation ^{90}Y-DOTATOC (a high-energy β^--emitter), and the third generation ^{177}Lu-DOTATATE (a low-energy β^--emitter and a γ-emitter). A major benefit of lutetium-177 is that its decay is associated with γ-emission, which allows imaging and dosimetry of absorbed doses to tumors and risk-organs (e.g., kidneys and bone marrow). The combination of the high-energy yttrium-90 β^--emitter for targeting lesions with a larger size and/or heterogeneous uptake (with more crossfire effect), and the medium-energy lutetium-177 emitter/γ-emitter for targeting smaller lesions (with a higher fraction of the total energy deposited within the tumor itself, and not in the surrounding tissue), is called "tandem or duo PRRT." Theoretically, a synergistic effect can be achieved by combining these two radionuclides with different absorption properties, but RCTs are awaited to demonstrate the superiority of this concept before widespread clinical use can take place. At present, ^{177}Lu-DOTATATE is considered the clinical standard and is the only radiopharmaceutical approved for PRRT by the American Food and Drug Administration (FDA 2018) and European Medicines Agency (EMA 2017). A promising fourth generation of PRRT-radiopharmaceuticals is emerging, with the entrance of α-emitters in the radionuclide therapy scene. PRRT α-emitters include ^{213}Bi-DOTATOC, ^{225}Ac-DOTATATE, and ^{212}Pb-DOTAMTATE. Preliminary clinical results provide proof-of-principle evidence that α-PRRT can overcome resistance to β-PRRT, reflected by higher objective response rates (ORRs) in favor of α-emitters [146].

Main Indications and Therapeutic Intent

Patients with advanced NET and clinical, biochemical, and/or radiological disease progression after first-line treatment

with SSA are eligible for second-line treatment with PRRT if sufficient tracer uptake on a so-called theranostics SSTR scintigraphy is present. The development of PRRT and its clinical trials were academia-driven which contrasts with the current novel anticancer drugs which are mainly pharma industry-driven. For a long period, no standard radiopharmaceutical or standard regimen was determined, which explains the heterogeneous literature involving PRRT [146]. At present, the only published randomized controlled trial with ^{177}Lu-DOTATATE is the phase III NETTER-1 trial, which included patients with advanced midgut NETs. One hundred sixteen patients were randomized to the PRRT arm (4 cycles of 7.4 GBq ^{177}Lu-DOTATATE plus best supportive care including octreotide long-acting repeatable (LAR) 30 mg) and 113 patients were randomized to the control arm (octreotide LAR 60 mg). An ORR of 18% was seen in the ^{177}Lu-DOTATATE group versus 3% in the control group ($p < 0.001$). An estimated progression-free survival (PFS) at 20 months of 65.2% (95% confidence interval (CI): 50.0–76.8%) was achieved in the PRRT arm and 10.8% (95% CI: 3.5–23.0%) in the control arm, with a hazard ratio for progression or death of 0.21 (95% CI: 0.13–0.33; $p < 0.001$) [147]. The final overall survival (OS) analysis revealed a median OS of 48 months in the ^{177}Lu-DOTATATE group versus 36.3 months in the control group. This difference was not statistically significant but can be considered as clinically significant. The lack of statistical significance was most likely caused by a high rate (36%) of crossover of patients in the control group to PRRT after progression. In addition, the NETTER-1 trial has confirmed that PRRT causes a significant improvement in the quality of life of patients and aids to substantially reduce tumoral symptoms (e.g., abdominal pain, diarrhea, and flushing) [146].

Treatment Course

The eligibility for PRRT is determined via mandatory pretreatment SSTR imaging, preferentially by SSTR PET, blood analysis, and clinical evaluation. ^{18}F-FDG PET/CT provides additional information, and all lesions should show sufficient SSTR expression, in particular the ^{18}F-FDG-avid ones. The conventional treatment schedule for ^{177}Lu-DOTATATE is based on the Rotterdam/NETTER-1 protocol. This consists of four cycles of 7.4 GBq administered in 8-week intervals. Nephroprotection is performed by administering a co-infusion of an amino acid solution during PRRT-administration; this solution will reduce renal uptake of the radiopeptide by ~25–50%. Acute side effects include nausea and vomiting which are provoked by the co-infusion of the nephroprotective amino acids and which can be controlled by an antiemetic treatment. Four to six weeks after each cycle of PRRT, a blood analysis and clinical evaluation are performed. After completion of the four cycles PRRT, further follow-up with SSTR and ^{18}F-FDG PET/CT, blood analysis, and clinical evaluation are warranted. The most severe long-term side effect of PRRT is the development of persistent hematological dysfunction (PHD) caused by bone marrow irradiation. However, PHD after PRRT has a low incidence of 1.8–4.8%, with a median latency of 41 months after completion of the treatment [146]. Other subacute (occurring within days/week) side effects include subacute myelosuppression (typically mild and transient), fatigue, and hair loss. Long-term side effects, besides PHD, are kidney failure, observed in up to 9.2% of patients treated with ^{90}Y-DOTATOC and <1% in patients with ^{177}Lu-DOTATATE [148, 149]. In patients with good response after a first PRRT regimen, with disease control for at least a year, a novel course of PRRT can be administered with ^{177}Lu-DOTATATE, called "salvage PRRT," if the patient's organ function is still adequate and SSTR expression is still present on all lesions. As such, PRRT has proven to be an adequate treatment in patients with advanced NETs. Several promising prospective trials are ongoing to further optimize PRRT (e.g., α-emitters, individualized dosimetry, and SSTR-antagonists) (Box 6.18).

Box 6.18 Peptide Receptor Radionuclide Therapy (PRRT)

- PRRT consists of the injection of a tumor-targeting radiolabeled peptide, which will subsequently bind to a specific receptor leading to tumor-specific binding and retention.
- Several radiopharmaceuticals were developed in the last two decades, with the third generation ^{177}Lu-DOTATATE being the current clinical standard and the only radiopharmaceutical approved for PRRT by the FDA and EMA.
- Multiple promising prospective trials are ongoing to further optimize PRRT (e.g., α-emitters, individualized dosimetry, and SSTR-antagonists).

6.8.4.2 Radioligand Therapy

Principles

At present, another well-known example of radioligand therapy (RLT) has demonstrated a significant survival benefit in patients with metastatic castration-resistant PCa. [^{177}Lu]Lu-PSMA-617 is a prostate-specific membrane antigen (PSMA) targeting small molecule consisting of PSMA-617 with the β^--emitting radionuclide lutetium-177 (Fig. 6.23). The PSMA-617 binds to the enzymatic pocket of PSMA after which it is internalized, resulting in the delivery of toxic doses of IR to PCa cells. The VISION trial has demonstrated

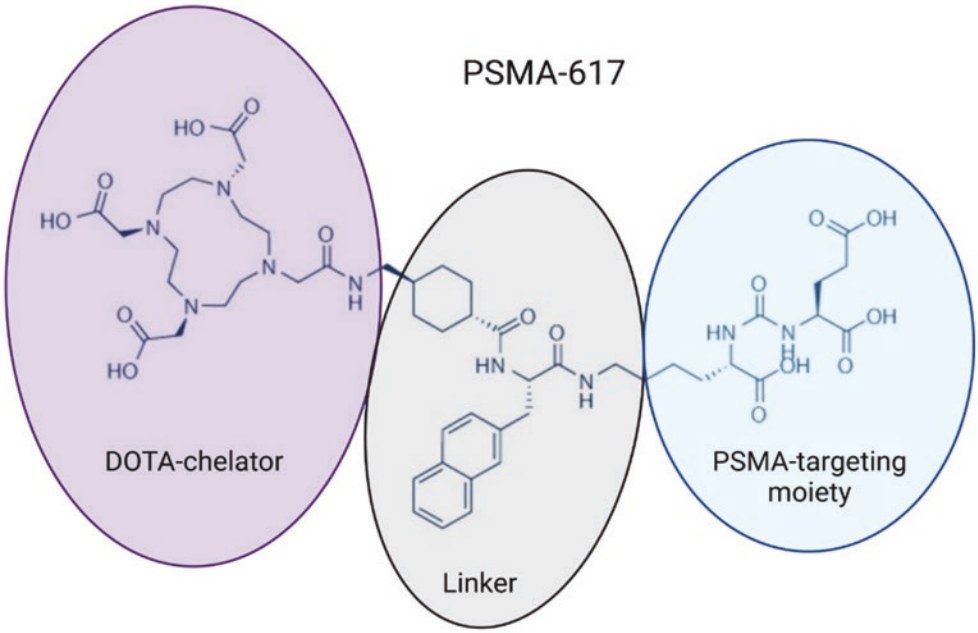

Fig. 6.23 Schematic representation of the structure of the PSMA-targeting compound PSMA-617. The blue circle shows the PSMA-targeting moiety. The purple circle highlights the DOTA-chelator used to entrap radionuclides. The grey circle represents the linker molecule that connects the PSMA-targeting moiety with the DOTA-chelator

a significant increase in imaging-based PFS and OS in a randomized controlled trial where it was compared to standard of care (i.e., chemotherapy, RT and ADT), resulting in the FDA approval of [^{177}Lu]Lu-PSMA-617 for patients with metastatic castration-resistant PCa in March 2022 [150]. Since PSMA poses such an interesting target for RLT, due to the high overexpression on PCa cells, more PSMA-targeting radioligands are currently under clinical investigation, as summarized in Table 6.10.

The development of RLT is not strictly limited to PCa and targeting PSMA. Several other compounds with other targets are also undergoing clinical trials. One such target is the bombesin receptor family. Many common tumors, including breast, prostate, and lung cancer, show overexpression of one of the bombesin receptors, resulting in the development of several compounds targeting this receptor family [151]. Compared to the development of PSMA-targeting compounds, the development of bombesin-targeting agents is still in its infancy as illustrated in Table 6.10 by the limited number of compounds undergoing clinical investigation. Thus, at present, research into bombesin-targeting compounds remains largely preclinical.

Besides PSMA and bombesin, other targets can also be used for RLT of a variety of human cancers. Other examples of clinical trials of radioligand therapy using other targets are summarized in Table 6.10.

Main Indications and Therapeutic Intent

At present, [^{177}Lu]Lu-PSMA-617 is FDA approved in PCa patients with metastatic castration-resistant disease in whom standard treatments, including hormone deprivation therapy

Table 6.10 Examples of RLT compounds under clinical investigation

Compound	Clinical trial phase	Trial number[a]	Disease
PSMA-targeting RLT			
[^{177}Lu] Lu-PSMA-617	Phase III	NCT03511664	Metastatic castration-resistant PCa
[^{64}Cu] Cu-SAR-PSMA	Phase II	NCT04868604	Metastatic castration-resistant PCa
[^{177}Lu] Lu-PSMA-I&T	Phase II	NCT04188587	Metastatic castration-resistant PCa
[^{225}Ac]Ac-PSMA	Early phase I	NCT04225910	Metastatic castration-resistant PCa
[^{177}Lu] Lu-PSMA-R2	Phase I/II	NCT03490838	Metastatic castration-resistant PCa
[^{131}I] I-PSMA-1095	Phase II	NCT04085991, NCT03939689	Metastatic castration-resistant PCa
Bombesin-targeting RLT			
[^{177}Lu]Lu-NeoB	Phase I/IIa	NCT03872778	Advanced or metastatic solid tumors: breast, lung, prostate, GIST, GBM tumor
Others			
[^{177}Lu] Lu-FAP-2286	Phase I	NCT04939610	Advanced metastatic solid tumor
[^{177}Lu] Lu-DOTA-Biotin (ST2210)	Phase I	NCT02053324	Colorectal cancer with liver metastases

[a]The trial number refers to its citation on https://clinicaltrials.gov/

and chemotherapy, have failed. Patients eligible for treatment also need to have at least one PSMA-positive lesion (observed by ^{68}Ga-PSMA-11 PET–CT imaging at baseline), a life-expectancy of at least 6 months, sufficient organ function (e.g., bone marrow, kidney), and capability of self-care (defined by Eastern Cooperative Oncology Group performance status ≤2) [150]. Other types of RLT are under investigation for treatment of other types of advanced tumors, such as advanced solid tumors of breast and lung or colorectal cancer with liver metastases.

Treatment Course

For the different types of RLT, treatment schedules can differ. For PSMA-RLT, and [^{177}Lu]Lu-PSMA-617 in particular, a conventional treatment schedule consists of four treatment cycles administered in 6-week intervals. In each cycle, the administered activity ranges from 6 to 7.5 GBq. After each therapy cycle, treatment response and the overall condition of the patient are monitored in order to decide if treatment can be continued or not [152]. The VISION trials showed that [^{177}Lu]Lu-PSMA-617 (hazard ratio 0.46) therapy was generally well tolerated and was able to improve both OS and PFS compared to standard of care treatment [150]. These clinical trials and the recent FDA approval of [^{177}Lu]Lu-PSMA-617 show the potential of RLT for treatment of PCa and in the future, results of the ongoing clinical trials of RLT using other targets will also be published and contribute to the development of RLT as a new cancer treatment modality (Box 6.19).

6.8.4.3 Radioimmunotherapy

In 1900, the German Nobel laureate Paul Ehrlich was the first person to introduce the "magic bullet" concept, with reference to antibodies that can be used to treat diseases by specifically targeting receptors or biochemical pathways in bacteria or cancer cells. More than half a century later, the invention of hybridoma technology by Georges Kohler and César Milstein paved the way for the production of monoclonal antibodies against almost any antigen. Kohler and Milstein received a Nobel Prize in 1984 for their work.

A large proportion of therapeutic antibodies have since then been developed and approved by the FDA or EMA for the treatment of cancer. There are several mechanisms through which immunoglobulins function in the body, including, but not limited to antibody-dependent cell-mediated cytotoxicity (ADCC), complement-dependent cytotoxicity (CDC), alteration of signal transduction, inhibition of angiogenesis, and immune checkpoint blockade [153].

Another important modality through which antibodies can mediate a therapeutic effect is through their conjugation to a radionuclide that emits IR in the form of α particles, β particles, γ-rays, or Auger electrons. By virtue of the antibody's specificity and selectivity, it will bind to a specific target overexpressed on a cancer cell and deliver a lethal dose of radiation to the cell. This approach is called radioimmunotherapy (RIT), though several other names have also been used in the literature. Most radioimmunoconjugates use the IgG class of antibodies, with an average molecular weight of 150 kDa and a biological half-life from 2 to 5 days.

Early clinical trials with radioimmunoconjugates used the readily available ^{131}I radionuclide which allowed for their application in SPECT imaging as well as therapy. Today, a wide arsenal of radionuclides has been used in different RIT studies, each with different properties.

There is currently only one FDA-approved RIT targeting the CD20 antigen on B-Cell Non-Hodgkin's Lymphoma (B-NHL): ^{90}Y-ibritumomab tiuxetan or Zevalin®. The immunoconjugate is a result of the conjugation of the monoclonal antibody ibritumomab to the chelator tiuxetan. The antibody is a murine IgG-1 kappa antibody toward CD20, and the tiuxetan chelator is ideal for the chelation of Indium-111 or Yttrium-90. In the following paragraphs, we will look with more details into the use of ^{90}Y-ibritumomab tiuxetan.

Main Indications and Therapeutic Intent of Zevalin®

The Zevalin® therapeutic regimen is used to treat adult patients either with newly diagnosed follicular NHL following a response to initial anticancer therapy, or patients with

Box 6.19 Radioligand Therapy

- Besides peptide receptor radionuclide therapy, other radioligand therapies are also under investigation for treatment of different cancer types (e.g., PCa).
- An FDA-approved compound for RLT is [^{177}Lu]Lu-PSMA-617 for the treatment of metastatic-castration resistant PCa.
- More compounds for RLT are under clinical investigation for multiple cancer types (summarized in Table 6.11).

Table 6.11 Comparison of the accelerator types used for therapy

Accelerator types	Properties
Cyclotron	Circular
	Small
	Mainly for protons
Synchrotron	Circular
	Large
	Suitable also for heavier ions
LINAC	Linear
	Long but slim
	Technically challenging

low-grade or follicular B-cell NHL that have relapsed during or after treatment with other chemotherapies. The prescription medication consists of three parts: two infusions of rituximab to reduce the number of B-cells in blood, and one injection of ^{90}Y-ibritumomab to treat the NHL.

Treatment Course of Zevalin®

The Zevalin® therapeutic regimen should be initiated between 6 and 12 weeks following the last dose of first-line chemotherapy, after platelet counts have recovered to 150,000/mm^3 or more. Patients with platelet counts less than 100,000/mm^3 are not treated with Zevalin®.

Treatment is initiated with an IV infusion of 20 mg/m^2 rituximab. The same infusion is re-administered 7–9 days after the first infusion. Within 4 h of administering the second rituximab infusion, an IV injection of ^{90}Y-ibritumomab tiuxetan is administered at a dose of 0.4 mCi/kg for patients with normal platelet count, or 0.3 mCi/kg for relapsed or refractory patients with lower platelet counts (100,000–149,000/mm^3). The total dose administered should not exceed 32 mCi (or 1184 MBq).

Although Zevalin® is the only FDA-approved RIT that is currently in use, there are a lot of other radioimmunoconjugates at different stages of clinical development, targeting different cancer-associated antigens. Figure 6.24 shows some of the antigens targeted in RIT.

Clinical trials designed with a direct comparison of the radiolabeled antibody with its non-radiolabeled counterpart allow to tease out the therapeutic benefit of RIT over conventional mAb immunotherapy for cancer patients. One example of such a study is a phase III randomized controlled trial of patients with relapsed or refractory CD20-positive NHL patients [154]. In this study, 143 patients were divided into two groups, a "control" group receiving intravenously (IV) the CD20-targeting antibody rituximab for 4 weeks, while the other group received a single (IV) dose of Zevalin® RIT. The latter group was pretreated with two rituximab doses to improve biodistribution and one dose of ^{111}In-ibritumomab tiuxetan for imaging and dosimetry. The control group had an overall response rate (ORR) of 56% while the RIT group showed an ORR of 80%. The complete response (CR) rates were 16% and 30%, respectively. The primary toxicity observed with Zevalin® was reversible

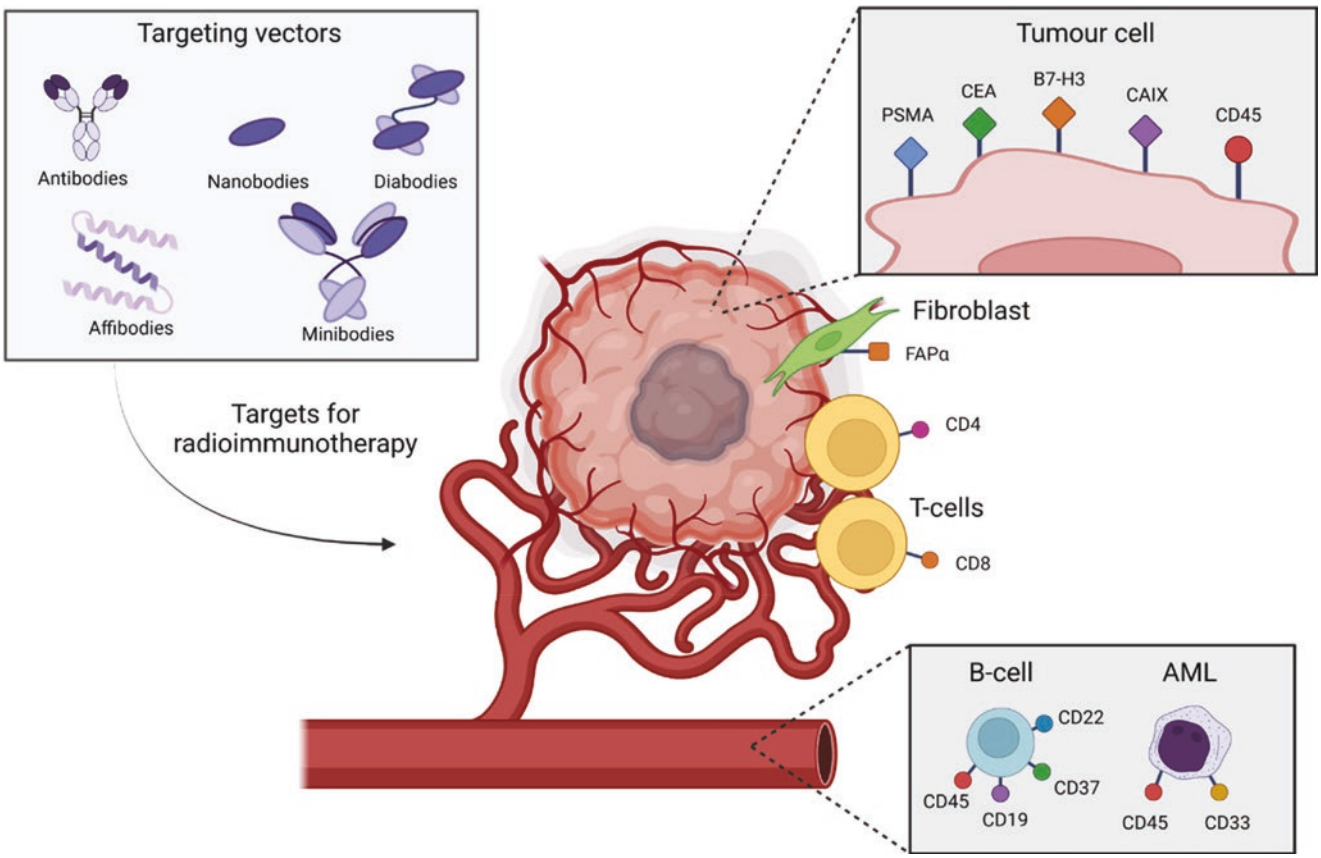

Fig. 6.24 Different targeting vectors and molecular targets used in RIT. In RIT, the targeting vectors are designed to recognize certain molecules present on the surface of tumor cells (e.g., PSMA, CEA, B7-H3, CAIX, or CD45), cancer-associated fibroblasts (FAPα), tumor-infiltrating T cells (CD4 or CD8), and/or circulating immune (e.g., CD45, CD19, CD37, or CD22) or tumor cells (e.g., CD45 or CD33)

myelosuppression, which is also the most common side effect of conventional cancer therapies [155].

It is worth mentioning that the clinical impact observed in RIT of hematological cancers has not been replicated in solid tumors yet, due to a number of outstanding challenges encountered which lead to high bone marrow absorbed doses and insufficient dose delivery to tumors. Several promising strategies have been developed to overcome these challenges, such as the use of antibody fragments (e.g., single-domain antibodies and affibodies) instead of whole immunoglobulins, allowing for higher imaging contrast, deeper tumor penetration, and improved pharmacokinetics [156]. Another important strategy, known as pretargeting, is based on separating the antibody from the radionuclide and letting the two agents combine in vivo. A review by Verhoeven et al. nicely summarizes the different RIT in which pretargeting has been applied [157].

6.8.5 Combination Therapies with Radionuclide Therapy

The undisputable efficacy of radionuclide therapy (RNT) has been documented in the last decade in a series of landmark trials. With a plethora of targeting vectors directed to tumor-specific molecular targets (some in routine clinical use, others in development) and a large panel of radionuclides characterized by different physical properties, the targeted treatment of both solid and hematological tumors is now a clinical reality. The concept of RNT emerged in the 1940s with the use of iodine-131 for thyroid cancer management and was the first FDA-approved radiopharmaceutical (in 1951). Since then, numerous other RNT radiopharmaceuticals have been developed and successfully used, including the most recent FDA- and EMA-approved radiopharmaceutical ^{177}Lu-DOTATATE. However, their success may be limited by healthy tissue toxicity and/or tumor intrinsic or acquired resistance. One strategy to overcome these limitations is the use of combination therapies aiming at achieving an increase in treatment efficacy while remaining at a low toxicity level [158]. This will subsequently lead to an increased therapeutic index and hence improved treatment outcome. If rationally designed, these combination therapies can lead to synergistic effects by targeting adequate molecular pathways, ultimately causing lethal damage to the tumor cell. Indeed, radiobiological mechanisms underlying the effects of RNTs could serve as a very promising basis for the design of combination clinical trials.

The rationale behind the use of the combination approach with RNT, using two or more therapeutic agents, may be multiple and vary according to the physical properties of the radioisotope used and the biology of the tumor considered. Combination strategies may aim at reducing hypoxia, improving the radiopharmaceutical delivery (in case of a poor tumor vasculature preventing drug delivery) via increased perfusion of the tumor, enhancing the therapeutic effect based on radiosensitization mechanisms, or improving the immune control. RNT has been basically evaluated in combination with all cancer pillar therapies, e.g., chemotherapy, external beam RT(EBRT), immune and targeted therapies. Different combination strategies with RNT are summarized in Fig. 6.25.

6.8.5.1 Radionuclide Therapy and Chemotherapy

The use of chemotherapy with EBRT in many common cancers (including lung, head and neck, cervical cancers) and different settings (e.g., neoadjuvant, curative, etc.) has fostered its combination with RNT.

Several clinical studies have been published combining PRRT with 5-fluorouracil (5-FU), capecitabine or temozolomide, a therapy called peptide receptor chemoradionuclide therapy (PRCRT). A population of interest for PRCRT are the highly proliferating NETs characterized by tumor dedifferentiation, higher tumor grade, worse OS outcome, and most commonly ^{18}F-FDG-avidity of the tumor lesions. PRCRT (combination of ^{177}Lu-DOTATATE and 5-FU) was retrospectively investigated in 52 patients with ^{18}F-FDG-avid disease and the majority having grade 2 advanced NETs [159]. A high DCR of 98% was achieved and 27% of the patients achieved complete metabolic response on ^{18}F-FDG PET/CT despite having residual SSTR-positive disease, most likely due to the eradication of the dedifferentiated lesions by PRCRT. It was expected that the prognosis in this patient cohort would be poor, however a median PFS of 48 months was achieved and a median OS was not reached during a median follow-up time of 36 months. Toxicity was low, despite the fact that 67% of the patients had received prior chemotherapy.

Capecitabine, a prodrug of 5-FU, has the additional advantage that it can be administered orally. A 2-arm cohort analysis compared concomitant ^{177}Lu-DOTATATE plus capecitabine (n = 88) with ^{177}Lu-DOTATATE monotherapy (n = 79) and revealed an increased OR in favor of ^{177}Lu-DOTATATE plus capecitabine (43.1% and 14%, respectively). In addition, a significant lengthening of OS in the ^{177}Lu-DOTATATE plus capecitabine group was observed compared to the ^{177}Lu-DOTATATE monotherapy group (median OS not reached vs. 48 months, respectively, after a mean follow-up of 32.4 months; $p = 0.0042$) [160]. The combination of ^{177}Lu-DOTATATE and capecitabine was also evaluated in paragangliomas, however the study failed to prove the superiority of the combination over ^{177}Lu-DOTATATE monotherapy [161] which might be attributed to a too small number of patients included and the typically lower proliferation rate in this cancer type.

A decreased sensitivity of tumors to the alkylating agent temozolomide has been associated with the expression of O(6)-methylguanine-DNA methyltransferase (MGMT), a DNA repair protein involved in the removal of O(6)-methylguanine DNA lesions induced by temozolomide. MGMT deficiency was more frequently observed in pancreatic NET (pNET) compared to lung or small intestine NET and may explain the different sensitivity profiles of pNET

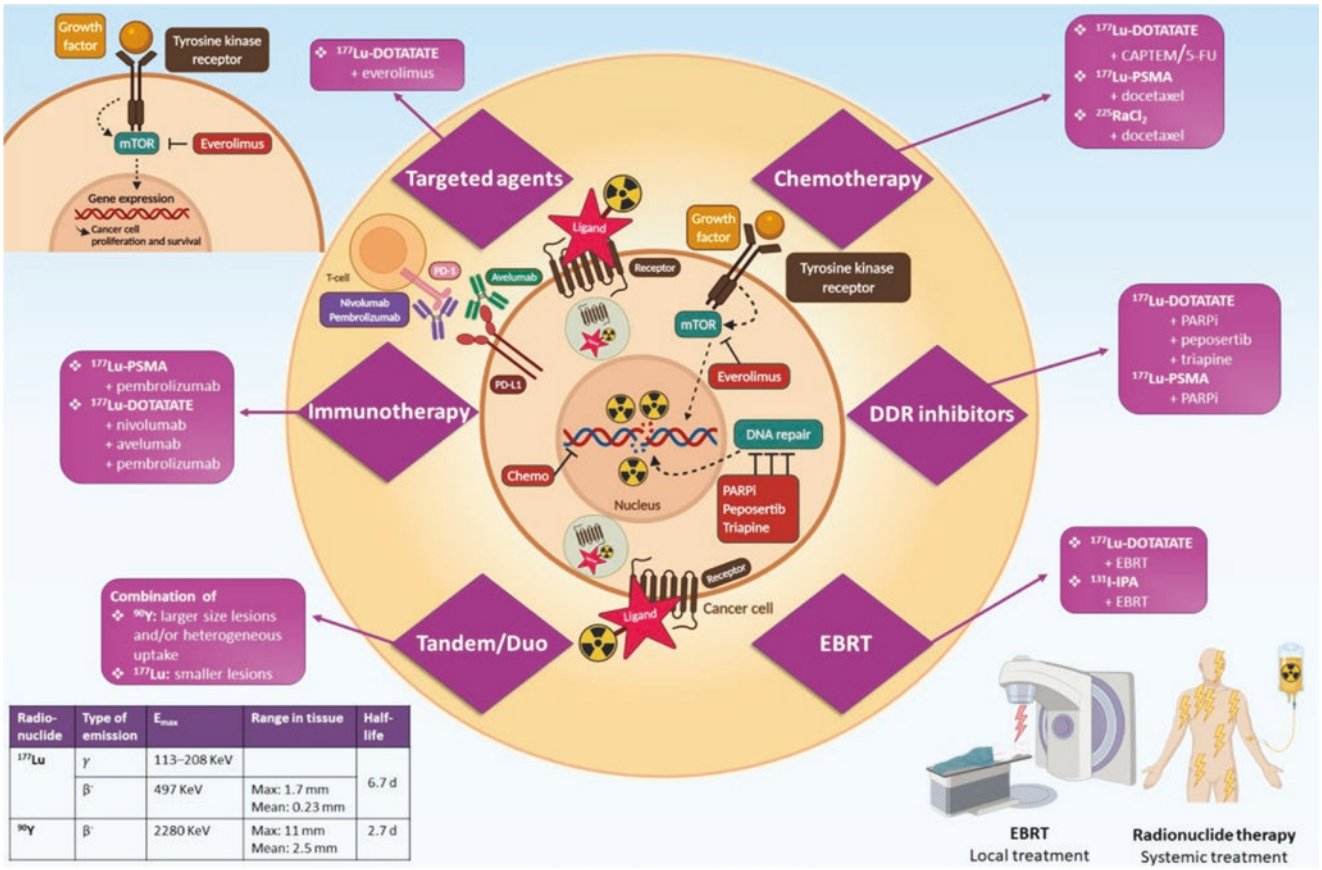

Radio-nuclide	Type of emission	E_{max}	Range in tissue	Half-life
^{177}Lu	γ	113–208 KeV		6.7 d
	β⁻	497 KeV	Max: 1.7 mm Mean: 0.23 mm	
^{90}Y	β⁻	2280 KeV	Max: 11 mm Mean: 2.5 mm	2.7 d

Fig. 6.25 Overview of combination therapies with radionuclide therapy

compared to NET of other origins. A synergistic effect is apparent when combining capecitabine and temozolomide (CAPTEM), most likely due to the depletion of MGMT caused by capecitabine, which strengthens the effect of temozolomide. This is the reason why the treatment regimens add temozolomide after substantial exposure to capecitabine [162]. Preliminary results of the phase II "CONTROL NET" RCT have been presented. This trial compares a combination of ^{177}Lu-DOTATATE plus CAPTEM (experimental arm) versus ^{177}Lu-DOTATATE monotherapy (control arm) in patients with low to intermediate grade midgut NETs. Forty-seven patients were included. The 15-months PFS was 90% versus 92% and ORR was 25% versus 15% for PRRT plus CAPTEM versus PRRT monotherapy, respectively. However, grade 3/4 toxicity occurred more frequently in the PRRT plus CAPTEM arm.

Overall, combining RNT with chemotherapy appears safe and efficient based on data with the beta-emitter lutetium-177. However, multicenter prospective RCTs are lacking to prove superiority of the combination over RNT alone. Although the mechanism of the radiosensitizing effect of chemotherapy is not elucidated, it is thought to act as a radiosensitizer of RNT by increasing DNA damage. However, one preclinical study also pointed out the effect of increased perfusion induced by a chemotherapeutic agent, temozolomide, which may improve ^{177}Lu-DOTATATE delivery to the tumor, as well as increase tumor oxygenation which may also have a radiosensitizing effect [163].

^{177}Lu-PSMA and radium-223 have also been combined with chemotherapy, although less data are available compared to ^{177}Lu-DOTATATE. A phase I/II study showed that the alpha-emitter radium-223 (55 kBq/kg every 6 weeks for 5 cycles) in combination with docetaxel (60 mg/m^2 every 3 week) was well tolerated in bone-predominant metastatic castration-resistant prostate cancer patients. Exploratory efficacy data even suggested enhanced antitumor activity in the combination arm [164]. This will be further explored in a phase III clinical trial that is currently recruiting patients (NCT03574571).

The combination of ^{177}Lu-PSMA with docetaxel, a taxane impairing microtubules polymerization dynamics and therefore preventing cell mitosis, is currently evaluated in metastatic hormone-naïve prostate cancer in a randomized phase II study (UpFrontPSMA trial—NCT04343885) [165]. Patients are randomized 1:1 to the ^{177}Lu-PSMA plus docetaxel arm (^{177}Lu-PSMA 7.5 GBq, 2 cycles intended, every 6 weeks followed 6 weeks later by docetaxel 75 mg/m^2, 6 cycles intended, every 3 weeks) or the docetaxel monotherapy arm.

6.8.5.2 Radionuclide Therapy and Targeted Agents

In addition to chemotherapy, RNT has also been evaluated in combination with targeted agents in order to potentiate the therapeutic effect of RNT. Targeting relevant pathways may aid in eliminating (radio-)resistant clones as well as overcoming tumor heterogeneity.

The mammalian target of rapamycin (mTOR) inhibitor everolimus was combined with ^{177}Lu-DOTATATE in the phase I NETTLE proof-of-concept study in order to establish an optimal safe dose of everolimus in this combination setting. Nephrotoxicity was the dose-limiting factor, leading to the maximum tolerated dose of 7.5 mg everolimus in combination with PRRT [166].

Among targeted agents, DNA damage response (DDR) inhibitors have recently been widely adopted. Preventing the repair of radiopharmaceutical-induced DNA damage by targeting DNA repair pathways is considered an interesting strategy. PARP is involved in the repair of DNA SSBs and has been targeted by PARP inhibitors (PARPi) in combination with chemotherapy and EBRT. Following favorable results from preclinical studies combining ^{177}Lu-DOTATATE and PARPi [167], the combination is now assessed in phase I/II clinical trials with ^{177}Lu-DOTATATE (NCT05053854, NCT04375267, NCT04086485) and ^{177}Lu-PSMA (NCT03874884). Different treatment schedules are used within the trials, with PARPi commencing either before or after RNT administration, and also with variable duration of PARPi (first few days of each RNT administration or daily continuous administration). Study results are awaited and might already provide some evidence about the optimal treatment schedule to be used.

Phase I studies evaluating the combination of ^{177}Lu-DOTATATE and other DDR inhibitors, such as peposertib (NCT04750954) and triapine (NCT04234568), are also underway. Peposertib is an inhibitor of DNA-PK, a serine/threonine protein kinase playing a critical role in DNA DSB repair via the NHEJ pathway while triapine is an inhibitor of ribonucleotide reductase, an essential enzyme for DNA replication and repair.

Other promising combinations are evaluated in the preclinical setting [168]. These include inhibitors of several pathways or molecules: DNA damage response, HSP 90, DNA topoisomerase, hedgehog signaling pathway, and EGFR.

6.8.5.3 Radionuclide Therapy and External Beam Radiation Therapy

Combining RNT with EBRT has several advantages [169]. Firstly, there should not be overlapping toxicities because of different dose-limiting organs, being the surrounding tissues (the ones close to the tumor or that are in the path of incident beams) for EBRT and mainly bone marrow and kidneys for RNT (but will depend according to the RNT type). Therefore, an escalation of the combined radiation absorbed dose without exceeding the maximum tolerated dose of the limiting organs should be allowed. Secondly, the advantages of both radiation-based therapies may be combined: EBRT delivers a precise and homogeneous high dose of radiation locally, to the bulk tumor, while the administration of RNT allows the targeted treatment of systemic disease, including (micro)-metastases and residual tumor cells, albeit with less control of the tumor dose and a heterogeneous dose depending on perfusion and target expression.

Very few clinical studies are being conducted, and most of them are based on sequential and not concurrent administration of both therapies. This combined regimen is mostly studied in bone metastases as well as in brain and liver tumors but also meningioma. Promising data have been obtained in meningioma where ^{177}Lu-DOTATATE and EBRT have been combined and showed the feasibility of such an approach. Interestingly, in seven patients out of ten, for which a follow-up ^{68}Ga-DOTATATE PET/CT was available, increased uptake of the radiotracer was observed compared to the pre-therapeutic scan [170]. This observation was corroborated in several preclinical studies in which up-regulation of somatostatin receptors was observed following low doses of EBRT [171]. Increased tumor perfusion might also be the cause of an increased radiotracer uptake seen on PET/CT. This finding is significant, as such a combination could be beneficial to patients currently not eligible for peptide receptor radionuclide therapy due to a too low uptake on ^{68}Ga-DOTA-SSA PET/CT.

A synergistic effect of 4-L-[131I]iodo-phenylalanine (^{131}I-IPA) and EBRT has been observed in preclinical models of glioblastoma multiforme, and the first results of a phase I/II trial (IPAX-1 trial—NCT03849105) should be available soon.

6.8.5.4 Radionuclide Therapy and Immunotherapy

RT with EBRT has been shown to increase tumor immunogenicity and antigen presentation and therefore enhance tumor cell destruction by T cells. Hence there is a rationale to investigate the combination of immunotherapy and RNT. Preclinical studies have shown the added value of an immune checkpoint blockade to RNT on survival.

The combination of PRRT with the immune checkpoint inhibitor nivolumab has recently been explored clinically in

a phase I study including nine patients with advanced lung neuroendocrine neoplasms [172]. Dose level 1 consisted of ^{177}Lu-DOTATATE 3.7 GBq (8-week interval, 4 cycles intended) plus nivolumab 240 mg (2-week interval), and dose level 2 consisted of ^{177}Lu-DOTATATE 7.4 GBq (8-week interval, 4 cycles intended) plus nivolumab 240 mg (2-week interval). Only one dose-limiting toxicity, consisting of a grade 3 rash, was noted in one patient being treated at dose level 2.

Phase I and II clinical trials combining ^{177}Lu-DOTATATE (NCT03325816, NCT04261855, NCT03457948) or ^{177}Lu-PSMA (PRINCE trial—NCT03658447, NCT03805594) with anti-PD1 or PD-L1 antibodies are under way.

There exists a huge potential in terms of a combined regimen with RNT. Promising combination strategies used with EBRT frequently serve as arguments to extrapolate to RNT. However, EBRT and RNT are characterized by major differences such as the delivery route (external versus "internal"), the dose (homogeneous dose versus heterogeneous dose), and the dose rate (very high and constant versus low and exponentially decreasing dose rate). The maximum therapeutic benefit one can derive from RNT will be achieved thanks to clever combinations exploiting synergistic interactions, used in the optimal doses and sequences [173] and using biomarkers with an individualized approach. Preclinical studies can bring valuable information and can serve as a basis to design proper clinical trials.

Novel treatment combinations are emerging and are now in the early phases of clinical trials, aiming at evaluating the feasibility and the toxicity of the combinations. Later, large prospective randomized trials will be needed to prove the superiority of the combinations over the monotherapies. Combination strategies might also enter in an entirely new realm when targeted alpha-emitters will become available for clinical trials in the upcoming years, with many new combination possibilities.

6.9 Charged Particles and High LET Radiotherapy

Compared to conventional RT (using X-rays), particle therapy has major advantages. The depth of penetration into the body is determined by the particle's acceleration energy and thus energy deposition increases over distance up to a high peak at the end of their range, the so-called Bragg peak. Simply said, the energy transfer is proportional to the inverse square of its velocity where the ionization density increases as the speed of the particle slows down:

$$E \alpha Z^2 / v^2 \tag{6.5}$$

where Z is the charge of the particle and v its velocity. This happens until very close to the end of their range where the high-dose Bragg peak phenomenon is formed (Fig. 6.26a). In the clinics, expanded Bragg peak also known as Spread out Bragg peak (SOBP) is then used to cover the entire tumor volume, this is formed by adding up all single Bragg curves for ions of different energy and therefore range (Fig. 6.26b).

Beyond the Bragg peak (known as tail), there is a rapid falloff of the dose, allowing for sparing of the normal tissue [177] as the tissue behind the tumor doesn't receive any radiation dose. Tumors which have an organ at risk (OAR) lying close to the tumor are especially suited for radiotherapy using particles, as this unique dose distribution can be exploited here. The OAR behind the tumor can thus effectively be spared from radiation damage (Fig. 6.26c).

At the moment, mainly protons are used in particle therapy but also carbon ions. Furthermore other ions such as helium are getting more and more in the focus of particle RT.

These physical advantages ensure precise localization of dose distribution to the tumor while minimizing dose (thus DNA damage) to the surrounding normal tissues. Currently, particles heavier than carbon are not well investigated for clinical purposes due to the dose distribution at the tail where the dose increases with the charge of the particle resulting in increased dose to normal tissue. Furthermore, for equal velocities, the ionization density for carbon ions (Z = six, A = 12) is 36 times greater than that of the proton. However, a carbon ion has 12 times more total kinetic energy, so the range of the carbon ion is about three times lower. Thus, the heavier the particle, the shorter the penetration depth. Finally, following the recommendations of the Ion Beam Therapy Workshop Report, heavy ion beam therapy should be limited to tumors (a) exhibiting a high risk of local failure post photon (or proton) RT, (b) radioresistance due to histology, hypoxia, and other factors, (c) recurring, (d) efficient at repairing cellular damage, or (e) adjacent to critical normal structures, in particular if resection could lead to a substantial loss of organ function.

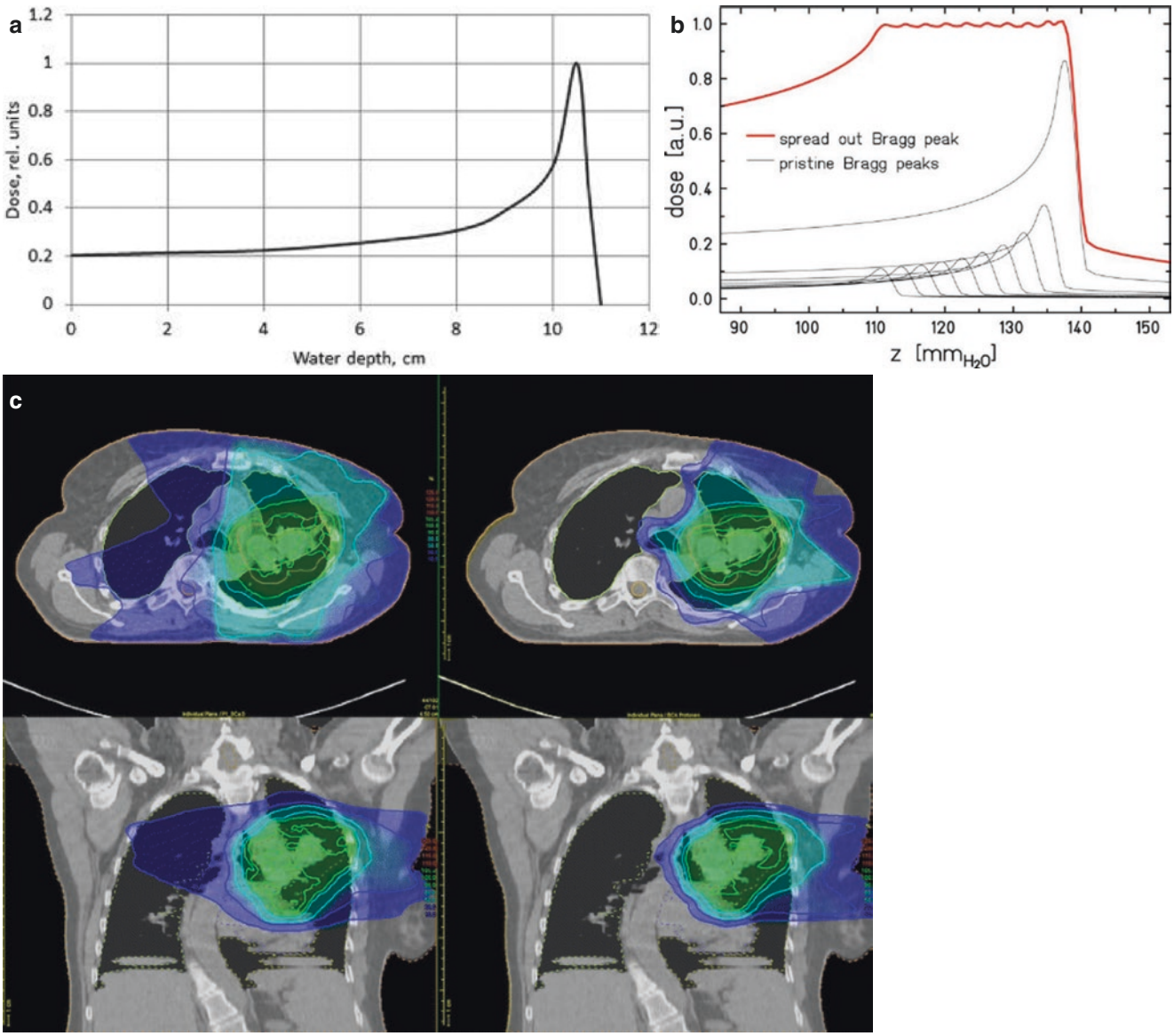

Fig. 6.26 (**a**) Absorbed dose of a 121 MeV proton in water forming the Bragg peak [174]. (**b**) Spread Out Bragg Peak formed by overlaying ions with different energy forms the spread out Bragg peak as used for therapy [175]. (**c**) Dose distribution of one patient with locally advanced non-small cell lung cancer (NSCLC) planned with intensity-modulated radiation therapy (IMRT) (left) or protons (right), depositing no dose behind the tumor [176

6.9.1 Proton Therapy

6.9.1.1 Introduction and History

Proton therapy is nowadays widely used all over the world and in some cases is more appropriate for patient treatment than the mostly used X-ray RT, due to the physical properties of protons (the Bragg curve). A detailed historical overview can be found in Elaimy et al. [178].

Clinical advantages of a proton beam were first suggested by Wilson in 1946 in his paper about the radiological use of high-energy protons. Animal studies began as soon as the first high-energy synchrocyclotron (340 MeV) was completed at the University of California Lawrence Berkeley Laboratory, USA (LBL). These first experiments on mice, Tradescantia microspores, and yeast cells showed that the RBE of high-energy protons (340 MeV) is comparable to that of 200 kVp X-rays.

The first patient proton treatment in LBL took place in 1954. A few years later, in the late 1950s, the Gustaf Werner Institute in Uppsala, Sweden also used protons for patient treatment. In 1961, the Massachusetts General Hospital began treating small intracranial targets with radiosurgical techniques at the Harvard Cyclotron Laboratory (HCL) in Cambridge. Prior to the patient treatment, a radiobiological investigation on monkeys demonstrated experimentally the

feasibility of the method. Later Koehler and others developed a technique to scatter the beam laterally and also range modulation wheels to produce SOBP to cover extended target volumes, thus it was possible to start treating larger treatment volumes in HLC in 1974.

During the late 1960s and in the decade of the 1970s, several Russian physics research facilities initiated their proton therapy programs. For example, the Joint Institute for Nuclear Research in Dubna in 1968, the Moscow Institute for Theoretical and Experimental Physics in 1969, and the Central Research Institute of Roentgenology and Radiology in Saint Petersburg in 1975.

The National Institute for Radiological Sciences in Chiba, Japan started proton therapy treatments in 1979. They were also the first that developed a spot scanning system for proton treatment delivery in 1980. Since then is proton therapy spread more and more—Clatterbridge, England in 1989, France at Nice and Orsay (1991), iThemba Labs in Cape Town, Africa (1993), Paul Scherrer Institut at Villigen, Switzerland (1996), Hahn Meitner Institute in Berlin, Germany (1998), National Cancer Center in Kashiwa, Japan (1998), and Joint Institute for Nuclear Research in Dubna, Russia (1999).

The first hospital specialized in proton therapy started treating patients in 1990 at the Loma Linda University Medical Center in Loma Linda, California, USA. In the same period, the Proton Therapy Cooperative Group was formed, later renamed to the Particle Therapy Cooperative Group (PTCOG) [179]. It is a non-profit organization making statistics and organizing meetings about protons, light ions, and heavy charged particles RT.

Nowadays, there are more than 100 proton therapy centers all over the world with technological equipment from several companies such as IBA, Varian, Mitsubishi, Sumitomo, Hitachi, Mevion, ProNova, Protom based on cyclotrons or synchrotrons. More about the facilities and also patient statistics can be found, for example, on the PTCOG website.

6.9.1.2 Proton Therapy Technology

The generation of protons is obtained via hydrogen ionization. Protons are then accelerated inside a particle accelerator, typically a cyclotron or a synchrotron. A cyclotron produces a proton beam with a fixed energy, on the other hand, the proton energy in a synchrotron is adjustable [180].

In both cases (cyclotron and synchrotron), the beam needs to be spread longitudinally, to produce an SOBP for the patient treatment. This is done by superposing several beams with different energies and weights. In the case of a cyclotron, an adjustable amount of material has to be placed in the way of the beam to reduce the beam energy to the one needed. This is achieved by the use of a degrader just after the beam extraction or by placing a stack with a variable number of plates (a range shifter), a plate with ripples (a ridge filter), or a rotating wheel with an azimuthally changing thickness (a range modulation wheel) inside the nozzle in the irradiation room. In the case of synchrotron, the energy is adjusted inside the accelerator, as was already mentioned, so there is no need for any additional devices [180].

The physical depth dose curve of a SOBP has a broad, quite homogeneous dose region, as is shown in Fig. 6.30. This makes it possible to deliver a higher dose to the tumor region than to the OAR, and therefore to spare these tissues.

There are two modes enabling the lateral beam spread, passive or active modes. Examples of passive modes are the Single or Double Scattering (SiS or DS) and an example of active mode is the Pencil Beam Scanning (PBS). For the passive modes, the beam passes through scatters (one or two, SiS or DS, respectively). In the active modes, scanning magnets are used, which redirect the narrow proton beam to several positions according to the treatment plan. The dose is then delivered to each layer of the volume spot by spot.

6.9.1.3 Proton Therapy and RBE

The energy spectrum, and thus the LET of protons in the SOBP is changing with depth in tissue, since the protons are slowing down traveling through the tissue. At the distal parts of the SOBP, the LET is much higher than in the proximal part. High LET values are connected to increased DNA damage, and thus to lower cell survival.

The International Commission on Radiation Units and Measurements (ICRU) has recommended the use of a generic RBE value equal to 1.1 in the whole range of proton therapy, and most of the proton therapy centers around the world have adopted this value [181]. This means that the same fractionation scheme as for X-ray RT can be used, with the difference that instead of 2 Gy 1.82 Gy per fraction will be used with protons.

This recommended value is based on experimental studies done in vitro and in vivo mostly using passive scattering modes in the early days of proton therapy. From the in vitro studies, mostly performed on Chinese Hamster cell lines, with cells placed in the middle of SOBP, the range of estimated RBE values was from 0.86 to 2.10 with a mean of 1.22 ± 0.02. The RBE from the mid-SOBP in vivo studies ranged from 0.73 to 1.55 with a mean of 1.10 ± 0.01 [181].

Later studies showed that the RBE is not a constant value but it varies depending on a wide range of parameters, such as the beam range, dose per fraction, position in the SOBP, cell line or tissue origin, and also the studied biological endpoint [182]. Another problem when comparing RBE values from different publications is the reference radiation used for the establishment of the RBE values. Several reviews on this topic exist, as, for example, where a collection of data from several groups are sorted by cell lines referring also to the used reference radiation [183].

Some studies report RBE values at the distal falloff of the SOBP near to 3 [184]. One of the claimed advantages of proton therapy is the steep distal falloff of the Bragg peak. Due to this fact, many times the proton beam is often directed to stop in the proximity of the patient's OAR. The mentioned studies highlight the inaccuracies in the generic RBE value used in the whole range of proton therapy. These inaccuracies are much more crucial at the distal falloff of the beam and can lead to the damage of healthy tissues behind the treatment volumes.

In recent years, there is an increased interest in using the PBS mode, thanks to the spot-weighted dose delivery, which facilitates a more conformal dose delivery to the treatment volumes and sparing of healthy tissue. Another advantage of PBS is the much lower secondary-induced radiation (mostly neutrons) from the components of the technological constructions or patient-specific devices (i.e., collimators and compensators) needed in passive modes.

The dose rate in each spot is however much higher than the dose rate in passive modes, which could maybe influence the cell response inside the treated volume in a different way than it is expected. Anyhow, there are several studies showing that there is not any significant difference between the biological response of cells using passive or active modes [185]. In clinical applications, there is some evidence that passive scattering may be associated with more toxicity than pencil beam scanning techniques [186].

6.9.2 Heavy Ion Radiotherapy

6.9.2.1 Carbon Ions

Carbon ion radiobiology finds its origin from the use of ions in cancer RT. Research on carbon ions and their clinical potential started in 1975, with the installation of the BEVALAC at the Lawrence Berkeley Laboratory [187]. In response to the initial success, the Japanese government began construction on the world's first heavy ion facility designated for medical applications at the National Institute of Radiological Sciences (NIRS) in 1984. The Heavy Ion Medical Accelerator in Chiba (HIMAC) was completed in 1993 and carbon ion RT clinical trials began in June 1994 [188].

Biological Advantages of Carbon Ions

Talking about energy deposition, it is important to mention the Linear Energy Transfer (LET—keV/μm) which is the energy deposited per unit of length along the particle track

$$\text{LET} = dE / dx \qquad (6.6)$$

with dE = deposited energy and dx = distance covered. Therapeutic beams of carbon ions (100–400 MeV/n) have LET ranging from 10 to 100 keV/μm [189]. LET is also at the origin of produced biological effects that cause radiation damage. As the particle species and their energy influence LET, the LET of carbon ions is higher than the LET of photons and hence causes a higher fraction of clustered DNA damage foci from direct DNA-ion interaction (Fig. 6.27).

Comparison of biological effects of different LET (beam qualities) is expressed as the relative biological effectiveness (RBE). For the same biological effect, RBE is described as the dose ratio of the reference beam quality experiment to the test beam quality experiment

$$\text{RBE} = Dr / D \qquad (6.7)$$

with Dr = Absorbed dose at reference beam quality experiment (usually photon) and D = Absorbed dose at test beam quality experiment.

RBE is a function of multiple parameters such as the dose, dose rate, LET, oxygen concentration, and cell cycle phase to mention a few. The dependency of these parameters is particularly true at low LET (<10 keV/μm) but less with increasing LET (>10 keV/μm) such as for carbon ions. The RBE value of photons (<10 keV/μm) is considered equal to ~1.0 and tends to increase gradually until it comes to a maximum at around LET = 100 keV/μm and finally decreases. This phenomenon is also known as the overkill effect. Generally, the RBE of carbon ions is around 3.0. However, with increasing LET, dose delivered to the surrounding tissue (entrance dose and tail) also increases. Therefore, a compromise between RBE and dose delivered to the surrounding tissue is needed. As an optimal RBE is said to be achieved around a LET of 100 keV/μm, carbon ions became the best compromise between RBE and dose delivered to the surrounding tissue and is therefore the most studied and clinically applied ion in particle therapy [188, 190]. Yet, little is known on healthy tissue toxicity and the correlated molecular and cellular mechanisms linked to carbon ion irradiation.

Under normoxic conditions, DNA damage caused by low LET radiation (such as photons or protons) is enhanced by generated DNA radicals, which in the presence of molecular oxygen are fixed or become permanent (also known as the

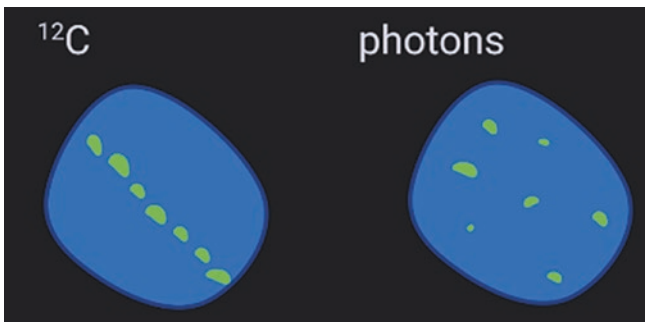

Fig. 6.27 Schematic representation of gH2AX after exposure to carbon ions versus photons. DAPI in blue, gH2AX in green

indirect interaction). The existing oxygen also hinders repair mechanisms. Under hypoxic conditions, this phenomenon is not present, DNA radicals become reduced by sulfhydryl groups causing less damage and repair mechanisms are promoted. Consequently, a major cause of radiation resistance in RTy has been attributed to hypoxic cancer cells. On the other hand, with high LET radiation (such as carbon ions), the particle directly acts on the phosphodiester bond of DNA inducing thus clustered damage which is then less amenable to be repaired. From these observations came the concept of Oxygen Enhancement Ratio (OER), which is an inverse relationship between dependence on oxygen, inducing cellular damage and the mass of the ion species (Fig. 6.28).

The cell cycle status has been shown to be influential in determining radiation sensitivity [191]. Cells in the G2/M phases of the cell cycle are most sensitive to radiation while cells in late S phase are most resistant. This increased radiation sensitivity in G2/M appears to be related to chromatin condensation as effective DNA damage repair is hindered. Unlike low LET radiation, no significant effects of radiation sensitivity on the cell cycle distribution were observed when employing high LET radiation such as carbon ions [192].

The rationale behind fractionated RT, beside the cell-sparing effect, is based on cell cycle radiation sensitivity. Fractionation allows tumor cells in a radiation resistant cell cycle phase to switch/move into a more radiation sensitive phase before the next fraction is applied [193]. However, as the cell cycle distribution is not affecting radiation sensitivity for high LET radiation, fractionated RT would therefore be less beneficial. Overall, carbon ion RT has several benefits (Fig. 6.29).

Indications and Clinical Trials of Carbon Therapy

Hadrontherapy with carbon ion (carbon therapy, CT) is a RT technique intended to destroy cells by irradiating them with a beam of carbon ions particles. This therapy requires heavy, specific equipment derived from research in particle physics including source and particle accelerator (synchrotron or cyclotron), device for controlling the treatment beam and preparation devices, for the conduct and control of processing. This equipment leads to very heavy material and financial investments and the need for multidisciplinary cooperation for their use.

Compared to X-rays (conventional RT) which pass through the whole body and therefore irradiate as healthy cells pass, the carbon ions stop at the desired depth (therefore at the level of the tumor). These ions, once arrived in the tumor cells, create more serious lesions than with other treatments at the level of its genetic material. As their action is intense and the beam precisely defined, tumor cells can be very precisely targeted. These tumor cells do not die immediately, but they are no longer able to multiply and lose their immortality. In addition, the number of sessions in carbon therapy can be much smaller than that required in conventional RT. Moreover, additional chemotherapy is rarely required, which means less fatigue for the patient.

Carbon therapy can target inoperable tumors and particularly radioresistant, in particular when they are in a situation of hypoxia, a common cause of failure of conventional RT. Accordingly, carbon therapy is intended for the treatment of inoperable tumors or incompletely resectable as well as radioresistant surrounded by radiosensitive healthy tissue.

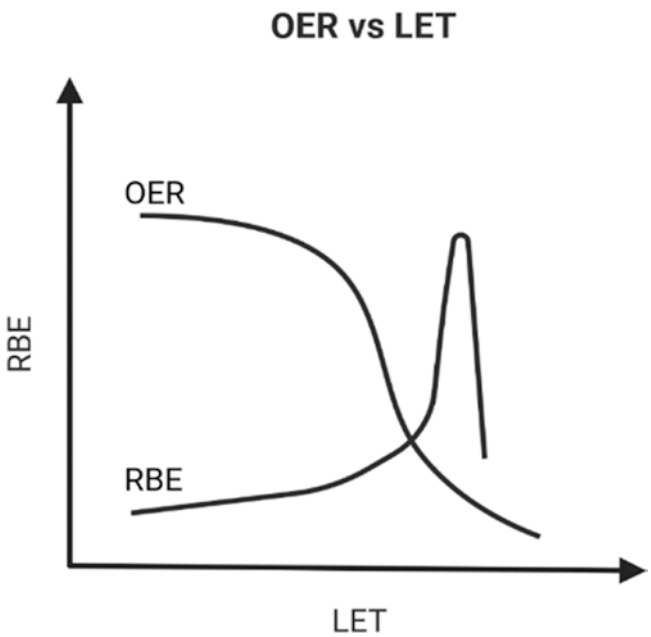

Fig. 6.28 Schematic representation of the relationship between OER and RBE in function of LET

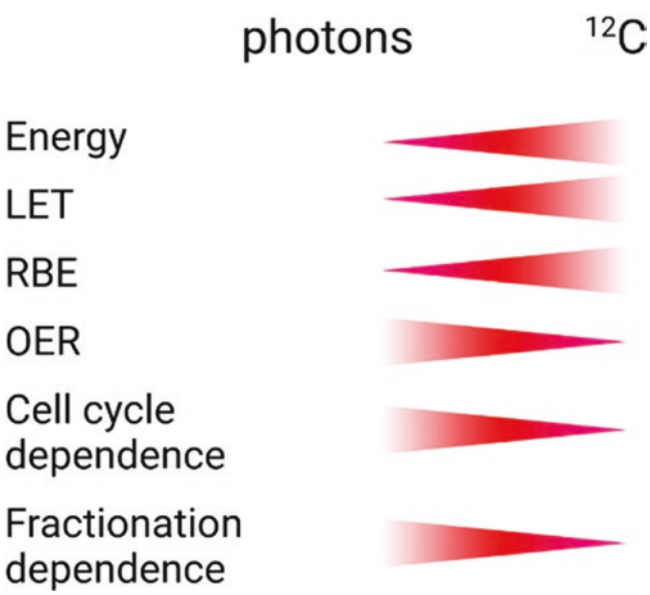

Fig. 6.29 Summary comparison between photon irradiation and carbon ion irradiation

The main indications of this therapy are cystic adenoid carcinomas, tumors of the sinuses of the face and salivary glands, mucous malignant melanomas, chordomas and chondrosarcomas of the base of the skull, sarcomas of the axial skeleton and soft tissues, unresectable or in resection incomplete, unresectable local recurrences of rectal cancer, large hepatocarcinomas (diameter greater than 4–5 cm), choroid malignant melanomas and eye tumors, prostate tumors, tumors of the cervix, and stage I NSCLC [188, 194].

All these pathologies to which carbon therapy is applied form a heterogeneous group for which there is a wide variety of therapeutic approaches ranging from surgery to very high-techRT, with or without the combination of several other treatments. According to the ClinicalTrials.gov website, 31 clinical trials comparing C-ions to either protons or photon therapy were found as recruiting, active or completed.

According to a global assessment of clinical experiences in Japan, the optimization of the therapeutic protocol has progressed over many years and is dependent on the tumor site [195]. For a given disease entity, the therapeutic schedule (e.g., carbon therapy alone, with chemotherapy or in a preoperative setting) is initially based on scientific evidence.

Some of the previously published clinical studies suggest that carbon-therapy would potentially be more effective than conventional RT in case of cystic adenoid carcinomas of the head and neck, tumors of the salivary glands in absence of complete resection, chordomas and chondrosarcomas of the base of the skull, and NSCLC tumors while late toxicities which have been reported in particular in some cases of chordomas and skull base chondrosarcomas, soft tissue and skeletal sarcomas axial, choroid melanomas and eye tumors [196–198].

In total, the analysis of the most recent literature and agency reports of evaluations are consistent to indicate that there is still little data available to conclude definitively on the efficiency-safety balance. Carbon therapy appears to be a promising technique for the treatment of certain not resectable or radioresistant tumors, surrounded by healthy radiosensitive tissue and is currently studied in clinical trials. The long-term side effects are also not yet well known. Indeed, looking at the dose/depth profile of particle beams, the effect of entrance dose and fragment tail on the surrounding healthy tissue is highly reduced compared to conventional therapy. Yet, this dose is not negligible and is an underdeveloped field in radiation research.

6.9.2.2 Other Ions

As described previously, only protons and carbon ions are the types of hadrons used to treat solid tumors so far, however several kind of hadrons, such as neutrons, charged pions, antiprotons, helium ions, and other light ions nuclei (like lithium, oxygen, up to silicon ions) have been either used or planned to be tested for oncological treatment [199].

Helium Ions

In recent years, thanks to their physical and biological properties complementary to protons and carbon ions, a renewed interest in using helium ions (4He) for RT has been observed. This is also tangible from the fact that the first European He-ion treatment is about to go into operation at the Heidelberg Ion-beam Therapy (HIT) center and that at NIRS, in Japan, a multi-ion therapy concept including He ions is currently set up [200, 201]. In addition, the National Center for Oncological Hadrontherapy (CNAO) in Italy is also planning to treat patients with He ions in the future since a source will be available for non-clinical/preclinical research by Spring 2023. In the past, about 2000 patients were successfully treated at the Lawrence Berkeley National Laboratory with passively scattered He ions in the US heavy ion therapy project [202].

He ions are very attractive for cancer treatment because they can overcome some of the limitations of protons and carbon ions, while keeping their advantages. Specifically, they can provide favorable biophysical characteristics like the reduced lateral scattering and enhanced biological damage to deep-seated tumors like heavier ions, while simultaneously lessening particle fragmentation in distal healthy tissues as observed with lighter protons [203].

Radiobiologically speaking, helium ions, being in a similar LET range as protons, offer an improved RBE and OER, while potentially allowing for less demanding biological modeling compared to carbon ions. The helium ions radiobiological characterizations performed so far showed a higher RBE in the Bragg Peak region of up to 1.6, and the OER at 10% survival was found to decrease from 2.9 to 2.6 in the peak region when compared to protons [204]. These are certainly advantageous features for eradication of radioresistant hypoxic tumors. In addition, helium offers a decreased lateral scatter effect versus proton, with less fragmentation tail dose versus carbon [205].

Especially for pediatric patients, helium ions could have the potential to reduce the volume of irradiated normal tissue, without bringing the disadvantage of additional dose caused by the fragmentation tail, like it is observed for carbon ions [206]. This could not only improve the dose distribution for small tumor lesions, but also reduce the total overall dose for children suffering from large tumors, also considering that it is expected that the number of secondary neutrons is very low and the dose due to neutrons may even be lower than in proton therapy [207]. Last but not least, it is important to take into account that helium hadrontherapy would also be less expensive than carbon ions, as they may be produced in cyclotrons rather than synchrotrons.

From the modeling point of view, the very few RBE models existing for these ions still need to be integrated and benchmarked by experimental data on radiation-induced tumor cell killing, as well as normal cell response. However, He-ion RBE data for cell survival are still very scarce, and intensive experimental campaigns need to be performed [203].

Oxygen Ions

Oxygen ions are currently considered as a potential alternative to carbon ions. Because of their mass, they have less lateral scattering which is in favor of the tumor conformality. The high LET of oxygen ions when compared to carbon ions is associated with higher RBE and therefore to better treatment effectiveness in particular with respect to hypoxic tumors. Compared to carbon ions, oxygen ions produce more nuclear fragments, which need to be carefully investigated, not only in-field but also out-of-field, laterally and beyond the Bragg peak, to study the effect of the mixed radiation field in the healthy tissues surrounding the tumor target [208] (Box 6.20).

Box 6.20 Helium Ions Versus Protons and Carbon Ions

- Helium ions versus Protons:
  - ↓ Lateral scattering
  - ↑ RBE
  - ↑ OER
  - ↓ Secondary neutrons
- Helium ions versus carbon ions:
  - ↓ Fragmentation tail
  - ↓ Costs

6.9.3 High-Energy Accelerators

Particles used for therapy need to have sufficient energy to penetrate the patient's body to the desired depth, i.e., several hundred MeV/u. At therapy centers, the acceleration is done by the use of circular accelerators, which can be divided into two types, the cyclotron and the synchrotron. Another way of accelerating particles is through the use of high-frequency linear accelerators, so-called LINACS, which at the moment are getting more and more in the focus. The different accelerator types are summarized in Table 6.11.

6.9.3.1 Cyclotron

A classical cyclotron consists of a large electromagnet with hollow, D-shaped electrodes, called Dees in-between. The Dees are separated by a small gap, which is the acceleration region of the cyclotron. The electromagnet has a constant magnetic field perpendicular to the plane of the movement of the particles. The electrodes induce a radiofrequency electric field, which is changing polarization in resonance with the particle movement. The particles are injected in the middle of the gap. In this gap, the ions are accelerated the first time, upon entering the first Dee there is no electric acceleration field, keeping the particle at constant velocity. Within the electrode, the magnetic field bends the particle due to the Lorentz force and brings it on a circular path with radius

$$r = \frac{m_0 v}{qB} \tag{6.8}$$

with m_0 the mass, v the velocity, q the charge of the particle, and B the magnetic field of the electromagnet. After a half circle, the particle enters the acceleration gap and is accelerated until the second Dee is entered, where again a half circle is formed, which has a larger radius but is traveled within the same time. Acceleration only happens if the frequency f of the electric field, the so-called cyclotron frequency, is adapted to the time, the particle needs to traverse the Dee and therefore to the charge q and the mass m of the particle and the magnetic field B:

$$f_0 = \frac{|q|}{2\pi m_0} B \tag{6.9}$$

but stays constant in time. This process happens until the radius corresponds to the extraction radius R and the particle is extracted with an energy of

$$E = \frac{q^2}{2m_0}(RB)^2 \tag{6.10}$$

Classical cyclotrons are using iron magnets which limit the magnetic field to 1–2 T, if superconducting magnets are used, the magnetic field can be increased, and therefore the size of the cyclotron decreased. This kind of cyclotron only works for non-relativistic particles with velocities $v \ll c$. For higher energies and thus higher velocities, the time for the half circle is not constant anymore. Therefore, they get asynchronous to the constant acceleration frequency. For relativistic particles, the mass m is no longer constant but increases by the factor

$$\gamma = \frac{1}{\sqrt{1-\left(\frac{v}{c}\right)^2}} \tag{6.11}$$

The cyclotron frequency is now dependent on particle velocity

$$f = \frac{|q|}{2\pi\gamma m_0} B \tag{6.12}$$

This limits the maximum energies achievable using classical cyclotrons to, e.g., approx. 20 MeV for protons, which is much smaller than the needed energies for particle therapy. This problem is overcome by two new types: the synchrocyclotron and the isochronous cyclotron. As the synchrocyclotron has a very low duty cycle, it is not usable for particle therapy.

The isochronous cyclotron makes use of a non-constant magnetic field. Here the magnetic field gets larger by the factor γ with increasing radius to increase the Lorentz force and balance the mass increase, resulting again in a constant travel time. This increase in magnetic field leads to a defocusing of the beam, which is compensated by alternating-gradient (also called strong) focusing. Technically it is realized by changing the magnet design, into the so-called hill-valley design, in so-called sector cyclotrons. This design results in regions with higher and lower magnetic fields as shown in Fig. 6.30b. At the transition between hill and valley, the magnetic field is bent and a defocusing (valley to hill) and focusing effect (hill to valley) can be achieved. Using this design acceleration to clinical relevant energies for protons is achievable. Furthermore using the isochronous mode together with superconducting magnets allows for small cyclotron sizes of only a few meters diameter. These properties make the isochronous cyclotron the most popular accelerator for proton therapy.

6.9.3.2 Synchrotron

A classical synchrotron consists of an injector, a set of bending and focusing magnets, guiding the particle on a circular track and linear acceleration tracks without magnetic field in between and an extractor as shown in Fig. 6.31a. The injector is basically a linear pre-accelerator, which injects the particles in the ring with a certain energy and a set of inflection magnets which initially bend the particles into the acceleration tube. In contrast to the cyclotron where the particle track is spiral, the particle track stays circular in the synchrotron at all times. To achieve a circular particle track,

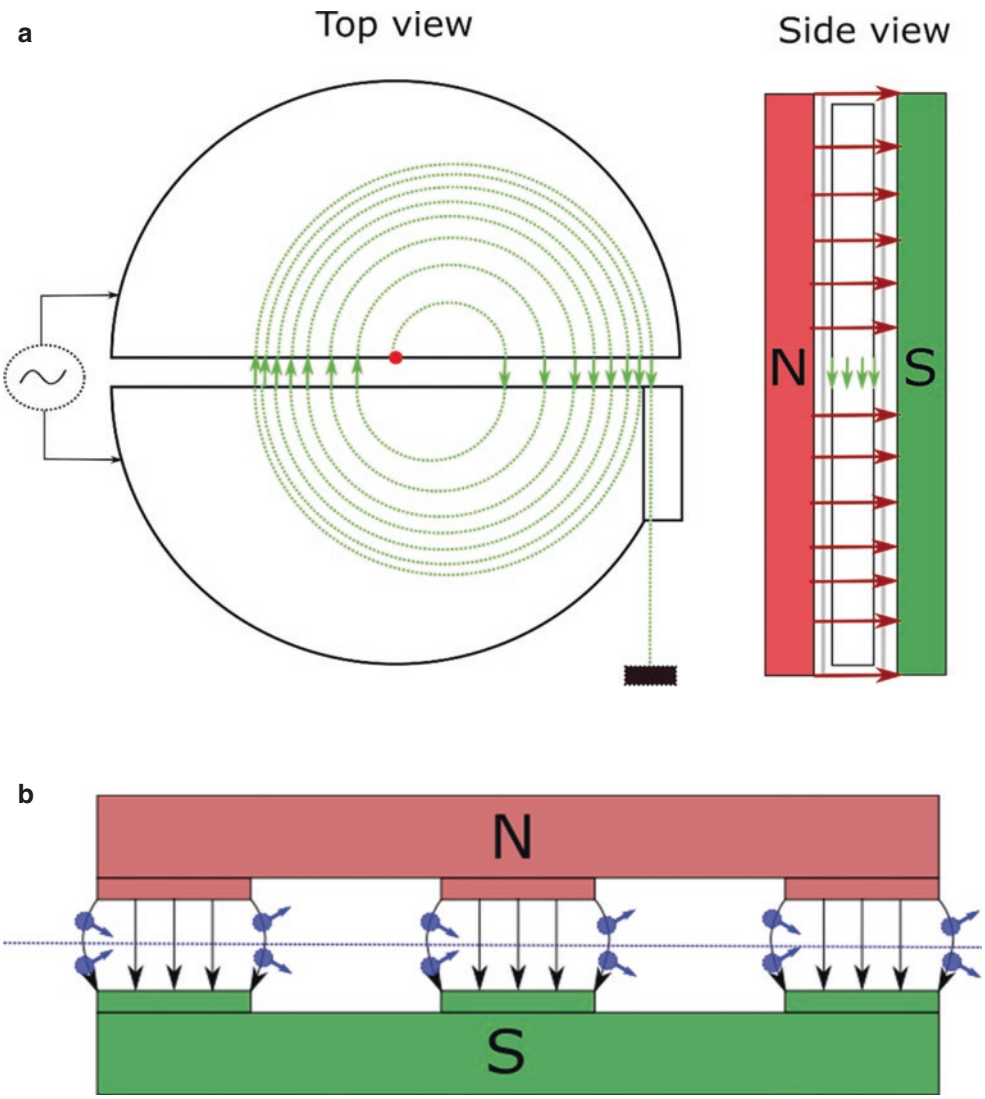

Fig. 6.30 (**a**) Principle of a classical cyclotron. (**b**) Hill-valley magnet design

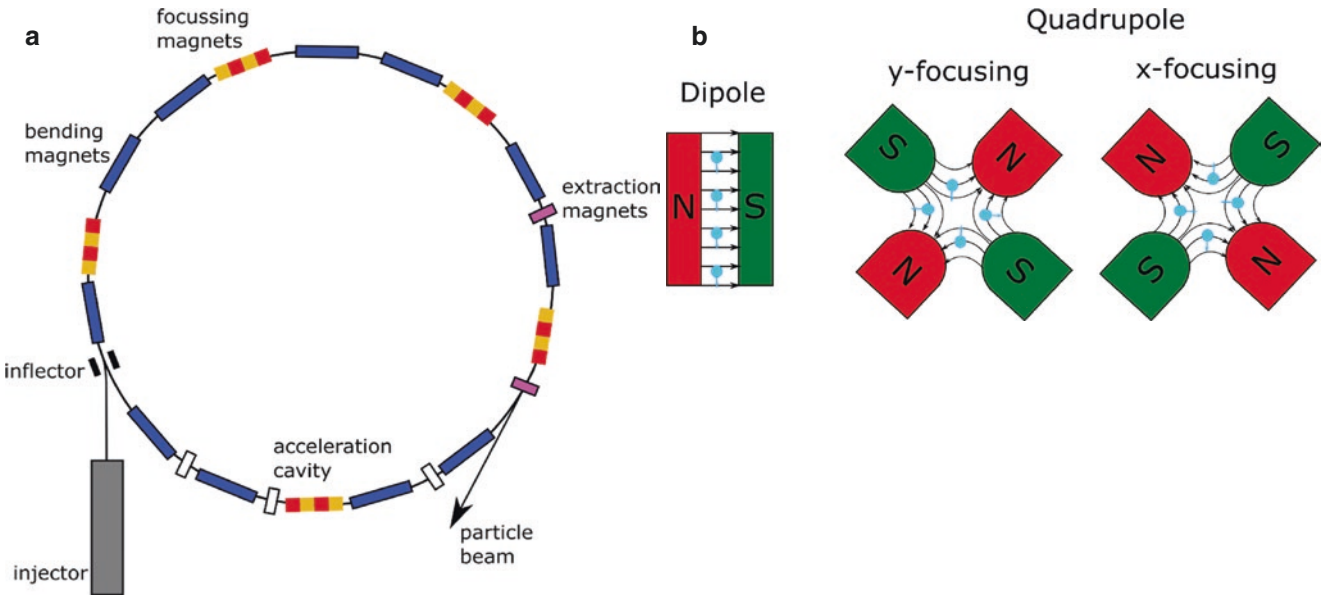

Fig. 6.31 (**a**) Principle of a synchrotron. (**b**) A positively charged beam coming from the front is deflected by Dipole magnets and focused by quadrupole magnets

dipole bending magnets, which bend the particles to stay in the circle, are placed all along the cyclotron. The magnetic field needs to be increased in synchronization with increasing energy and therefore velocity of the accelerated particle, to keep the particles on track. The particles are accelerated close to the speed of light; therefore, the processes happen in the relativistic regime. In the synchrotron, the following requirement, due to the Lorentz force, has to be fulfilled at all times:

$$B = \frac{m_0 \gamma v}{qr} \tag{6.13}$$

One can see that the magnetic field has to be increased proportionally to the increased velocity and therefore energy of the particles. Furthermore, quadrupole and even higher order magnets are necessary to focus the particle beam within the vacuum acceleration tube. The quadrupole magnets are able to spatially focus the beam and therefore work as a lens. In contrast to optical lenses, magnetic lenses only focus in one direction and even worse defocuses in the other direction. Therefore magnetic lenses always come in units of pairs, one focusing the x-direction and the other the y-direction. The higher order magnets are able to correct even the smallest aberrations and therefore ensure that the beam keeps on track. Modern synchrotrons also take advantage of the strong focusing to further reduce beam diameter, as in the isochronous cyclotron. The energy of the particles is increased in the linear acceleration tracks, where high-frequency electric fields are applied in cavity resonators, which again have to be synchronized with the velocity of the particles. Both magnetic field strength and phase of the electric field have to be adapted to the particle's energy in each circle. The vacuum chamber for particles in a synchrotron can, due to the circular path, be a thin torus rather than a disk as it is for cyclotrons, which allows a more cost-efficient construction. The last part is the extractor, which consist of sets of dipole magnets which extract the particles once the desired energy is reached. The synchrotron by design can only operate in a quite slow pulsed mode, but has the advantage that the energy can be easily varied pulse by pulse. Synchrotrons are mainly used when different particle types (protons, carbon ions, and others) are used in the same facility, as the magnet tuning allows flexibility to flexibly change the accelerated ions, which is not possible in cyclotrons (Box 6.21).

Box 6.21 Cyclotron and Synchrotron

- Cyclotrons consist of a big magnet and two, complex shaped electrodes.
- Compact design of asynchronous cyclotrons allows for small sizes of a few meters diameter.
- Asynchronous cyclotrons most popular accelerator for proton therapy.
- Synchrotrons consist of a set of bending and focusing magnets and field free drift tracks, which are arranged in a circle.
- Synchrotrons can accelerate different particle types (protons, helium, carbon, and also heavier ions) with the same design.

6.9.3.3 Particle LINAC

A high-frequency linear accelerator (LINAC) represents a complementary type of accelerator compared to cyclotron and synchrotron. It is based on the same principle as the modern clinical LINACs for X-ray therapy, as commonly used worldwide to accelerate electrons to high energies and stimulate them to emit X-rays at several MeV energies. Due to the light weight of the electrons, these accelerators can be very compact and directly mounted on the application gantry. For particles such as protons and heavier ions in contrast, more complex technological developments are necessary. Although already proposed in the 1990s, the technology for particle LINACs still is in its infancy, with only a few projects worldwide [209, 210]. Radiofrequency LINACs are based on the principle to accelerate a bunch of particles in cavity resonators as shown in Fig. 6.32a. The particles are synchronized to the applied alternating electric field. They are accelerated when they are in the acceleration space.

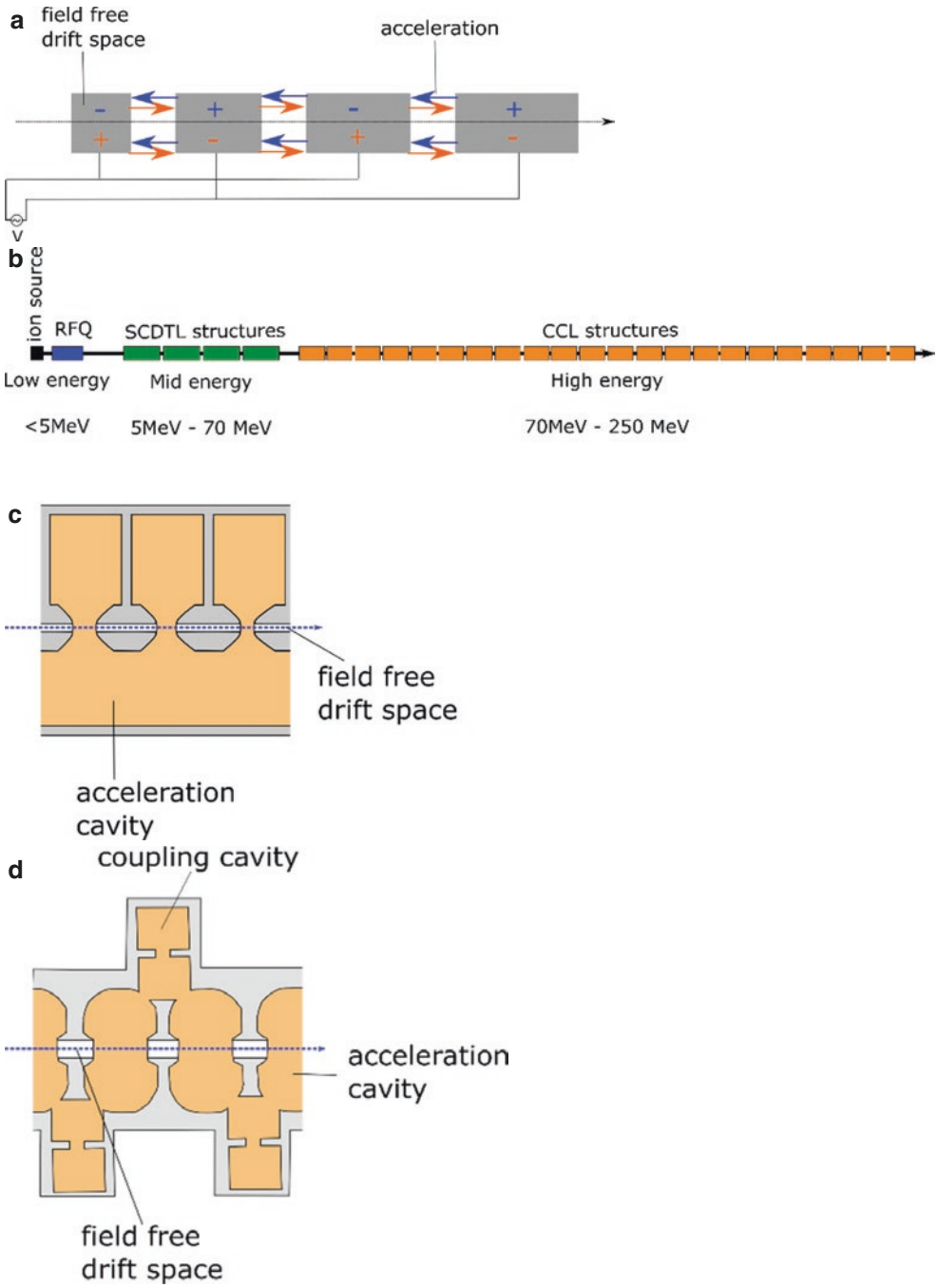

Fig. 6.32 (**a**) Linear acceleration principle. (**b**) A proton LINAC system. (**c**) Principle of a side-coupled drift tube LINAC (SCDTL) structure (cut through). (**d**) Principle of a coupled cavity LINAC structure (cut through)

When the field commutes, the particles are shielded in a field free drift space. The shielding also serves as electrodes for the electric field. When the particles enter the next acceleration space, due to alternation of field again see an acceleration electric field. This process is continued until the final energy is reached. Particle LINACs in the so-called all-linac approach consist of different types of acceleration cavities shown in Fig. 6.32b, after the ion source, each suited for a different particle energy range. For energies up to ~5 MeV, a radiofrequency quadrupole (RFQ) is used for acceleration. For energies between 5 and 70 MeV, the acceleration is performed in a SCDTL (side-coupled drift tube LINAC), followed by the coupled cavity LINAC (CCL) up to the maximum energies of ~250 MeV. The acceleration is performed in an electric field in which the resonators are oscillating with 3 GHz allowing for high electric fields and a shrink the system length to approximate of ~30 m, which can be fit into a clinical building. The RFQ is a quadrupole electromagnet, which is oscillating with a 3 GHz radiofrequency. Special longitudinal design of the electrodes makes it possible to push the particle beam through the RFQ and therefore accelerate it. Furthermore, the RFQ bunches the particle beam so that it fits the needs of the SCDTL and CCL structures, which can only accelerate a bunch of particles. The SCDTL accelerates the beam in the mid energy range 5 and 70 MeV. The SCDTL structure as shown in Fig. 6.32c consists of a huge cavity resonator where drift tubes are mounted. In the cavity, the alternating electric field is built and the tubes serve as field free drift space. The length of the drift tube must be synchronized to the velocity of the particles, so that the particles only see the acceleration of the oscillating field. The length of the *i*th tube is:

$$L_i = \beta_i \lambda_{RF} \tag{6.14}$$

with

$$\beta = \frac{v}{c} \tag{6.15}$$

describing the velocity v of the particle in units of velocity of light c and λ_{RF} being the wavelength of the oscillating field. For a 3 GHz radiofrequency, the wavelength is

$$\lambda_{RF} = \frac{c}{f} \approx 10\,\text{cm} \tag{6.16}$$

For an acceleration between 5 MeV ($\beta = 0.1$) and 70 MeV ($\beta = 0.36$), this results in a drift tube length of 1–3.6 cm. For higher energies, a coupled cavity LINAC (CCL) system is used (Fig. 6.32d). The design of the structure is different compared to SCDTL. Here the field is coupled in through a cavity, which makes them more efficient for higher particle velocities. The manufacturing of SCDTL and CCL structures is quite complicated as material defects such as welding seams or supernatant material will disturb the electric field. New production techniques such as 3D metal printing will offer possibilities of high precision manufacturing of such structures.

6.9.3.4 Beam Transport and Gantries

After the accelerator, the particle beam needs to be guided to the patient. For beam guiding as in the acceleration process of the synchrotron, sets of magnets are used. Dipole magnets are used for bending the beam, whereas quadrupole magnets are used to keep the beam on track in the vacuum tube. Before the patient also beam diagnostics, such as a dosimetry chamber is placed. A quite important step is also the beam shaping, which defines the energy and size of the beam. In most centers, pencil beam scanning is used, which allows to get rid of a collimator close to the patient and therefore reduce unwanted exposure of the patient with neutrons coming from the collimator. The energy selection can be done away from the patient, and it must only be guaranteed that the beam has a defined profile modern therapy centers mostly rely on the application of radiation from different angles, which makes it necessary to move the beam around the patient. This is done by the use of so-called gantries, which are rotatable. The beam is deflected on the gantry and then can be delivered at a defined position. In particle therapy, due to the velocity of the particles and their rigidity, i.e., the resistance of a particle to be bent by a magnetic field, huge and especially heavy magnets must be used, which make gantries quite large and heavy. A conventional proton gantry is in the order of 150 t with a size of several meters, whereas for carbon ions it can be up to 600–700 t (Box 6.22).

Box 6.22 Particle LINAC

- High-frequency LINACs for particle therapy are an emerging technology.
- Complex cavities accelerate beams with a GHz frequency.
- Cavity size has to be precisely aligned with particle velocity.

6.10 Nanoparticles in Cancer Therapy

Box 6.23 Nanoparticles in Cancer Therapy

- Nano-objects exhibit different physical and chemical properties compared to the related bulk materials due to a high surface-to-volume ratio, a metric that decreases with the size of the object.
- The surface of nanoparticles can be functionalized to actively target cancer cells opening avenues for a use in nanomedicine field. Recognition and clearance of the nano-objects from the bloodstream by the reticuloendothelial system (i.e., resident macrophages in liver, spleen, lungs) remain the main challenge.
- Nanoparticles have the potential to be used to efficiently and specifically deliver drugs to the tumor, to produce heat in hyperthermia therapy, and to sensitize cancer cells to radiotherapy.
- Translation of nanoparticles to the clinic remains poor due to hurdles related to their large-scale manufacturing and toxicity studies.

In the last few decades, the use of nanomaterials in medicine has attracted increased interest. A nanoparticle is a particle with at least one of its external dimensions in the size range of 1–100 nm. Due to this small size, nanoparticles exhibit physical, chemical, and optical properties that significantly differ from those of their bulk material, which makes them emerge as promising tools to improve the efficacy of cancer diagnosis and therapy. This section describes how nanoparticles have the potential to contribute to certain cancer therapies that are discussed in Sects. 6.4 and 6.5, including the delivery of chemotherapeutic drugs, targeted therapy, hyperthermia, and RT (Box 6.23).

6.10.1 The Properties of Nanoparticles

Nanoparticles can typically be classified based upon their material (organic or inorganic), shape, surface, or size (Fig. 6.33). As such, a broad and versatile spectrum of nanoparticles exists. Organic nanoparticles include liposomes, polymeric nanoparticles, dendrimers, and micelles. On the other hand, examples of inorganic nanoparticles are metallic nanoparticles, magnetic nanoparticles, silica nanoparticles, carbon-based nanoparticles, and quantum dots. The type of nanoparticle to use depends on its application in medicine.

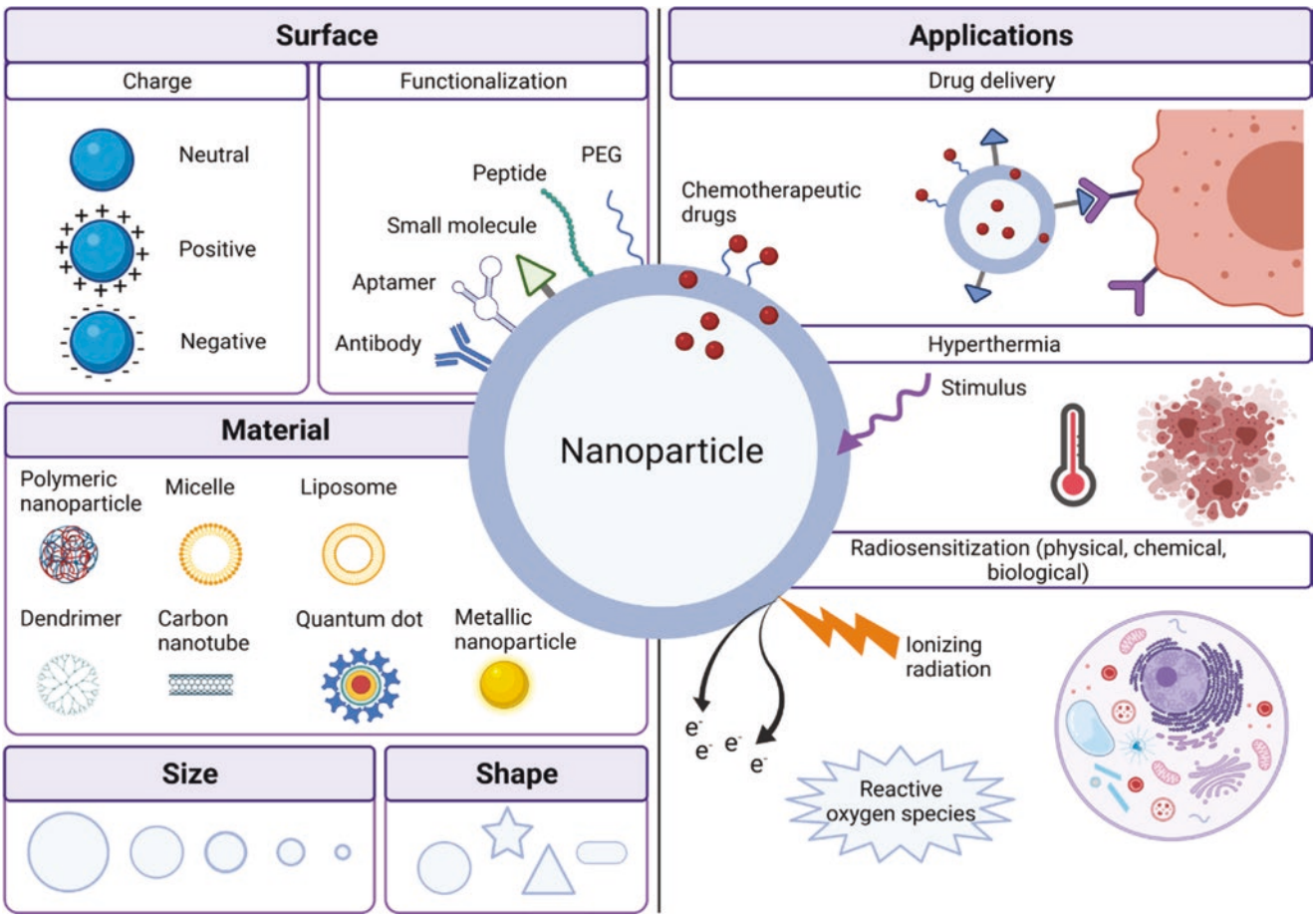

Fig. 6.33 The versatility of nanoparticles and their potential applications in cancer therapy

A major challenge in nanomedicine is the immediate and inevitable "masking" of nanoparticles by proteins, lipids, carbohydrates, and nucleic acids once the nanoparticles are introduced into the blood circulation, forming a "biocorona." Subsequently, the adsorbed surface proteins are recognized by the abundant phagocytic cells in the liver and the spleen, causing the rapid trapping and removal of nanoparticles from the bloodstream. A limited blood circulation time prevents nanoparticles from reaching the tumor cells. In order to improve the biocompatibility, solubility, and stability of the nanoparticles in physiological media, the surface of nanoparticles is usually coated with polymers, generating an electrostatic repulsion and/or a physical barrier between the nanoparticles. Depending on the applied coating, the net surface charge of the nanoparticle can be positive, negative, or neutral, which strongly influences the biological fate and effects of the nanoparticles. One of the most commonly used polymers for nanoparticle coating is polyethylene glycol (PEG), which reduces the biocorona formation by neutralizing the nanoparticle surface charge and giving the nanoparticle a "stealth" character. This delays their recognition and subsequent sequestration of the nanoparticles by the reticuloendothelial system (RES), prolonging the blood circulation time.

An important physical property of nanoparticles is the large surface area-to-volume ratio. When the size of the nanoparticles decreases, a larger proportion of their atoms or molecules are displayed on the particle's surface, rather than in the particle's core, increasing the surface area-to-volume ratio. This ratio decreases with the size of nanoparticles modifying their physical and chemical properties compared to bulk materials. Furthermore, the large surface area-to-volume ratio facilitates the functionalization of the nanoparticle surface with multiple moieties, supporting their multifunctional applications in cancer diagnosis and therapy, which is discussed in more detail below.

6.10.2 Tumor Accumulation and Tumor Targeting

In order to use nanoparticles in cancer remediation applications, nanoparticles need to reach and accumulate in the tumor tissue. Rapidly growing tumors stimulate the formation of new blood vessels to supply the tumor cells with a sufficient amount of oxygen and nutrients. The newly formed tumor vasculature is usually characterized by the presence of abnormal, leaky, and immature blood vessels, which are poorly aligned with a defective endothelium. Consequently, nano-sized particles can efficiently pass through inter-endothelial gaps and accumulate in the tumor. Furthermore, the decreased level of lymphatic drainage promotes the nanoparticle tumor retention. This "passive" process is known as the enhanced permeability and retention (EPR) effect. Importantly, the efficacy of the EPR effect is limited due to the heterogeneity of the vascular structure within the tumor, at different tumor stages and between different tumor types. Furthermore, despite the success of the EPR effect in preclinical tumor models, the efficacy and clinical translation of cancer nanomedicine remain poor, indicating that the EPR effect is less reliable in human tumors. In fact, research demonstrated that extravasation of nanoparticles into the tumor via active trans-endothelial transport pathways occurs more frequently than passive diffusion and thus should not be underestimated [211].

A strategy to complement the EPR effect and to improve the tumor accumulation efficiency of nanoparticles is the functionalization of the nanoparticle surface with cancer-targeting ligands. Cancer-targeting ligands are often specific for factors that are unique or upregulated in cancer cells and that are mostly involved in processes such as tumor progression, invasion, metastasis, and angiogenesis. In general, these targeting ligands can be categorized in five main classes: small molecules, peptides, protein domains, antibodies, and nucleic-acid based aptamers. Examples of cancer-specific targeting ligands are folic acid (FA) (essential for DNA synthesis), cyclic arginine-glycine-aspartic acid (cRGD) peptide (a cell adhesion motif with a high affinity for αβ-integrins), and targeting ligands that can bind to membrane receptors, such as EGFR or VEGFR. Thanks to the large surface area-to-volume ratio of nanoparticles, multiple targeting molecules can be conjugated to the nanoparticles, which enables multivalent interaction with membrane receptors, increasing the tumor uptake and the intratumoral retention time.

6.10.3 Application in Cancer Therapy

Nanoparticles can be used as promising tools to enhance the efficiency of multiple anticancer therapies, including the delivery of chemotherapeutic drugs, hyperthermal therapy, and RT.

6.10.3.1 Drug Delivery

The conventional chemotherapeutic treatment strategies have certain drawbacks linked to the systemic administration and nonspecific distribution of the drugs through the body. This can, for instance, result in limited accessibility of the drug to the tumor, requiring high therapeutic doses and causing off-target toxicity due to damage to healthy cells. Besides, cancers can develop resistance to chemotherapeutic drugs, which is an important factor in treatment failure. Nanoparticles have the potential to improve these aspects by acting as drug delivery systems (DDS). In fact, nanoparticles can efficiently hold a massive payload of the drug, improving the solubility and stability of the drug in the blood circulation. In addition, they enable targeted delivery of the drug

to the tumor sites and promote transport across membranes. Altogether, nanoparticle-based drug delivery has the potential to enhance the efficacy of the chemotherapeutic treatment, while minimizing the side effects. Furthermore, in order to counteract multidrug resistance, nanoparticles can be used to deliver multiple therapeutic agents, including chemo-sensitizers, small interfering RNA, microRNA, enhancing antitumor effects.

Therapeutic agents can typically be loaded on nanoparticles through physical packaging, covalent binding, or electrostatic complexation. Lipid-based nanoparticles, such as liposomes, consisting out of a double lipid layer are the most popular structures in nanoparticle-based drug delivery thanks to their excellent biocompatibility and biodegradability. Furthermore, they can transport both hydrophilic and hydrophobic drugs, encapsulated in the aqueous core and the bilayer membrane, respectively. Other organic nanoplatforms used for drug delivery include polymers, micelles, and dendrimers. On the other hand, inorganic nanoparticles such as carbon-based nanotubes, gold nanoparticles, silica nanoparticles, and iron oxide nanoparticles are also used as drug delivery systems because of their advanced multi-functionality, excellent stability, high drug payload, and unique surface properties.

To improve the precision of drug delivery, it is possible to engineer a cancer-targeted, stimulus-sensitive DDS, which releases the drug at the tumor site in a controlled and sustained manner upon encountering an endogenous or exogenous trigger, without affecting the regions near the tumor site. The tumor microenvironment features conditions that substantially differ from those in normal tissues, such as an acidic pH, high enzyme levels of matrix metalloproteinases (MMPs) and proteases, hypoxia, metabolic shift to anaerobic glycolysis, and a high redox activity. These endogenous stimuli can induce nanoparticle degradation and subsequent drug release. The development of nanocarriers sensitive for exogenous stimuli such as near infrared light, heat or sound waves enables an "on-demand" drug delivery that is tightly controlled from outside the body [212].

6.10.3.2 Nanoparticle-Mediated Hyperthermal Therapy

As mentioned in a previous section, hyperthermia can help in tumor control thanks to its tumor vasculature effect. Briefly, hyperthermia triggers vasodilation. In healthy vasculature, it helps to efficiently dissipate the heat and avoid tissue damage. However, in the aberrant organization and structure of tumor vasculature, it initially increases the blood flow and oxygen supply to the tumor tissue until the heat accumulated in the tissue reaches 42 °C triggering the collapse of tumor blood vessels that promotes cancer cell death. Therefore, it is important to localize hyperthermia to the tumor tissue while avoiding prolonged exposure of healthy cells to elevated temperatures.

Interestingly, the increase in tumor blood flow induced by hyperthermia can be used to sensitize cancer cells and to enhance the delivery of drugs improving the efficacy of chemotherapy and RT, respectively. Nanoparticles have unique properties, which enables them to efficiently convert incident energy into heat. For instance, alternating magnetic fields activate magnetic nanoparticles, such as iron oxide nanoparticles, stimulating heat production. On the other hand, plasmonic nanoparticles, such as gold nanoparticles, typically hold a unique optical characteristic called the surface plasmon resonance (SPR). This phenomenon implies the interaction of light of a specific wavelength with the free electrons on the surface of the nanoparticle, resulting in the absorbance and scattering of light, and the generation of heat [213]. Finally, carbon nanotubes absorb electromagnetic radiation over an extremely broad frequency spectrum, ranging from near infrared light to radiofrequency waves. The absorbance of electromagnetic energy induces electron excitation and relaxation within the nanoparticle, causing heat production. The ability to target and accumulate nanoparticles in the tumor tissue allows the nanoparticle-mediated heat generation to be localized at the tumor site.

6.10.3.3 Radiosensitization

In 2004, it was demonstrated that gold nano-objects injected in tumors can enhance the effect of radiation by improving tumor control in mice treated with kilovoltage X-rays. Since this pioneering work, extensive experimental validations were performed evidencing the potential of a large series of metal-based nanoparticles as radiosensitizer at preclinical level. However, the mechanism(s) of action, a complex mixture between physical, chemical, and biological contributions is still under debate [214]. Physical contribution resides in their ability to increase the dose deposited (radioenhancement effect) via the emission of secondary Auger and photoelectrons following the interaction with IR. The capacity of nanoparticles to increase radiolysis processes leading to a higher oxidative stress in cellular systems constitutes a chemical contribution to the mechanism of action. Finally, the biological effect is based on cell detoxification and DNA repair system impairment, enabling to potentiate the effect of irradiation (radiosensitization effect) [215, 216].

6.10.4 Theranostics and Combination Therapy (Clinical Potential)

Researchers designed complex and multimodal nanoplatforms enabling the simultaneous use of nano-objects for diagnostic and therapeutic applications. These nano-objects are called "theranostics" agents. They enable a non-invasive and real-time tracking of the in vivo nanomaterial distribution and facilitate the dose and toxicity management, as dis-

cussed previously, fine-tuning the patient-specific treatment protocol [217]. Superparamagnetic iron oxide nanoparticles (SPIONs) is one interesting example of theranostic agent. While it has been used for years as contrast agents in MRI, enabling to increase the quality of images used for diagnostics (with higher spatial resolution), these nanoparticles have recently shown radiosensitizing properties. The presence of these nano-objects within the tumor allows to better define the area to treat and to increase the efficiency of the treatment. These SPIONs can also be coupled to chemotherapeutic drugs, such as doxorubicin, further increasing their therapeutic impact.

6.10.5 Challenges

Currently, only a relatively small amount of nano-objects are FDA approved for cancer treatment, since the translation toward clinics is an expensive and time-consuming process that is associated with two main challenges [218]:

- Large-Scale Manufacture

  To enable large clinical trials, drugs have to be produced on a large scale. The Good Manufacturing Practices (GMP) of nanoparticle technology is characterized by a high complexity compared to conventional formulation technologies that usually contain free drug dispersed in a given medium. Indeed, the efficacy of nano-objects is determined by optimal parameters that should be preserved during the scaling-up process. Therefore, nanoparticles have to be manufactured with proper quality standards and with a strict batch-to-batch reproducibility to ensure product specification. Finally, they have to be stable during long-duration storage ensuring the product quality at the time of clinical administration.
- Extensive Toxicity Studies

  Before a drug candidate can be tested in humans, its safety profile must be proven in animal models. These preliminary tests allow a thorough understanding of its pharmacokinetics and toxicity as well as the establishment of safe limits for further clinical trials.

  Preclinical in vivo studies have demonstrated nano-object accumulation in liver and spleen for several months post intravenous injection, raising the question of long-term toxicity for which time-consuming approaches are needed. These toxicological studies are governed by specific rules and regulations of Good Laboratory Practice (GLP), a quality system ensuring the uniformity, consistency, reproducibility, and reliability of non-clinical safety tests. Nevertheless, the current regulatory approaches used for the toxicological assessment of conventional drugs may not be appropriate to fully assess the toxicity of nanomaterials requiring the development of new specific approaches.

6.11 Second and Secondary Cancers in Radiotherapy Patients

Although often used interchangeably, there is a fundamental difference between second and secondary cancers. Second cancer is a more general name for any tumor occurring in patients who have been treated earlier for a first cancer, while the development of a secondary cancer can be ascribed to the treatment for the first cancer. This is not uncommon and should be discussed as part of the process of taking informed consent when explaining the treatment with chemotherapy or RT.

The risk of developing a secondary malignancy following RT depends on:

- The organs irradiated
- The age at treatment, with younger patients having an increased risk compared to a teenager or adult
- The total dose of radiation received
- The time from treatment
- The prior use of alkylating agent chemotherapy
- Underlying genetic predisposition

The risk of developing a secondary tumor is cumulative and increasing over time. However, as age increases, the risk relative to the normal population decreases as cancer becomes more common in the general population as well.

Well-known examples are breast cancer, meningiomas, thyroid cancer, and sarcomas. There is an increased risk of development of breast cancer in girls treated for Hodgkin lymphoma under 16 years of age, with a 20% cumulative incidence of breast cancer by the age of 45 [219]. Girls treated with whole lung RT for Wilms tumor are also at risk of breast cancer. There is a well-documented increased incidence of meningiomas associated with cranial RT, with young age at time of RT and time from treatment associated with higher risk. An excess of thyroid cancer and bone and soft tissue sarcoma are also seen in relation to previous RT [220].

There have been concerns about the "low-dose bath" effect of modern RT techniques such as intensity modulated radiotherapy or arc therapy (IMRT/IMAT) increasing the risk of secondary cancers, compared with simple conformal RT. However, IMRT results in greater conformality and reduces the non-target high dose volume. This may offset the increased volume of normal tissue receiving low-dose irra-

diation. As of today, the feared increase in secondary cancers has not been proven. A major advantage of proton beam RT is the expected reduced risk of secondary malignancy.

Molecular RT may lead to an increased risk of secondary leukemias and cancers, both from the general effects of irradiation of the whole body, and from organ-specific dose, e.g., thyroid uptake of free radioiodine in meta-iodobenzylguanidine (mIBG) therapy, despite the use of thyroid blockade.

RT is not alone in causing cancer. Chemotherapy, particularly alkylating agents, may predispose to the development of myelodysplasia, secondary leukemias, and other malignancies. Chemotherapy and RT may be synergistic in this regard.

Predisposing genetic factors such as retinoblastoma, Li–Fraumeni syndrome, or neurofibromatosis type 1 (NF1) also increase the risk of induction of secondary, but also second, malignancies.

The risk is also related to the underlying cancer, with an increase seen after treatment for Hodgkin lymphoma and sarcoma.

Finally, lifestyle factors contribute to the risk, hence the importance of emphasizing healthy living choices, for example, smoking cessation, normal body weight, and good intake of fruit and vegetables, in survivors to try to mitigate this where possible.

6.12 Exercises and Self-Assessment

Q1. Which statement is true? The Continuous Hyperfractionated Accelerated RadioTherapy (CHART) irradiation protocol is characterized by:
- (a) A fraction size <2 Gy.
- (b) Reduced overall treatment time compared with conventional fractionation.
- (c) Irradiation is continued during the weekend.
- (d) a, b, and c are all correct.

Q2. Why is hyperfractionation potentially beneficial when it comes to late normal tissue sparing relative to conventional fractionation?
- (a) The α/β ratio is high.
- (b) The repair of sublethal damage is very effective.
- (c) The fraction size <2 Gy.
- (d) The number of fractions is larger.

Q3. On the basis of radiobiological aspects, what would be the optimal number of fractions in a hypofractionated treatment regimen?

Q4. Which of the following *is not true* about Stereotactic Body Radiation Therapy (SBRT)
- (a) In SBRT a high dose per fraction is used.
- (b) SBRT has high conformality.
- (c) SBRT has a large margin for the beam penumbra.
- (d) In SBRT image guidance is required for geometric verification of targets.

Q5. Please indicate which of the following statements *is wrong* when it comes to the SBRT treatment planning.
- (a) The dose is prescribed to lower isodose lines.
- (b) A homogeneous dose distribution is seen.
- (c) There is a sharp dose falloff outside target volume.
- (d) An isotropic grid size of 2 mm or finer is recommended for dose calculation.

Q6. Below are some statements related to how targeted therapy may sensitize tumors to radiation therapy (RT). Please indicate which statements are correct or wrong:
- (a) Inhibition of the DNA repair enzyme PARP1 with small molecules is a possible RT sensitizer for all types of tumors.
- (b) To increase the function of Bcl-2 is a RT sensitizing strategy.
- (c) Inhibitors toward EGFR is a promising RT sensibilization option for some tumors.
- (d) Reverting hypoxia is a way for RT sensitization.

Q7. Please name a key reason why RT can be combined with some immune therapies?

Q8. Hyperthermia has been shown to increase the effect of radiation therapy. Describe a DNA repair pathway that hyperthermia can inhibit.

Q9. Name an advantage and a disadvantage of photon spatially fractionated radiation therapy (SFRT), proton minibeam radiotherapy (pMBRT) and ion MBRT?

Q10. Give an example of a vectorized radiopharmaceutical used in the clinic and outline how it works.

Q11. Helium ions are good candidates in RT of tumors. What makes them good candidates?
- (a) Helium ions produce more secondary neutrons compared to protons.
- (b) Helium ions produce more nuclear fragments compared to carbon ions.
- (c) Helium ions have higher radiobiological effect (RBE) compared to protons.
- (d) Helium ions have lower oxygen enhancement ratio (OER) compared to protons.

6.13 Exercise Solutions

SQ1. Alternative (d). All statements (a, b, c) about the CHART irradiation protocol are correct. It involves a fraction size of <2 Gy and treatments are given dur-

ing weekends giving a reduced treatment time compared to a conventional fractionation scheme.

SQ2. Alternative (c). The fraction size <2 Gy.

SQ3. Taking the normal tissue dose-volume constraints into account and considering, e.g., the kinetics of reoxygenation, the activation of the immune system and the abscopal effect, a number of six to eight medium sized fractions spaced 72 h might be optimal regarding tumor control. However, this is still a point of debate.

SQ4. Alternative (c). In SBRT, small or no margin is given for beam penumbra to improve sharp dose falloff.

SQ5. Alternative (b). SBRT treatment plans have a heterogenous dose distribution.

SQ6. (a). The statement is wrong. PARP1 is primarily a target in tumors that have mutations in *BRCA1*/*BRAC2* or have a "BRACAness" phenotype. Such tumors lack functional DNA repair via HR and hence blocking PARP can impair repair of RT-induced DNA DSB. This is called synthetic lethality. PARP inhibition can also be applied for tumors with impairment in ATM or ATR. (b). The statement is wrong. Bcl-2 is an anti-apoptotic protein. Its activity/expression needs to be inhibited in order for RT to more prominently trigger cell death. (c). The statement is correct. EGFR inhibitors work in *EGFR*-mutant tumors, i.e., NSCLC or in tumors over-expressing EGFR. (d). The statement is correct. Tumor hypoxia can be attacked for RT sensitization purpose in several different ways.

SQ7. Since radiotherapy (RT) does exert both, immune stimulatory and immune suppressive effects, immune therapies aim to switch off the immune suppressive effects of RT or to boost the immune activating ones can be applied. This may result in effective local and systemic antitumor immune responses.

SQ8. Hyperthermia can temporarily downregulate the BRCA2 protein, thereby blocking the homologous recombination.

SQ9.

	Photon SFRT	Proton MBRT	Ion MBRT
Advantage	Easy implementation in clinic	Homogeneous tumor irradiation already from one direction	(Almost) no widening on the way to the tumor
Disadvantage	Low PVDR compared to MBRT	Widening of the beams on the way to the tumor	Technically challenging as interlacing necessary for homogeneous tumor irradiation

SQ10. Examples of vectorized radionuclide therapy are ^{177}Lu-PSMA-617 for the treatment of prostate cancer, ^{177}Lu-NeoB for the treatment of solid metastatic tumors, ^{177}Lu-DOTATATE for the treatment of neuroendocrine tumors, and ^{90}Y-ibritumomab tiuxetan (Zevalin®) for the treatment of CD20-positive Non-Hodgkin lymphoma. Brief description of the principle: A radiopharmaceutical comprises a targeting moiety, which targets a specific molecule expressed on certain cells, and a radionuclide, which emits IR. By linking the targeting moiety to the radionuclide, molecules (e.g., somatostatin receptors, PSMA, CD20, etc.) that are highly expressed on the target tissue can be targeted to treat disease. Thus, the targeting moiety ensures specific delivery of toxic IR to the targeted cells which ensures treatment of the tumor disease, while causing minimal damage to surrounding healthy tissues.

SQ11. Alternative (c). Helium ions have higher RBE compared to protons.

Appendix: Therapeutic BNCT Clinical Trials in the Last Two Decades

Cancer subsite	First author and year	Number of cases	^{10}B-carrier agent	Results/comments
Glioblastoma (newly diagnosed/recurrent)	Joensuu et al. (2003) [221]	18	BPA	Protocol P-01: 1-year overall survival was 61% in newly diagnosed glioblastoma.
		3	BPA	Protocol P-03: No death reported in re-irradiated patients.
	Capala et al. (2003) [222]	17	BPA	Short follow-up, no severe acute toxicities.
	Busse et al. (2003) [223]	22	BPA-Fructose (BPA-F)	2/22 patients had complete radiographic response while 13/17 evaluable subjects had measurable reduction in tumor volume.
	Henriksson et al. (2008) [224]	30	BPA-F	Median time to progression was 5.8 months and median survival time was 14.2 months. 4/30 patients had grade 3–4 toxicities.
	Kawabata et al. (2011) [225]	21	BSH and BPA	Protocol 1—BNCT. Protocol 2—BNCT followed by external beam RT. Median survival time was 15.6 months overall and 23.5 months in protocol 2.
Gliomas (high grade, malignant/recurrent)	Yamamoto et al. (2004) [226]	9	BSH	Interim analysis—median survival time was 23 months for glioblastoma and 25.9 months for anaplastic astrocytoma.
	Miyatake et al. (2005) [227]	13	BPA	In 8/12 patients, >50% of contrast enhanced lesions disappeared.
	Miyatake et al. (2009) [228]	22	BPA	Median survival for all patients was 10.8 months and high-risk RPA classes was 9.1 months.
	Kankaanranta et al. (2011) [229]	22	BPA-F	Median survival time was 7 months in malignant gliomas that recur after surgery and conventional radiotherapy.
Meningioma (high grade, malignant/recurrent)	Miyatake et al. (2007) [230]	7	BPA	18F-BPA-PET was taken before BNCT. 2/3 anaplastic meningioma patients showed complete response. 6/7 patients available for follow-up had radiographic improvements.
	Kawabata et al. (2013) [231]	20	BPA	Median survival time after BNCT was 14.1 months and after diagnosis was 45.7 months.
Malignant melanoma	Fukuda et al. (2003) [232]	22	BPA	Complete response was seen in 73% (16/22) and 3/22 patients developed severe skin damage.
	Menéndez et al. (2009) [233]	7	BPA	69.3% overall response, 30.7% no change, and 30% grade 3 skin toxicities.
	Hiratsuka et al. (2020) [233]	8	BPA	6/8 patients had complete response. On long-term follow-up, 88% control rate (7/8) and no >grade 2 adverse events.
Liver metastasis	Koivunoro et al. (2004) [233]	2	BPA	Liver extirpated, irradiated in a nuclear reactor, and reimplanted. One patient survived for 3 years after the procedure.
Head and neck cancers (recurrent/locally advanced)	Kato et al. (2004) [236]	6	BPA and BSH	46–100% reduction in tumor size with improved quality of life and very mild side effects.
	Kankaanranta et al. (2007) [237]	16	BPA-F	Median duration of response was 12.1 months. At median follow-up of 14 months, 33% (4/12) were alive. 2/12 had grade 3 toxicity.
	Kato et al. (2009) [238]	26	BPA	Response rate was 85%. Six-year overall rate was 24%.
	Kankaanranta et al. (2012) [238]	30	BPA	Two fractions of RT at 30-day interval. Tolerable early toxicities.
	Suzuki et al. (2014) [240]	62	BSH and BPA or BPA alone	Median survival time was 10.1 months. The overall survival rate was 43.1% and 24.2% at 1-year and 2-year, respectively.
	Aihara et al. (2014) [241]	20	BPA	Complete remission seen in 11 patients and partial remission in 7 patients. No severe acute or chronic toxicity.
	Wang et al. (2016) [242]	17	BPA	Two-year overall survival was 47% and locoregional control was 28%.
	Koivunoro et al. (2019) [243]	79	BPA	Two-year overall survival was 21% and locoregional progression-free survival was 38%.
	Hirose et al. (2021) [244]	21	Borofalan	Two-year overall survival was 58% in recurrent cases and 100% in locally advanced cases.

References

1. Brown A, Suit H. The centenary of the discovery of the Bragg peak. Radiother Oncol. 2004;73(3):265–8.
2. Marcu LG. Altered fractionation in radiotherapy: from radiobiological rationale to therapeutic gain. Cancer Treat Rev. 2010;36(8):606–14.
3. Shrieve DC, Loeffler JS. Human radiation injury. Wolters Kluwer Health/Lippincott Williams & Wilkins; 2011.
4. Bentzen SM, Atasoy BM, Daley FM, Dische S, Richman PI, Saunders MI, et al. Epidermal growth factor receptor expression in pretreatment biopsies from head and neck squamous cell carcinoma as a predictive factor for a benefit from accelerated radiation therapy in a randomized controlled trial. J Clin Oncol. 2005;23(24):5560–7.
5. Grimm J, Marks LB, Jackson A, Kavanagh BD, Xue J, Yorke E. High dose per fraction, hypofractionated treatment effects in the clinic (HyTEC): an overview. Int J Radiat Oncol Biol Phys. 2021;110(1):1–10.
6. Brown JM, Brenner DJ, Carlson DJ. Dose escalation, not "new biology," can account for the efficacy of stereotactic body radiation therapy with non-small cell lung cancer. Int J Radiat Oncol Biol Phys. 2013;85(5):1159–60.
7. Shibamoto Y, Miyakawa A, Otsuka S, Iwata H. Radiobiology of hypofractionated stereotactic radiotherapy: what are the optimal fractionation schedules? J Radiat Res. 2016;57(Suppl 1):i76–82.
8. Park HJ, Griffin RJ, Hui S, Levitt SH, Song CW. Radiation-induced vascular damage in tumors: implications of vascular damage in ablative hypofractionated radiotherapy (SBRT and SRS). Radiat Res. 2012;177(3):311–27.
9. Shuryak I, Hall EJ, Brenner DJ. Dose dependence of accelerated repopulation in head and neck cancer: supporting evidence and clinical implications. Radiother Oncol. 2018;127(1):20–6.
10. Shuryak I, Hall EJ, Brenner DJ. Optimized hypofractionation can markedly improve tumor control and decrease late effects for head and neck cancer. Int J Radiat Oncol Biol Phys. 2019;104(2):272–8.
11. Boustani J, Grapin M, Laurent PA, Apetoh L, Mirjolet C. The 6th R of radiobiology: reactivation of anti-tumor immune response. Cancers (Basel). 2019;11(6):860.
12. Formenti SC. Optimizing dose per fraction: a new chapter in the story of the abscopal effect? Int J Radiat Oncol Biol Phys. 2017;99(3):677–9.
13. Daguenet E, Khalifa J, Tolédano A, Borchiellini D, Pointreau Y, Rodriguez-Lafrasse C, et al. To exploit the 5 'R' of radiobiology and unleash the 3 'E' of immunoediting: 'RE'-inventing the radiotherapy-immunotherapy combination. Ther Adv Med Oncol. 2020;12:1758835920913445.
14. Franken NA, Oei AL, Kok HP, Rodermond HM, Sminia P, Crezee J, et al. Cell survival and radiosensitisation: modulation of the linear and quadratic parameters of the LQ model (Review). Int J Oncol. 2013;42(5):1501–15.
15. Schneider U, Besserer J, Mack A. Hypofractionated radiotherapy has the potential for second cancer reduction. Theor Biol Med Model. 2010;7:4.
16. Potters L, Kavanagh B, Galvin JM, et al. American society for therapeutic radiology and oncology (ASTRO) and American college of radiology (ACR) practice guideline for the performance of stereotactic body radiation therapy. Int J Radiat Oncol Biol Phys. 2010;76(2):326–32.
17. Khan FM, Gibbons JP. Stereotactic body radiation therapy. In: Khan FM, Gibbons JP, editors. Khan's the physics of radiation therapy. (5th edition) ed. Philadelphia, PA: Lippincott Williams & Wilkins; 2014. p. 467–74.
18. Fowler JF, Welsh JS, Howard SP. Loss of biological effect in prolonged fraction delivery. Int J Radiat Oncol Biol Phys. 2004;59(1):242–9.
19. Tilki D, Kilic N, Sevinc S, et al. Zone-specific remodeling of tumor blood vessels affects tumor growth. Cancer. 2007;110:2347–62.
20. Kavanagh BD, Bradley JD, Timmerman RD. Stereotactic irradiation of tumors outside the central nervous system. In: Halperin EC, Wazer DE, Perez CA, Brady LW, editors. Principle and practice of radiation oncology. (7th edition) ed. Philadelphia, PA: Wolters Kluwer; 2019. 426–34.
21. Park C, Papiez L, Zhang S, et al. Universal survival curve and single fraction equivalent dose: useful tools in understanding potency of ablative radiotherapy. Int J Radiat Oncol Biol Phys. 2008;70:847–52.
22. Benedict SH, Yenice KM, Followill D, et al. Stereotactic body radiation therapy: the report of AAPM Task Group 101. Med Phys. 2010;37:4078–101.
23. Simpson DR, Mell LK, Mundt AJ, et al. Image-guided radiation therapy. In: Halperin EC, Wazer DE, Perez CA, Brady LW, editors. Principle and practice of radiation oncology. (7th edition) ed. Philadelphia, PA: Wolters Kluwer; 2019. 288–302.
24. Wu QJ, Wang Z, Kirkpatrick JP, et al. Impact of collimator leaf width and treatment technique on stereotactic radiosurgery and radiotherapy plans for intra- and extracranial lesions. Radiat. Oncol. 2009;4
25. Martel MK, Ten Haken RK, Hazuka MB, et al. Estimation of tumor control probability model parameters from 3-D dose distributions of non-small cell lung cancer patients. Lung Cancer. 1999;24:31–7.
26. Niemierko A. Reporting and analyzing dose distributions: a concept of equivalent uniform dose. Med. Phys. 1997;24:103–10.
27. Matuszak MM, Yan D, Grills I, et al. Clinical applications of volumetric modulated arc therapy. Int J Radiat Oncol Biol Phys. 2010;77(2):608–16.
28. Zwahlen DR, Lang S, Hrbacek J, et al. The use of photon beams of a flattening filter-free linear accelerator for hypofractionated volumetric modulated arc therapy in localized prostate cancer. Int J Radiat Oncol Biol Phys. 2012;83(5):1655–60.
29. Kry SF, Vassiliev ON, Mohan R. Out-of-field photon dose following removal of the flattening filter from a medical accelerator. Phys. Med. Biol. 2010;55:2155–66.
30. R.A. Sethi, I.J. Barani, D.A. Larson, M. Roach III (Eds.). Handbook of evidence-based stereotactic radiosurgery and stereotactic body radiotherapy. Switzerland: Springer. 2016.
31. Timmerman RD, Bizekis CS, Pass HI, Fong Y, Dupuy DE, Dawson LA, et al. Local surgical, ablative, and radiation treatment of metastases. CA Cancer J Clin. 2009;59(3):145–70.
32. Favaudon V, Labarbe R, Limoli CL. Model studies of the role of oxygen in the FLASH effect. Med Phys. 2022;49(3):2068–81.
33. Bourhis J, Sozzi WJ, Jorge PG, Gaide O, Bailat C, Duclos F, et al. Treatment of a first patient with FLASH-radiotherapy. Radiother Oncol. 2019;139:18–22.
34. Jansen J, Knoll J, Beyreuther E, Pawelke J, Skuza R, Hanley R, et al. Does FLASH deplete oxygen? Experimental evaluation for photons, protons, and carbon ions. Med Phys. 2021;48(7):3982–90.
35. Montay-Gruel P, Bouchet A, Jaccard M, Patin D, Serduc R, Aim W, et al. X-rays can trigger the FLASH effect: Ultra-high dose-rate synchrotron light source prevents normal brain injury after whole brain irradiation in mice. Radiother Oncol. 2018;129(3):582–8.
36. Formenti SC, Demaria S. Systemic effects of local radiotherapy. Lancet Oncol. 2009;10(7):718–26.
37. Nakamura N, Kusunoki Y, Akiyama M. Radiosensitivity of CD4 or CD8 positive human T-lymphocytes by an in vitro colony formation assay. Radiat Res. 1990;123(2):224–7.
38. Chadwick J, Goldhaber M. Disintegration by slow neutrons. Nature. 1935;135:65.
39. Coleman CN, Prasanna PG, Capala J, et al. SMART radiotherapy. In: Halperin EC, Wazer DE, Perez CA, Brady LW, editors. Principle and practice of radiation oncology. (7th edition) ed. Philadelphia, PA: Wolters Kluwer; 2019. p. 146.

40. Halperin EC. The discipline of radiation oncology. In: Halperin EC, Wazer DE, Perez CA, Brady LW, editors. Principle and practice of radiation oncology. (7th edition) ed. Philadelphia, PA: Wolters Kluwer; 2019. p. 36–8.
41. Hall EJ, Giaccia AJ. Alternative radiation modalities. In: Hall EJ, Giaccia AJ, editors. Radiobiology for the radiologist. (8th edition) ed. Philadelphia, PA: Wolters Kluwer; 2019. p. 805–7.
42. Laramore GE. Neutron therapy and boron neutron capture therapy. In: Halperin EC, Wazer DE, Perez CA, Brady LW, editors. Principle and practice of radiation oncology. 7th ed. Philadelphia, PA: Wolters Kluwer; 2019. p. 487–8.
43. Ishiwata K, Ido T, Honda C, Kawamura M, Ichihashi M, Mishima Y. 4-Borono-2-[18F]fluoro-D,L-phenylalanine: a possible tracer for melanoma diagnosis with PET. Int J Rad Appl Instrum B. 1992;19(3):311–8.
44. Yanch JC, Shefer RE, Busse PM. Boron neutron capture therapy. Sci Med. 1999;6:18–27.
45. Coderre JA, Morris GM. The radiation biology of boron neutron capture therapy. Radiat Res. 1999;151:1–18.
46. Chin MP, Spyrou NM. A detailed Monte Carlo accounting of radiation transport in the brain during BNCT. Appl Radiat Isot. 2009;67(7-8 Suppl):S164–7.
47. Godwin JT, Farr LE, Sweet WH, et al. Pathological study of eight patients with glioblastoma multiforme treated by neutron capture therapy using boron 10. Cancer. 1956;8:601.
48. Hatanaka H, Amano K, Kanemitsu H, et al. Boron uptake by human brain tumors and quality control of boron compounds. In: Hatanaka H, editor. Boron-neutron capture therapy for tumors. Niigata, Japan: Nishimura; 1986. p. 77–106.
49. Laramore GE, Spence AM. Boron neutron capture therapy (BNCT) for highgrade gliomas of the brain. A cautionary note. Int J Radiat Oncol Biol Phys. 1996;36:241.
50. Rockhill JK, Laramore GE. Neutron radiotherapy. In L.L.Gunderson, J.E.Tepper (Eds.). Clinical radiation oncology (4th edition). Elsevier. 2019. p. 376–79.
51. Capala J, Barth RF, Bendayan M, et al. Boronated epidermal growth factor as a potential targeting agent for boron neutron capture therapy of brain tumors. Bioconjug Chem. 1996;7(1):7–15.
52. Carlsson J, Kullberg EB, Capala J, et al. Ligand liposomes and boron neutron capture therapy. J Neurooncol. 2003;62(1–2):47–59.
53. Murshed H, editor. Fundamentals of radiation oncology. Elsevier; 2019.
54. Tepper JE, Foote RL, Michalski JM. Gunderson & Tepper's clinical radiation oncology. 5th ed. Philadelphia: Elsevier; 2020.
55. Sureka CS, Armpilia C, editors. Radiation biology for medical physicists. 1st ed. Boca Raton: CRC Press; 2017.
56. Joiner MC, van der Kogel A. In: Joiner MC, van der Kogel A, editors. Basic clinical radiobiology. 4th ed. London: CRC press; 2009.
57. Hanahan D, Weinberg RA. Hallmarks of cancer: the next generation. Cell. 2011;144(5):646–74.
58. Pilié PG, Tang C, Mills GB, Yap TA. State-of-the-art strategies for targeting the DNA damage response in cancer. Nat Rev Clin Oncol. 2019;16(2):81–104.
59. van Bussel MTJ, Awada A, de Jonge MJA, Mau-Sørensen M, Nielsen D, Schöffski P, et al. A first-in-man phase 1 study of the DNA-dependent protein kinase inhibitor peposertib (formerly M3814) in patients with advanced solid tumours. Br J Cancer. 2021;124(4):728–35.
60. Myers SH, Ortega JA, Cavalli A. Synthetic lethality through the lens of medicinal chemistry. J Med Chem. 2020;63(23): 14151–83.
61. Teknos TN, Grecula J, Agrawal A, Old MO, Ozer E, Carrau R, et al. A phase 1 trial of Vorinostat in combination with concurrent chemoradiation therapy in the treatment of advanced staged head and neck squamous cell carcinoma. Investig New Drugs. 2019;37(4):702–10.
62. Cuneo KC, Morgan MA, Sahai V, Schipper MJ, Parsels LA, Parsels JD, et al. Dose escalation trial of the Wee1 inhibitor adavosertib (AZD1775) in combination with gemcitabine and radiation for patients with locally advanced pancreatic cancer. J Clin Oncol. 2019;37(29):2643–50.
63. Bosacki C, Bouleftour W, Sotton S, Vallard A, Daguenet E, Ouaz H, et al. CDK 4/6 inhibitors combined with radiotherapy: a review of literature. Clin Transl Radiat Oncol. 2021;26:79–85.
64. Zerp SF, Stoter TR, Hoebers FJP, van den Brekel MWM, Dubbelman R, Kuipers GK, et al. Targeting anti-apoptotic Bcl-2 by AT-101 to increase radiation efficacy: data from in vitro and clinical pharmacokinetic studies in head and neck cancer. Radiat Oncol. 2015;10(1):158.
65. Blaes J, Thomé CM, Pfenning PN, Rübmann P, Sahm F, Wick A, et al. Inhibition of CD95/CD95L (FAS/FASLG) signaling with APG101 prevents invasion and enhances radiation therapy for glioblastoma. Mol Cancer Res. 2018;16(5):767–76.
66. Sun XS, Tao Y, Le Tourneau C, Pointreau Y, Sire C, Kaminsky MC, et al. Debio 1143 and high-dose cisplatin chemoradiotherapy in high-risk locoregionally advanced squamous cell carcinoma of the head and neck: a double-blind, multicentre, randomised, phase 2 study. Lancet Oncol. 2020;21(9):1173–87.
67. Tchelebi LT, Batchelder E, Wang M, Lehrer EJ, Drabick JJ, Sharma N, et al. Radiotherapy and receptor tyrosine kinase inhibition for solid cancers (ROCKIT): a meta-analysis of 13 studies. JNCI Cancer Spectr. 2021;5(4):pkab050.
68. Wrona A, Dziadziuszko R, Jassem J. Combining radiotherapy with targeted therapies in non-small cell lung cancer: focus on anti-EGFR, anti-ALK and anti-angiogenic agents. Transl Lung Cancer Res. 2021;10(4):2032–47.
69. Huang CY, Tai WT, Wu SY, Shih CT, Chen MH, Tsai MH, et al. Dovitinib acts as a novel radiosensitizer in hepatocellular carcinoma by targeting SHP-1/STAT3 signaling. Int J Radiat Oncol Biol Phys. 2016;95(2):761–71.
70. Boland PM, Meyer JE, Berger AC, Cohen SJ, Neuman T, Cooper HS, et al. Induction therapy for locally advanced, resectable esophagogastric cancer: a phase I trial of vandetanib (ZD6474), paclitaxel, carboplatin, 5-fluorouracil, and radiotherapy followed by resection. Am J Clin Oncol. 2017;40(4):393–8.
71. Saran F, Chinot OL, Henriksson R, Mason W, Wick W, Cloughesy T, Dhar S, Pozzi E, Garcia J, Nishikawa R. Bevacizumab, temozolomide, and radiotherapy for newly diagnosed glioblastoma: comprehensive safety results during and after first-line therapy. Neuro Oncol. 2016;18(7):991–1001. https://doi.org/10.1093/neuonc/nov300. PMID: 26809751; PMCID: PMC4896538.
72. Saksø M, Jensen K, Andersen M, Hansen CR, Eriksen JG, Overgaard J. DAHANCA 28: a phase I/II feasibility study of hyperfractionated, accelerated radiotherapy with concomitant cisplatin and nimorazole (HART-CN) for patients with locally advanced, HPV/p16-negative squamous cell carcinoma of the oropharynx, hypopharynx, larynx and oral cavity. Radiother Oncol. 2020;148:65–72.
73. Toulany M. Targeting DNA Double-strand break repair pathways to improve radiotherapy response. Genes (Basel). 2019;10(1):25.
74. Lee EF, Fairlie WD. Discovery, development and application of drugs targeting BCL-2 pro-survival proteins in cancer. Biochem Soc Trans. 2021;49(5):2381–95.
75. Rödel F, Reichert S, Sprenger T, Gaipl US, Mirsch J, Liersch T, et al. The role of survivin for radiation oncology: moving beyond apoptosis inhibition. Curr Med Chem. 2011;18(2):191–9.
76. Tuomainen K, Hyytiäinen A, Al-Samadi A, Ianevski P, Ianevski A, Potdar S, et al. High-throughput compound screening identifies navitoclax combined with irradiation as a candidate therapy for HPV-negative head and neck squamous cell carcinoma. Sci Rep. 2021;11(1):14755.
77. Salazar R, Capdevila J, Manzano JL, Pericay C, Martínez-Villacampa M, López C, et al. Phase II randomized trial of

capecitabine with bevacizumab and external beam radiation therapy as preoperative treatment for patients with resectable locally advanced rectal adenocarcinoma: long term results. BMC Cancer. 2020;20(1):1164.
78. Frey B, Rubner Y, Kulzer L, Werthmöller N, Weiss EM, Fietkau R, et al. Antitumor immune responses induced by ionizing irradiation and further immune stimulation. Cancer Immunol Immunother. 2014;63(1):29–36.
79. Falcke SE, Rühle PF, Deloch L, Fietkau R, Frey B, Gaipl US. Clinically relevant radiation exposure differentially impacts forms of cell death in human cells of the innate and adaptive immune system. Int J Mol Sci. 2018;19(11):3574.
80. Rückert M, Flohr AS, Hecht M, Gaipl US. Radiotherapy and the immune system: more than just immune suppression. Stem Cells. 2021b;39(9):1155–65.
81. Weichselbaum RR, Liang H, Deng L, Fu YX. Radiotherapy and immunotherapy: a beneficial liaison? Nat Rev Clin Oncol. 2017;14(6):365–79.
82. Frey B, Rückert M, Deloch L, Rühle PF, Derer A, Fietkau R, et al. Immunomodulation by ionizing radiation-impact for design of radio-immunotherapies and for treatment of inflammatory diseases. Immunol Rev. 2017;280(1):231–48.
83. Rückert M, Deloch L, Frey B, Schlücker E, Fietkau R, Gaipl US. Combinations of radiotherapy with vaccination and immune checkpoint inhibition differently affect primary and abscopal tumor growth and the tumor microenvironment. Cancers (Basel). 2021a;13(4):714.
84. Demaria S, Guha C, Schoenfeld J, Morris Z, Monjazeb A, Sikora A, et al. Radiation dose and fraction in immunotherapy: one-size regimen does not fit all settings, so how does one choose? J Immunother Cancer. 2021;9(4):e002038.
85. Shu CA, Cascone T. What is neo? Chemoimmunotherapy in the neoadjuvant setting for resectable non–small-cell lung cancer. J Clin Oncol. 2021;39(26):2855–8.
86. Chargari C, Toillon RA, Macdermed D, Castadot P, Magné N. Concurrent hormone and radiation therapy in patients with breast cancer: what is the rationale? Lancet Oncol. 2009;10(1):53–60.
87. Azria D, Larbouret C, Cunat S, et al. Letrozole sensitizes breast cancer cells to ionizing radiation. Breast Cancer Res. 2004;7:1–8(R156).
88. Abraham J, Staffurth J. Hormonal therapy for cancer. Medicine. 2016;44(1):30–3.
89. Philippou Y, Sjoberg H, Lamb AD, Camilleri P, Bryant RJ. Harnessing the potential of multimodal radiotherapy in prostate cancer. Nat Rev Urol. 2020;17(6):321–38.
90. Bolla M, Van Tienhoven G, Warde P, Dubois JB, Mirimanoff RO, Storme G, Bernier J, Kuten A, Sternberg C, Billiet I, Torecilla JL, Pfeffer R, Cutajar CL, Van der Kwast T, Collette L. External irradiation with or without long-term androgen suppression for prostate cancer with high metastatic risk: 10-year results of an EORTC randomised study. Lancet Oncol. 2010;11:1066–73. https://doi.org/10.1016/S1470-2045(10)70223-0. Epub 2010 Oct 7
91. Hader M, Frey B, Fietkau R, Hecht M, Gaipl US. Immune biological rationales for the design of combined radio- and immunotherapies. Cancer Immunol Immunother. 2020a;69(2):293–306.
92. Hader M, Savcigil DP, Rosin A, Ponfick P, Gekle S, Wadepohl M, et al. Differences of the immune phenotype of breast cancer cells after ex vivo hyperthermia by warm-water or microwave radiation in a closed-loop system alone or in combination with radiotherapy. Cancers (Basel). 2020b;12(5):1082.
93. Sugarbaker PH. Laboratory and clinical basis for hyperthermia as a component of intracavitary chemotherapy. Int J Hyperth. 2007;23(5):431–42.
94. Issels R, Kampmann E, Kanaar R, Lindner LH. Hallmarks of hyperthermia in driving the future of clinical hyperthermia as targeted therapy: translation into clinical application. Int J Hyperth. 2016;32(1):89–95.
95. Oei AL, Kok HP, Oei SB, Horsman MR, Stalpers LJA, Franken NAP, et al. Molecular and biological rationale of hyperthermia as radio- and chemosensitizer. Adv Drug Deliv Rev. 2020;163–164:84–97.
96. Narayan P, Crocker I, Elder E, Olson JJ. Safety and efficacy of concurrent interstitial radiation and hyperthermia in the treatment of progressive malignant brain tumors. Oncol Rep. 2004;11(1):97–103.
97. Elming PB, Sørensen BS, Oei AL, Franken NAP, Crezee J, Overgaard J, et al. Hyperthermia: the optimal treatment to overcome radiation resistant hypoxia. Cancers (Basel). 2019;11(1):60.
98. Kok HP, Cressman ENK, Ceelen W, Brace CL, Ivkov R, Grüll H, et al. Heating technology for malignant tumors: a review. Int J Hyperth. 2020;37(1):711–41.
99. Schildkopf P, Frey B, Ott OJ, Rubner Y, Multhoff G, Sauer R, et al. Radiation combined with hyperthermia induces HSP70-dependent maturation of dendritic cells and release of pro-inflammatory cytokines by dendritic cells and macrophages. Radiother Oncol. 2011;101(1):109–15.
100. Multhoff G. Activation of natural killer cells by heat shock protein 70. 2002. Int J Hyperth. 2009;25(3):169–75.
101. Datta NR, Ordóñez SG, Gaipl US, Paulides MM, Crezee H, Gellermann J, et al. Local hyperthermia combined with radiotherapy and-/or chemotherapy: recent advances and promises for the future. Cancer Treat Rev. 2015;41(9):742–53.
102. Lindner LH, Blay JY, Eggermont AMM, Issels RD. Perioperative chemotherapy and regional hyperthermia for high-risk adult-type soft tissue sarcomas. Eur J Cancer. 2021;147:164–9.
103. Issels RD, Lindner LH, Verweij J, Wust P, Reichardt P, Schem BC, et al. Neo-adjuvant chemotherapy alone or with regional hyperthermia for localised high-risk soft-tissue sarcoma: a randomised phase 3 multicentre study. Lancet Oncol. 2010;11(6):561–70.
104. van der Zee J, González González D, van Rhoon GC, van Dijk JD, van Putten WL, Hart AA. Comparison of radiotherapy alone with radiotherapy plus hyperthermia in locally advanced pelvic tumours: a prospective, randomised, multicentre trial. Dutch Deep Hyperthermia Group. Lancet. 2000;355(9210):1119–25.
105. Kroesen M, Mulder HT, van Holthe JML, Aangeenbrug AA, Mens JWM, van Doorn HC, et al. The effect of the time interval between radiation and hyperthermia on clinical outcome in 400 locally advanced cervical carcinoma patients. Front Oncol. 2019;9:134.
106. van Leeuwen CM, Oei AL, Ten Cate R, Franken NAP, Bel A, Stalpers LJA, et al. Measurement and analysis of the impact of time-interval, temperature and radiation dose on tumour cell survival and its application in thermoradiotherapy plan evaluation. Int J Hyperth. 2018;34(1):30–8.
107. Nencioni A, Caffa I, Cortellino S, Longo VD. Fasting and cancer: molecular mechanisms and clinical application. Nat Rev Cancer. 2018;18(11):707–19.
108. Buono R, Longo VD. Starvation, stress resistance, and cancer. Trends Endocrinol Metab. 2018;29(4):271–80.
109. Köhler A. A method of deep Roentgen irradiation without injury to the skin. Arch Roentgen Ray. 1909;14(5):141–2.
110. Prezado Y, Renier M, Bravin A. A new method of creating minibeam patterns for synchrotron radiation therapy: a feasibility study. J Synchrotron Radiat. 2009;16(Pt 4):582–6.
111. Zlobinskaya O, Girst S, Greubel C, Hable V, Siebenwirth C, Walsh DW, et al. Reduced side effects by proton microchannel radiotherapy: study in a human skin model. Radiat Environ Biophys. 2013;52(1):123–33.
112. Sammer M, Greubel C, Girst S, Dollinger G. Optimization of beam arrangements in proton minibeam radiotherapy by cell survival simulations. Med Phys. 2017;44(11):6096–104.
113. Reindl J, Girst S. pMB FLASH - status and perspectives of combining proton minibeam with FLASH radiotherapy. J Cancer Immunol. 2019; https://doi.org/10.33696/cancerimmunol.1.003.

114. Yan W, Khan MK, Wu X, Simone CB, Fan J, Gressen E, et al. Spatially fractionated radiation therapy: history, present and the future. Clin Transl Radiat Oncol. 2020;20:30–8.
115. Billena C, Khan AJ. A current review of spatial fractionation: back to the future? Int J Radiat Oncol Biol Phys. 2019;104(1):177–87.
116. Blanco Suarez JM, Amendola BE, Perez N, Amendola M, Wu X. The use of lattice radiation therapy (LRT) in the treatment of bulky tumors: a case report of a large metastatic mixed Mullerian ovarian tumor. Cureus. 2015;7(11):e389.
117. Fernandez-Palomo C, Fazzari J, Trappetti V, Smyth L, Janka H, Laissue J, et al. Animal models in microbeam radiation therapy: a scoping review. Cancers. 2020;12(3):527.
118. Trappetti V, Fazzari JM, Fernandez-Palomo C, Scheidegger M, Volarevic V, Martin OA, et al. Microbeam radiotherapy—a novel therapeutic approach to overcome radioresistance and enhance anti-tumour response in melanoma. Int J Mol Sci. 2021;22(14):7755.
119. Sammer M, Girst S, Dollinger G. Optimizing proton minibeam radiotherapy by interlacing and heterogeneous tumor dose on the basis of calculated clonogenic cell survival. Sci Rep. 2021;11(1):3533.
120. Lamirault C, Doyère V, Juchaux M, Pouzoulet F, Labiod D, Dendale R, et al. Short and long-term evaluation of the impact of proton minibeam radiation therapy on motor, emotional and cognitive functions. Sci Rep. 2020;10(1):13511.
121. Lansonneur P, Mammar H, Nauraye C, Patriarca A, Hierso E, Dendale R, et al. First proton minibeam radiation therapy treatment plan evaluation. Sci Rep. 2020;10(1):7025.
122. Mohiuddin M, Lynch C, Gao M, Hartsell W. Early clinical results of proton spatially fractionated GRID radiation therapy (SFGRT). Br J Radiol. 2020;93(1107):20190572.
123. Skowronek J. Current status of brachytherapy in cancer treatment - short overview. J Contemp Brachyther. 2017;9(6):581–9.
124. Njeh CF, Saunders MW, Langton CM. Accelerated partial breast irradiation (APBI): a review of available techniques. Radiat Oncol. 2010;5(1):90.
125. Pötter R, Tanderup K, Kirisits C, de Leeuw A, Kirchheiner K, Nout R, et al. The EMBRACE II study: the outcome and prospect of two decades of evolution within the GEC-ESTRO GYN working group and the EMBRACE studies. Clin Transl Radiat Oncol. 2018;9:48–60.
126. ICRU-Report-89. ICRU report 89: prescribing, recording, and reporting brachytherapy for cancer of the cervix. J ICRU. 2013;13(1–2)
127. Sminia P, Schneider CJ, van Tienhoven G, Koedooder K, Blank LE, González González D. Office hours pulsed brachytherapy boost in breast cancer. Radiother Oncol. 2001;59(3):273–80.
128. Harms W, Weber KJ, Ehemann V, Zuna I, Debus J, Peschke P. Differential effects of CLDR and PDR brachytherapy on cell cycle progression in a syngeneic rat prostate tumour model. Int J Radiat Biol. 2006;82(3):191–6.
129. Nicolay NH, Berry DP, Sharma RA. Liver metastases from colorectal cancer: radioembolization with systemic therapy. Nat Rev Clin Oncol. 2009;6(12):687–97.
130. Cremonesi M, Chiesa C, Strigari L, Ferrari M, Botta F, Guerriero F, et al. Radioembolization of hepatic lesions from a radiobiology and dosimetric perspective. Front Oncol. 2014;4:210.
131. Vouche M, Vanderlinden B, Delatte P, Lemort M, Hendlisz A, Deleporte A, et al. New imaging techniques for 90Y microsphere radioembolization. J Nucl Med Radiat Ther. 2011;2(1):113.
132. Levillain H, Bagni O, Deroose CM, Dieudonné A, Gnesin S, Grosser OS, et al. International recommendations for personalised selective internal radiation therapy of primary and metastatic liver diseases with yttrium-90 resin microspheres. Eur J Nucl Med Mol Imaging. 2021;48(5):1570–84.
133. Salem R, Padia SA, Lam M, Bell J, Chiesa C, Fowers K, et al. Clinical and dosimetric considerations for Y90: recommendations from an international multidisciplinary working group. Eur J Nucl Med Mol Imaging. 2019;46(8):1695–704.
134. Garin E, Tselikas L, Guiu B, Chalaye J, Edeline J, de Baere T, et al. Personalised versus standard dosimetry approach of selective internal radiation therapy in patients with locally advanced hepatocellular carcinoma (DOSISPHERE-01): a randomised, multicentre, open-label phase 2 trial. Lancet Gastroenterol Hepatol. 2021;6(1):17–29.
135. Sherman M, Levine R. Nuclear medicine and wall street: an evolving relationship. J Nucl Med. 2019;60(Suppl 2):20s–4s.
136. Puranik AD, Dromain C, Fleshner N, Sathekge M, Pavel M, Eberhardt N, et al. Target heterogeneity in oncology: the best predictor for differential response to radioligand therapy in neuroendocrine tumors and prostate cancer. Cancers. 2021;13(14):3607.
137. Yordanova A, Eppard E, Kürpig S, Bundschuh RA, Schönberger S, Gonzalez-Carmona M, et al. Theranostics in nuclear medicine practice. Onco Targets Ther. 2017;10:4821–8.
138. Qaim SM, Scholten B, Neumaier B. New developments in the production of theranostic pairs of radionuclides. J Radioanal Nucl Chem. 2018;318(3):1493–509.
139. Burkett BJ, Dundar A, Young JR, Packard AT, Johnson GB, Halfdanarson TR, et al. How we do it: a multidisciplinary approach to (177)Lu DOTATATE peptide receptor radionuclide therapy. Radiology. 2021;298(2):261–74.
140. Fersing C, Bouhlel A, Cantelli C, Garrigue P, Lisowski V, Guillet B. A comprehensive review of non-covalent radiofluorination approaches using aluminum [(18)F]fluoride: will [(18)F]AlF replace (68)Ga for metal chelate labeling? Molecules. 2019;24(16):2866.
141. Radhi HT, Jamal HF, Sarwani AA, Abdullah AJ, Al-Alawi MF, Alsabea AS, et al. Efficacy of a single fixed 131I dose of Radioactive iodine for the treatment of hyperthyroidism. Clin Investig. 2019;9(4):111–20.
142. Parker C, Nilsson S, Heinrich D, Helle SI, O'Sullivan JM, Fosså SD, et al. Alpha emitter radium-223 and survival in metastatic prostate cancer. N Engl J Med. 2013;369(3):213–23.
143. Poeppel TD, Handkiewicz-Junak D, Andreeff M, Becherer A, Bockisch A, Fricke E, et al. EANM guideline for radionuclide therapy with radium-223 of metastatic castration-resistant prostate cancer. Eur J Nucl Med Mol Imaging. 2018;45(5):824–45.
144. Pryma DA, Mandel SJ. Radioiodine therapy for thyroid cancer in the era of risk stratification and alternative targeted therapies. J Nucl Med. 2014;55(9):1485–91.
145. Luster M, Clarke SE, Dietlein M, Lassmann M, Lind P, Oyen WJ, et al. Guidelines for radioiodine therapy of differentiated thyroid cancer. Eur J Nucl Med Mol Imaging. 2008;35(10):1941–59.
146. Ahmadi Bidakhvidi N, Goffin K, Dekervel J, Baete K, Nackaerts K, Clement P, et al. Peptide receptor radionuclide therapy targeting the somatostatin receptor: basic principles, clinical applications and optimization strategies. Cancers. 2022;14(1):129.
147. Strosberg J, El-Haddad G, Wolin E, Hendifar A, Yao J, Chasen B, et al. Phase 3 trial of (177)Lu-dotatate for midgut neuroendocrine tumors. N Engl J Med. 2017;376(2):125–35.
148. Brabander T, van der Zwan WA, Teunissen JJM, Kam BLR, Feelders RA, de Herder WW, et al. Long-term efficacy, survival, and safety of [(177)Lu-DOTA(0),Tyr(3)]octreotate in patients with gastroenteropancreatic and bronchial neuroendocrine tumors. Clin Cancer Res. 2017;23(16):4617–24.
149. Imhof A, Brunner P, Marincek N, Briel M, Schindler C, Rasch H, et al. Response, survival, and long-term toxicity after therapy with the radiolabeled somatostatin analogue [90Y-DOTA]-TOC in metastasized neuroendocrine cancers. J Clin Oncol. 2011;29(17):2416–23.

150. Sartor O, de Bono J, Chi KN, Fizazi K, Herrmann K, Rahbar K, et al. Lutetium-177-PSMA-617 for metastatic castration-resistant prostate cancer. N Engl J Med. 2021;385(12):1091–103.
151. Moreno P, Ramos-Álvarez I, Moody TW, Jensen RT. Bombesin related peptides/receptors and their promising therapeutic roles in cancer imaging, targeting and treatment. Expert Opin Ther Targets. 2016;20(9):1055–73.
152. von Eyben FE, Bauman G, von Eyben R, Rahbar K, Soydal C, Haug AR, et al. Optimizing PSMA radioligand therapy for patients with metastatic castration-resistant prostate cancer. A systematic review and meta-analysis. Int J Mol Sci. 2020;21(23):9054.
153. Weiner GJ. Building better monoclonal antibody-based therapeutics. Nat Rev Cancer. 2015;15(6):361–70.
154. Witzig TE, Gordon LI, Cabanillas F, Czuczman MS, Emmanouilides C, Joyce R, et al. Randomized controlled trial of yttrium-90-labeled ibritumomab tiuxetan radioimmunotherapy versus rituximab immunotherapy for patients with relapsed or refractory low-grade, follicular, or transformed B-cell non-Hodgkin's lymphoma. J Clin Oncol. 2002;20(10):2453–63.
155. Wang Y, Probin V, Zhou D. Cancer therapy-induced residual bone marrow injury-mechanisms of induction and implication for therapy. Curr Cancer Ther Rev. 2006;2(3):271–9.
156. Altunay B, Morgenroth A, Beheshti M, Vogg A, Wong NCL, Ting HH, et al. HER2-directed antibodies, affibodies and nanobodies as drug-delivery vehicles in breast cancer with a specific focus on radioimmunotherapy and radioimmunoimaging. Eur J Nucl Med Mol Imaging. 2021;48(5):1371–89.
157. Verhoeven M, Seimbille Y, Dalm SU. Therapeutic applications of pretargeting. Pharmaceutics. 2019;11(9):434.
158. Gill MR, Falzone N, Du Y, Vallis KA. Targeted radionuclide therapy in combined-modality regimens. Lancet Oncol. 2017;18(7):e414–e23.
159. Kashyap R, Hofman MS, Michael M, Kong G, Akhurst T, Eu P, et al. Favourable outcomes of (177)Lu-octreotate peptide receptor chemoradionuclide therapy in patients with FDG-avid neuroendocrine tumours. Eur J Nucl Med Mol Imaging. 2015;42(2):176–85.
160. Ballal S, Yadav MP, Damle NA, Sahoo RK, Bal C. Concomitant 177Lu-DOTATATE and capecitabine therapy in patients with advanced neuroendocrine tumors: a long-term-outcome, toxicity, survival, and quality-of-life study. Clin Nucl Med. 2017;42(11):e457–e66.
161. Yadav MP, Ballal S, Bal C. Concomitant 177Lu-DOTATATE and capecitabine therapy in malignant paragangliomas. EJNMMI Res. 2019;9(1):13.
162. Strosberg JR, Fine RL, Choi J, Nasir A, Coppola D, Chen DT, et al. First-line chemotherapy with capecitabine and temozolomide in patients with metastatic pancreatic endocrine carcinomas. Cancer. 2011;117(2):268–75.
163. Bison SM, Haeck JC, Bol K, et al. Optimization of combined temozolomide and peptide receptor radionuclide therapy (PRRT) in mice after multimodality molecular imaging studies. EJNMMI Res. 2015;5(1):62. https://doi.org/10.1186/s13550-015-0142-y.
164. Morris MJ, Loriot Y, Sweeney CJ, Fizazi K, Ryan CJ, Shevrin DH, et al. Radium-223 in combination with docetaxel in patients with castration-resistant prostate cancer and bone metastases: a phase 1 dose escalation/randomised phase 2a trial. Eur J Cancer. 2019;114:107–16.
165. Dhiantravan N, Emmett L, Joshua AM, Pattison DA, Francis RJ, Williams S, et al. UpFrontPSMA: a randomized phase 2 study of sequential 177Lu-PSMA-617 and docetaxel vs docetaxel in metastatic hormone-naïve prostate cancer (clinical trial protocol). BJU Int. 2021;128(3):331–42.
166. Claringbold PG, Turner JH. NeuroEndocrine tumor therapy with lutetium-177-octreotate and everolimus (NETTLE): a phase I study. Cancer Biother Radiopharm. 2015;30(6):261–9.
167. Cullinane C, Waldeck K, Kirby L, Rogers BE, Eu P, Tothill RW, et al. Enhancing the anti-tumour activity of 177Lu-DOTA-octreotate radionuclide therapy in somatostatin receptor-2 expressing tumour models by targeting PARP. Sci Rep. 2020;10(1):10196.
168. Suman SK, Subramanian S, Mukherjee A. Combination radionuclide therapy: a new paradigm. Nucl Med Biol. 2021;98–99:40–58.
169. Dietrich A, Koi L, Zöphel K, Sihver W, Kotzerke J, Baumann M, et al. Improving external beam radiotherapy by combination with internal irradiation. Br J Radiol. 2015;88(1051):20150042.
170. Kreissl MC, Hänscheid H, Löhr M, Verburg FA, Schiller M, Lassmann M, et al. Combination of peptide receptor radionuclide therapy with fractionated external beam radiotherapy for treatment of advanced symptomatic meningioma. Radiat Oncol. 2012;7(1):99.
171. Oddstig J, Bernhardt P, Nilsson O, Ahlman H, Forssell-Aronsson E. Radiation induces up-regulation of somatostatin receptors 1, 2, and 5 in small cell lung cancer in vitro also at low absorbed doses. Cancer Biother Radiopharm. 2011;26(6):759–65.
172. Kim C, Liu SV, Subramaniam DS, Torres T, Loda M, Esposito G, et al. Phase I study of the (177)Lu-DOTA(0)-Tyr(3)-Octreotate (lutathera) in combination with nivolumab in patients with neuroendocrine tumors of the lung. J Immunother Cancer. 2020;8(2):e000980.
173. Shah RG, Merlin MA, Adant S, Zine-Eddine F, Beauregard JM, Shah GM. Chemotherapy-induced upregulation of somatostatin receptor-2 increases the uptake and efficacy of (177)Lu-DOTA-octreotate in neuroendocrine tumor cells. Cancers (Basel). 2021;13(2):232.
174. Obodovskiy I. Chapter 5—Passing of charged particles through matter. In: Obodovskiy I, editor. Radiation. Elsevier; 2019. p. 103–36.
175. Rietzel E, Bert C. Respiratory motion management in particle therapy. Med Phys. 2010;37(2):449–60.
176. Zschaeck S, Simon M, Löck S, Troost EGC, Stützer K, Wohlfahrt P, et al. PRONTOX – proton therapy to reduce acute normal tissue toxicity in locally advanced non-small-cell lung carcinomas (NSCLC): study protocol for a randomised controlled trial. Trials. 2016;17(1):543.
177. Park SH, Kang JO. Basics of particle therapy I: physics. Radiat Oncol J. 2011;29(3):135–46.
178. Elaimy AL, Ding L, Bradford C, Geng Y, Bushe H, Kuo I-L, et al. History and overview of proton therapy. IntechOpen; 2021.
179. Smith AR. Proton therapy. Phys Med Biol. 2006;51(13):R491–504.
180. Paganetti H, editor. Proton therapy physics. 1st ed. Boca Raton: CRC Press; 2012.
181. Jones B, McMahon SJ, Prise KM. The radiobiology of proton therapy: challenges and opportunities around relative biological effectiveness. Clin Oncol. 2018;30(5):285–92.
182. Michaelidesová A, Vachelová J, Puchalska M, Brabcová KP, Vondráček V, Sihver L, et al. Relative biological effectiveness in a proton spread-out Bragg peak formed by pencil beam scanning mode. Australas Phys Eng Sci Med. 2017;40(2):359–68.
183. Paganetti H. Relative biological effectiveness (RBE) values for proton beam therapy. Variations as a function of biological endpoint, dose, and linear energy transfer. Phys Med Biol. 2014;59(22):R419–R72.
184. Wouters BG, Skarsgard LD, Gerweck LE, Carabe-Fernandez A, Wong M, Durand RE, et al. Radiobiological intercomparison of the 160 MeV and 230 MeV proton therapy beams at the Harvard Cyclotron Laboratory and at Massachusetts General Hospital. Radiat Res. 2015;183(2):174–87.
185. Michaelidesová A, Vachelová J, Klementová J, Urban T, Pachnerová Brabcová K, Kaczor S, et al. In vitro comparison of passive and active clinical proton beams. Int J Mol Sci. 2020;21(16):5650.

186. Breen WG, Paulino AC, Hartsell WF, Mangona VS, Perkins SM, Indelicato DJ, et al. Factors associated with acute toxicity in pediatric patients treated with proton radiation therapy: a report from the Pediatric Proton Consortium Registry. Pract Radiat Oncol. 2022;12(2):155–62.
187. Castro JR, Quivey JM, Lyman JT, Chen GT, Phillips TL, Tobias CA. Radiotherapy with heavy charged particles at Lawrence Berkeley Laboratory. J Can Assoc Radiol. 1980;31(1):30–4.
188. Mohamad O, Makishima H, Kamada T. Evolution of carbon ion radiotherapy at the National Institute of Radiological Sciences in Japan. Cancers (Basel). 2018;10(3):66.
189. IAEA-Report. Dose reporting in ion beam therapy. Vienna: International Atomic Energy Agency; 2007.
190. Malouff TD, Mahajan A, Krishnan S, Beltran C, Seneviratne DS, Trifiletti DM. Carbon ion therapy: a modern review of an emerging technology. Front Oncol. 2020;10:82.
191. Syljuåsen R. Cell cycle effects in radiation oncology. In: Wenz F, editor. Radiation oncology. Cham: Springer International Publishing; 2019. p. 1–8.
192. Held KD, Kawamura H, Kaminuma T, Paz AE, Yoshida Y, Liu Q, et al. Effects of charged particles on human tumor cells. Front Oncol. 2016;6:23.
193. Durante M, Loeffler JS. Charged particles in radiation oncology. Nat Rev Clin Oncol. 2010;7(1):37–43.
194. Lodge M, Pijls-Johannesma M, Stirk L, Munro AJ, De Ruysscher D, Jefferson T. A systematic literature review of the clinical and cost-effectiveness of hadron therapy in cancer. Radiother Oncol. 2007;83(2):110–22.
195. Kamada T, Tsujii H, Blakely EA, Debus J, De Neve W, Durante M, et al. Carbon ion radiotherapy in Japan: an assessment of 20 years of clinical experience. Lancet Oncol. 2015;16(2):e93–e100.
196. Chen J, Mao J, Ma N, Wu KL, Lu J, Jiang GL. Definitive carbon ion radiotherapy for tracheobronchial adenoid cystic carcinoma: a preliminary report. BMC Cancer. 2021;21(1):734.
197. Kaneko T, Suefuji H, Koto M, Demizu Y, Saitoh JI, Tsuji H, et al. Multicenter study of carbon-ion radiotherapy for oropharyngeal non-squamous cell carcinoma. In Vivo. 2021;35(4):2239–45.
198. Lu VM, O'Connor KP, Mahajan A, Carlson ML, Van Gompel JJ. Carbon ion radiotherapy for skull base chordomas and chondrosarcomas: a systematic review and meta-analysis of local control, survival, and toxicity outcomes. J Neurooncol. 2020;147(3):503–13.
199. Degiovanni A, Amaldi U. History of hadron therapy accelerators. Phys Med. 2015;31(4):322–32.
200. Inaniwa T, Kanematsu N, Noda K, Kamada T. Treatment planning of intensity modulated composite particle therapy with dose and linear energy transfer optimization. Phys Med Biol. 2017;62(12):5180–97.
201. Mizushima KA-O, Iwata YA-O, Muramatsu M, Lee SH, Shirai T. Experimental study on monitoring system of clinical beam purity in multiple-ion beam operation for heavy-ion radiotherapy. Rev Sci Instrum. 2020;91:023309.
202. Horst F, Schardt D, Iwase H, Schuy C, Durante M, Weber U. Physical characterization of 3He ion beams for radiotherapy and comparison with 4He. Phys Med Biol. 2021;66(9):095009.
203. Mein S, Dokic I, Klein C, Tessonnier T, Böhlen TT, Magro G, et al. Biophysical modeling and experimental validation of relative biological effectiveness (RBE) for 4He ion beam therapy. Radiat Oncol. 2019;14(1):123.
204. Knäusl B, Fuchs H, Dieckmann K, Georg D. Can particle beam therapy be improved using helium ions? - A planning study focusing on pediatric patients. Acta Oncol. 2016;55(6):751–9.
205. Ebner DK, Frank SJ, Inaniwa T, Yamada S, Shirai T. The emerging potential of multi-ion radiotherapy. Front Oncol. 2021;11:624786.
206. Winkelmann T, Cee R, Haberer T, Naas B, Peters A. Test bench to commission a third ion source beam line and a newly designed extraction system. Rev Sci Instrum. 2012;83(2):02b904.
207. Jäkel O. Physical advantages of particles: protons and light ions. Br J Radiol. 2020;93(1107):20190428.
208. Ying C, Bolst D, Rosenfeld A, Guatelli S. Characterization of the mixed radiation field produced by carbon and oxygen ion beams of therapeutic energy: a Monte Carlo simulation study. J Med Phys. 2019;44(4):263–9.
209. Degiovanni A, Adam J, Aguilera Murciano D, Ballestrero S, Benot-Morell A, Bonomi R, et al., editors. Status of the Commissioning of the LIGHT Prototype. The 9th International Particle Accelerator Conference; 2018-06; Vancouver. Geneva, Switzerland: JACoW Publishing; 2018.
210. Ronsivalle C, Picardi L, Ampollini A, Bazzano G, Marracino F, Nenzi P, et al. First acceleration of a proton beam in a side coupled drift tube linac. Europhys Lett. 2015;111(1):14002.
211. Sindhwani S, Syed AM, Ngai J, Kingston BR, Maiorino L, Rothschild J, et al. The entry of nanoparticles into solid tumours. Nat Mater. 2020;19(5):566–75.
212. Mitchell MJ, Billingsley MM, Haley RM, Wechsler ME, Peppas NA, Langer R. Engineering precision nanoparticles for drug delivery. Nat Rev Drug Discov. 2021;20(2):101–24.
213. Kaur P, Aliru ML, Chadha AS, Asea A, Krishnan S. Hyperthermia using nanoparticles—promises and pitfalls. Int J Hyperth. 2016;32(1):76–88.
214. Penninckx S, Heuskin A-C, Michiels C, Lucas S. Gold nanoparticles as a potent radiosensitizer: a transdisciplinary approach from physics to patient. Cancers. 2020;12(8):2021.
215. Penninckx S, Heuskin AC, Michiels C, Lucas S. The role of thioredoxin reductase in gold nanoparticle radiosensitization effects. Nanomedicine (Lond). 2018;13(22):2917–37.
216. Penninckx S, Heuskin AC, Michiels C, Lucas S. Thioredoxin reductase activity predicts gold nanoparticle radiosensitization effect. Nanomaterials (Basel). 2019;9(2):295.
217. Zhong D, Zhao J, Li Y, Qiao Y, Wei Q, He J, et al. Laser-triggered aggregated cubic α-Fe(2)O(3)@Au nanocomposites for magnetic resonance imaging and photothermal/enhanced radiation synergistic therapy. Biomaterials. 2019;219:119369.
218. Schuemann J, Bagley AF, Berbeco R, Bromma K, Butterworth KT, Byrne HL, et al. Roadmap for metal nanoparticles in radiation therapy: current status, translational challenges, and future directions. Phys Med Biol. 2020;65(21):21rm02.
219. Scorsetti M, Cozzi L, Navarria P, Fogliata A, Rossi A, Franceschini D, et al. Intensity modulated proton therapy compared to volumetric modulated arc therapy in the irradiation of young female patients with Hodgkin's lymphoma. Assessment of risk of toxicity and secondary cancer induction. Radiat Oncol. 2020;15(1):12.
220. Yamanaka R, Hayano A, Kanayama T. Radiation-induced meningiomas: an exhaustive review of the literature. World Neurosurg. 2017;97:635–44.e8.
221. Joensuu H, Kankaanranta L, Seppälä T, Auterinen I, Kallio M, Kulvik M, et al. Boron neutron capture therapy of brain tumors: clinical trials at the Finnish facility using boronophenylalanine. J Neurooncol. 2003;62(1–2):123–34.
222. Capala J, Stenstam BH, Sköld K, Munck af Rosenschöld P, Giusti V, Persson C, et al. Boron neutron capture therapy for glioblastoma multiforme: clinical studies in Sweden. J Neurooncol. 2003;62(1–2):135–44.
223. Busse PM, Harling OK, Palmer MR, Kiger WS III, Kaplan J, Kaplan I, et al. A critical examination of the results from the Harvard-MIT NCT program phase I clinical trial of neutron capture therapy for intracranial disease. J Neurooncol. 2003;62(1–2):111–21.
224. Henriksson R, Capala J, Michanek A, Lindahl SA, Salford LG, Franzén L, et al. Boron neutron capture therapy (BNCT) for glioblastoma multiforme: a phase II study evaluating a prolonged high-dose of boronophenylalanine (BPA). Radiother Oncol. 2008;88(2):183–91.

225. Kawabata S, Miyatake S, Hiramatsu R, Hirota Y, Miyata S, Takekita Y, et al. Phase II clinical study of boron neutron capture therapy combined with X-ray radiotherapy/temozolomide in patients with newly diagnosed glioblastoma multiforme—study design and current status report. Appl Radiat Isot. 2011;69(12):1796–9.
226. Yamamoto T, Matsumura A, Nakai K, Shibata Y, Endo K, Sakurai F, et al. Current clinical results of the Tsukuba BNCT trial. Appl Radiat Isot. 2004;61(5):1089–93.
227. Miyatake S, Kawabata S, Kajimoto Y, Aoki A, Yokoyama K, Yamada M, et al. Modified boron neutron capture therapy for malignant gliomas performed using epithermal neutron and two boron compounds with different accumulation mechanisms: an efficacy study based on findings on neuroimages. J Neurosurg. 2005;103(6):1000–9.
228. Miyatake S, Kawabata S, Yokoyama K, Kuroiwa T, Michiue H, Sakurai Y, et al. Survival benefit of Boron neutron capture therapy for recurrent malignant gliomas. J Neurooncol. 2009;91(2):199–206.
229. Kankaanranta L, Seppälä T, Koivunoro H, Välimäki P, Beule A, Collan J, et al. L-Boronophenylalanine-mediated boron neutron capture therapy for malignant glioma progressing after external beam radiation therapy: a Phase I study. Int J Radiat Oncol Biol Phys. 2011;80(2):369–76.
230. Miyatake S, Tamura Y, Kawabata S, Iida K, Kuroiwa T, Ono K. Boron neutron capture therapy for malignant tumors related to meningiomas. Neurosurgery. 2007;61(1):82–90; discussion –1.
231. Kawabata S, Hiramatsu R, Kuroiwa T, Ono K, Miyatake S. Boron neutron capture therapy for recurrent high-grade meningiomas. J Neurosurg. 2013;119(4):837–44.
232. Fukuda H, Hiratsuka J, Kobayashi T, Sakurai Y, Yoshino K, Karashima H, et al. Boron neutron capture therapy (BNCT) for malignant melanoma with special reference to absorbed doses to the normal skin and tumor. Australas Phys Eng Sci Med. 2003;26(3):97–103.
233. Menéndez PR, Roth BM, Pereira MD, Casal MR, González SJ, Feld DB, et al. BNCT for skin melanoma in extremities: updated Argentine clinical results. Appl Radiat Isot. 2009;67(7–8 Suppl):S50–3.
234. Hiratsuka J, Kamitani N, Tanaka R, Tokiya R, Yoden E, Sakurai Y, et al. Long-term outcome of cutaneous melanoma patients treated with boron neutron capture therapy (BNCT). J Radiat Res. 2020;61(6):945–51.
235. Koivunoro H, Bleuel DL, Nastasi U, Lou TP, Reijonen J, Leung KN. BNCT dose distribution in liver with epithermal D-D and D-T fusion-based neutron beams. Appl Radiat Isot. 2004;61(5):853–9.
236. Kato I, Ono K, Sakurai Y, Ohmae M, Maruhashi A, Imahori Y, et al. Effectiveness of BNCT for recurrent head and neck malignancies. Appl Radiat Isot. 2004;61(5):1069–73.
237. Kankaanranta L, Seppälä T, Koivunoro H, Saarilahti K, Atula T, Collan J, et al. Boron neutron capture therapy in the treatment of locally recurred head and neck cancer. Int J Radiat Oncol Biol Phys. 2007;69(2):475–82.
238. Kato I, Fujita Y, Maruhashi A, Kumada H, Ohmae M, Kirihata M, et al. Effectiveness of boron neutron capture therapy for recurrent head and neck malignancies. Appl Radiat Isot. 2009;67(7–8 Suppl):S37–42.
239. Kankaanranta L, Seppälä T, Koivunoro H, Saarilahti K, Atula T, Collan J, et al. Boron neutron capture therapy in the treatment of locally recurred head-and-neck cancer: final analysis of a phase I/II trial. Int J Radiat Oncol Biol Phys. 2012;82(1):e67–75.
240. Suzuki M, Kato I, Aihara T, Hiratsuka J, Yoshimura K, Niimi M, et al. Boron neutron capture therapy outcomes for advanced or recurrent head and neck cancer. J Radiat Res. 2014;55(1):146–53.
241. Aihara T, Morita N, Kamitani N, et al. BNCT for advanced or recurrent head and neck cancer. Appl Radiat Isot. 2014;88:12–5.
242. Wang LW, Chen YW, Ho CY, Hsueh Liu YW, Chou FI, Liu YH, et al. Fractionated boron neutron capture therapy in locally recurrent head and neck cancer: a prospective phase I/II trial. Int J Radiat Oncol Biol Phys. 2016;95(1):396–403.
243. Koivunoro H, Kankaanranta L, Seppälä T, Haapaniemi A, Mäkitie A, Joensuu H. Boron neutron capture therapy for locally recurrent head and neck squamous cell carcinoma: an analysis of dose response and survival. Radiother Oncol. 2019;137:153–8.
244. Hirose K, Konno A, Hiratsuka J, Yoshimoto S, Kato T, Ono K, et al. Boron neutron capture therapy using cyclotron-based epithermal neutron source and borofalan ((10)B) for recurrent or locally advanced head and neck cancer (JHN002): an open-label phase II trial. Radiother Oncol. 2021;155:182–7.

Further Reading

Adant S, Shah GM, Beauregard JM. Combination treatments to enhance peptide receptor radionuclide therapy of neuroendocrine tumours. Eur J Nucl Med Mol Imaging. 2020;47(4):907–21.
Ahmadzadehfar H, Biersack HJ, Freeman LM, Zuckier LS, editors. Clinical nuclear medicine. 2nd ed. Switzerland: Springer Cham; 2020. 584 p
Billena C, Khan AJ. A current review of spatial fractionation: back to the future? Int J Radiat Oncol Biol Phys. 2019;104(1):177–87.
Bragg WH, Kleeman R. LXXIV. On the ionization curves of radium. London Edinburgh Dublin Philos Mag J Sci. 1904;8(48):726–38.
Chan TG, O'Neill E, Habjan C, Cornelissen B. Combination strategies to improve targeted radionuclide therapy. J Nucl Med. 2020;61(11):1544–52.
Douglass M, Hall EJ, Giaccia AJ. Radiobiology for the radiologist. Australas Phys Eng Sci Med. 2018;41(4):1129–30.
Dymova MA, Taskaev SY, Richter VA, Kuligina EV. Boron neutron capture therapy: current status and future perspectives. Cancer Commun (Lond). 2020;40(9):406–21.
Feijtel D, de Jong M, Nonnekens J. Peptide receptor radionuclide therapy: looking back, looking forward. Curr Top Med Chem. 2020;20(32):2959–69.
Herrmann K, Schwaiger M, Lewis JS, Solomon SB, McNeil BJ, Baumann M, et al. Radiotheranostics: a roadmap for future development. Lancet Oncol. 2020;21(3):e146–e56.
Jadvar H, Chen X, Cai W, Mahmood U. Radiotheranostics in cancer diagnosis and management. Radiology. 2018;286(2):388–400.
Joiner MC, van der Kogel AJ, editors. Basic clinical radiobiology. Boca Raton: CRC Press; 2018. 360 p
Kaplon H, Reichert JM. Antibodies to watch in 2021. MAbs. 2021;13(1):1860476.
Kraeber-Bodéré F, Barbet J, Chatal J-F. Radioimmunotherapy: from current clinical success to future industrial breakthrough? J Nucl Med. 2016;57(3):329.
Kraeber-Bodéré F, Bodet-Milin C, Rousseau C, Eugène T, Pallardy A, Frampas E, et al. Radioimmunoconjugates for the treatment of cancer. Semin Oncol. 2014;41(5):613–22.
Macià IGM. Radiobiology of stereotactic body radiation therapy (SBRT). Rep Pract Oncol Radiother. 2017;22(2):86–95.
Malik A, Afaq S, Tarique M, editors. Nanomedicine for cancer diagnosis and therapy. 1st ed. Singapore: Springer Singapore; 2021.
Miyatake SI, Wanibuchi M, Hu N, Ono K. Boron neutron capture therapy for malignant brain tumors. J Neurooncol. 2020;149(1):1–11.
Reynolds TS, Bandari RP, Jiang Z, Smith CJ. Lutetium-177 labeled bombesin peptides for radionuclide therapy. Curr Radiopharm. 2016;9(1):33–43.

Schuemann J, Bagley AF, Berbeco R, Bromma K, Butterworth KT, Byrne HL, et al. Roadmap for metal nanoparticles in radiation therapy: current status, translational challenges, and future directions. Phys Med Biol. 2020;65(21):21rm02.

Shi J, Kantoff PW, Wooster R, Farokhzad OC. Cancer nanomedicine: progress, challenges and opportunities. Nat Rev Cancer. 2017;17(1):20–37.

Suzuki M. Boron neutron capture therapy (BNCT): a unique role in radiotherapy with a view to entering the accelerator-based BNCT era. Int J Clin Oncol. 2020;25(1):43–50.

Thomadsen B. Comprehensive brachytherapy: physical and clinical aspects. Med Phys. 2013;40(11)

Trifiletti DM, Chao ST, Sahgal A, Sheehan JP, editors. Stereotactic radiosurgery and stereotactic body radiation therapy: a comprehensive guide. 1st ed. Switzerland: Springer Cham; 2019. 435 p

Vugts DJ, van Dongen GAMS. Immunoglobulins as radiopharmaceutical vectors. In: Lewis JS, Windhorst AD, Zeglis BM, editors. Radiopharmaceutical chemistry. Cham: Springer International Publishing; 2019. p. 163–79.

Wiedemann H, editor. Particle accelerator physics. 4th ed. Cham: Springer; 2015. 475 p

Yan W, Khan MK, Wu X, Simone CB, Fan J, Gressen E, et al. Spatially fractionated radiation therapy: history, present and the future. Clin Transl Radiat Oncol. 2020;20:30–8.